# PLATTE RIVER RECOVERY IMPLEMENTATION PROGRAM

Data Synthesis Compilation

Sediment Augmentation



**PLATTE RIVER**
**RECOVERY IMPLEMENTATION PROGRAM**

Prepared by staff of the Executive Director's Office for the Governance Committee of the Platte River Recovery Implementation Program

December 10, 2024

# PREFACE

This document was prepared by the Executive Director's Office (EDO) of the Platte River Recovery Implementation Program ("Program" or "PRRIP"). The information and analyses presented herein are focused on informing the use of Program land, water, and fiscal resources to achieve the Program's long-term goal of improving and maintaining the associated habitats for the target species (interior least tern, piping plover, whooping crane, and pallid sturgeon). While the sediment regime and effect of sediment augmentation apply for the entire suite of target species, these actions have the highest potential to effect the channel planform as it relates to whooping crane habitat; as such, the Program has focused efforts on informing the relationship between sediment augmentation and the whooping crane management objective: contribute to the survival of whooping cranes by increasing habitat suitability and thus use of the Associated Habitat Reach (AHR) along the central Platte River in Nebraska. The Program has invested fourteen years in implementation of an adaptive management program (AMP) to reduce uncertainties about proposed management strategies and learn about river and species responses to management actions. During that time, the Program has implemented management actions, collected a large body of physical and species response data, and developed modeling and analysis tools to aid in the interpretation and synthesis of data.

Implementation of the Program's AMP has proceeded with the understanding that management uncertainties, expressed as hypotheses and summarized as Big Questions, encompass complex physical and ecological responses to limited treatments that occur within a larger ecosystem that cannot be controlled by the Program. The lack of experimental control and complexity of response precludes the sort of controlled experimental setting necessary to cleanly follow the strong inference path of testing alternative hypotheses by devising crucial experiments (Platt, 1964). Instead, adaptive management in the Platte River ecosystem must rely on a combination of monitoring of physical and biological response to management treatments, predictive modeling, and retrospective analyses (Walters, 1997).

One of the Program's primary management uncertainties is the need for long-term sediment (sand) augmentation. Due to significant variation and uncertainty in the sediment balance throughout the central Platte River, the Program focused its efforts at the upper end of the Associated Habitat Reach (AHR) to offset the largest and most well-known historical sediment deficit in the central Platte River due to clearwater hydropower return flows. Stakeholders have long been concerned that incision and narrowing due to erosion of sediment from the bed of the channel downstream of the return will migrate downstream and impact habitat suitability for the Program's target species. Efforts to quantify the magnitude of the sediment deficit and develop augmentation methods began soon after Program initiation in 2007. By 2016, Program stakeholders reached consensus that the best next step in evaluating sediment augmentation would be implementation of a full-scale sediment augmentation experiment immediately downstream of the hydropower return. The full-scale augmentation experiment was initiated in 2017 with augmentation occurring annually from 2017 through 2021. In 2022, the Executive Director's Office began analysis of the effectiveness of sediment augmentation, producing multiple lines of evidence across a range of spatial and temporal scales.

The results of our analyses are organized into a four-chapter synthesis report. The Executive Summary provides a condensed and consolidated summary of the findings presented in the following chapters. The Data Summary provides relevant information regarding all the sources of data used in our analyses. Chapter 1 provides history and context including a summarization of modeling and research conducted during the First Increment of the Program. Chapter 2 is comprised of retrospective analyses of spatial and temporal patterns of incision prior to initiation of the sediment augmentation experiment. Chapter 3 focuses on two-dimensional longitudinal channel response to sediment augmentation. Chapter 4 is comprised of an analysis of volumetric change in the period prior to and during the sediment augmentation experiment.

**References**

Platt, J. R. 1964. Strong inference. Science, 146(3642), 347-353.

Walters, C. 1997. Challenges in adaptive management of riparian and coastal ecosystems. Conservation ecology, 1(2), 1.

# CONTENTS

# LIST OF ACRONYMS

| | |
|---|---|
| 1D | One dimensional |
| 2D | Two dimensional |
| ADCP | Acoustic doppler current profilers |
| AHR | Associated Habitat Reach |
| AMP | Adaptive management plan |
| CNPPID | Central Nebraska Public Power and Irrigation District |
| CWR | Cottonwood Ranch |
| DEM | Digital elevation model |
| EDO | Executive Directors Office |
| EIS | Environmental impact statement |
| GAM | Generalized additive model |
| GAMM | Generalized additive mixed model |
| GC | Governance Committee |
| GGL | Geomorphic Grade Line |
| GSD | Ground Sample Distance |
| ISAC | Independent Scientific Advisory Committee |
| J2 Return | Johnson No. 2 Hydropower Return |
| KCD | Kearney Canal Diversion |
| LiDAR | Light Detection and Ranging |
| MUCW | Maximum unobstructed channel width |
| NE | Nebraska |
| PRRIP | Platte River Recovery Implementation Program, or Program |
| QSI | Quantum Spatial Inc. |
| REM | Relative elevation model |
| SED-VEG | Platte River Sediment Transport and Riparian Vegetation Model |
| USBR | United States Bureau of Reclamation |
| USGS | United States Geological Survey |
| Ft | Foot |
| cfs | Cubic feet per second |
| $yd^3$ | Cubic yard |

# EXECUTIVE SUMMARY

## *E.1      Why did we conduct a sediment augmentation management experiment?*

Extension Science Plan Big Question 3[1] asks if sediment augmentation is necessary to create and/or maintain suitable whooping crane habitat in the future. More specifically, clearwater hydropower return flows entering the south channel of the Platte between Lexington and Overton (the J2 Return Channel) have resulted in incision and narrowing in that reach. We hypothesized that annual sand augmentation of 60,000 to 80,000 tons (40,000 to 53,000 yd$^3$)[2] might be necessary to supply sediment in sufficient quantities to stabilize channel incision and prevent it from progressing downstream past the Overton Bridge and negatively impacting whooping crane habitat suitability.[3] Alternative hypotheses include the need for more or less sediment and/or alternate augmentation locations, as well as the hypothesis that incision is progressing slowly enough that it does not pose a threat to downstream habitat.

To answer this question, the Program initiated a full-scale sediment augmentation management experiment in 2017 that involves mechanically augmenting 40,000–60,000 yd$^3$ of sand into the channel immediately downstream of the J2 Return each year. A combination of transect surveys and LiDAR data has been analyzed to evaluate channel response to the increase in sediment supply. Preliminary findings, along with a map of the augmentation evaluation reach and features, follow.

---

[1] Big Questions are priority uncertainties identified by policymakers. The answers to these questions will inform future decision-making.

[2] Earlier work computed sediment deficit and transport in units of tons, while current work is computed in cubic yards. In 2016, Twin Rivers Testing and Environmental determined an average sediment density and proposed 1 yd$^3$ would be equal to 1.5 T. This conversion rate was used to approximate volumes from sediment masses where necessary.

[3] The narrow, incised reach of the J2 Return Channel does not meet minimum habitat suitability requirements for whooping crane roosting habitat. If impacts progress downstream past the Overton Bridge, habitat suitability at the Cottonwood Ranch habitat complex will be negatively impacted.
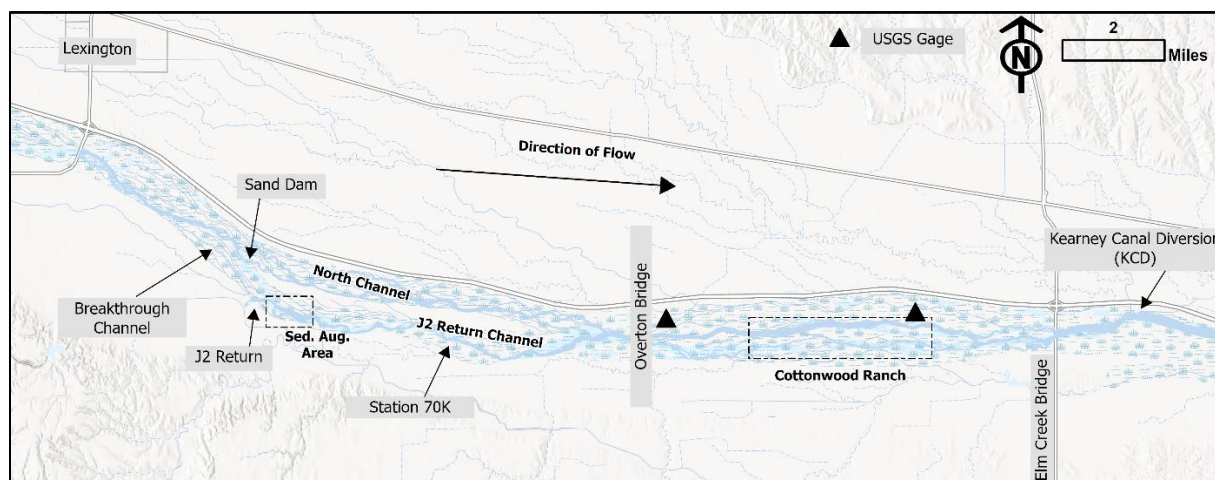
**Figure E.1** Overview map of sediment augmentation evaluation reach and features. There is no permanent surface flow connection between the north channel and the upstream end of the J2 Return Channel.

### E.2     What have we learned about historical degradation in the J2 Return Channel prior to augmentation?

The J2 Return began clearwater hydropower returns in 1942. Since then, J2 Return Channel has incised and its slope has decreased, diverging markedly from historical elevations (Figures 2.5-2.6; relative elevation model). Limited transect survey data prior to LiDAR gives an indication of the progression of this change. In 1989, transect data indicated that the thalweg below the return had incised 14 feet (0.3 ft/yr) below the floodplain, followed by an additional six feet of incision by 2002 (0.5 ft/yr). After this point, however, incision seems to have slowed with no measurable lowering between 2002 and 2016. This period of slowing incision coincided with a steady increase in sinuosity (i.e. more lateral channel movement).

Classic braided channels are multithreaded, where flow is separated by temporary, unvegetated sediment bars; meandering channels are single-threaded, sinuous and associated with pools along cut banks and riffles between subsequent pools; and wandering channels can be considered transitionary between braided and meandering. The shift from vertical incision to lateral migration may be linked to the channel slope dropping below the range needed to maintain a straight braided channel, causing it to transition to a wandering planform. Lateral erosion now comprises >50% of total erosion in the channel, supplying downstream reaches with sediment from bank material rather than bed material.

Overall, we assess that a wave of vertical incision propagated down through the study area after J2 Return began operations. In the early 2000s, the primary mechanism of channel degradation shifted from incision to lateral migration, with the highest intensity of migration occurring in upper half of the J2 Return Channel.

### E.3    What have we learned about the J2 Return Channel during the sediment augmentation management experiment?

Mechanical augmentation operations began in 2017 and full-scale augmentation of 40,000–60,000 yd$^3$ occurred annually from 2018–2021.[4] Calculation of year-to-year volume change in the augmentation area indicates most augmented material was mobilized downstream out of the augmentation area annually. Annual comparisons of volume change downstream of the augmentation area found that rates of bed erosion decreased by 20,000–40,000 yd$^3$ (45%–60%) from the pre-augmentation period.  This roughly equals the annual increase in sediment transported out of the sediment augmentation area (36,000 yd$^3$) during augmentation operations.

The decrease in bed erosion occurred in the first three miles downstream of the augmentation area. Bed elevations in that segment were stable to slightly aggradational. However, incision was observed farther down the J2 Return Channel. A 6,000 ft reach near Station 70,000 was identified as an area of interest where rapid channel consolidation and incision seems to be occurring. This area will continue to be monitored closely for evidence of transition from braided to wandering channel planforms.

These findings indicate that the annual augmentation volume was sufficient to offset approximately half the bed erosion in the J2 Return Channel Reach while bed erosion and possible planform change continued in the downstream half of the reach.

### E.4    What have we learned about sediment balance downstream of Overton during the sediment augmentation management experiment?

When compared to the pre-augmentation period and normalized for discharge, we observed no major difference in the volume of bed erosion during the pre- and post-augmentation periods downstream of Overton Bridge. The one substantial difference we did observe was significant lateral erosion that occurred because of the prolonged peak flow event in 2015 which increased mean channel width by more than 200 ft. Channel widths have remained stable since.

Overall, we assess that effects of sediment augmentation were not detectable downstream of Overton Bridge.  The reach continues to be dynamic and highly variable but generally stable and the increase in channel width that occurred during the pre-augmentation period has been maintained.[5]

### E.5    What is our overall assessment of the performance of the sediment augmentation management experiment?

Augmentation operations reduced annual bed erosion in the J2 Return Channel by approximately 20,000–40,000 yd$^3$ (45%–60%) which is consistent with the 35,000 yd$^3$ increase in sediment transported out of the augmentation area following augmentation operations. Nonetheless, we observe continued incision and planform change midway down the J2 Return Channel (Station

---

[4] Full-scale augmentation also occurred in 2022 but remote sensing data was not available in time to include in this analysis.
[5] Whooping crane habitat suitability in the CWR reach is being maintained at the highest level in 60-70 years.

70,000). In the absence of augmentation, we would expect bed erosion in the J2 Return Channel to return to pre-augmentation levels and for incision and planform change to accelerate near Station 70,000. We are unable to predict short term changes in the rate of incision because:

1) The absence of detailed thalweg elevation data during the pre-augmentation period (no topo-bathymetric LiDAR) prevented a detailed analysis of thalweg incision rates immediately prior to augmentation.
2) The absence of a complete hydrologic record in the J2 Return Channel obscures the relationship between flow and incision. This is being remedied for future analysis with the installation of a stream gage.

Regardless of these uncertainties we can say with confidence that there is a substantial sediment deficit in the J2 Return Channel that has, and continues to, impact channel form. At present the most serious planform impact (transition from braided to wandering) has not progressed downstream of Overton Bridge but may at some unknown point in the future. As such, mechanical augmentation at the upper end of the J2 Return Channel has been shown to reduce the sediment deficit, theoretically reducing future risk to downstream habitat. However, near- and long-term benefits are difficult to quantitatively predict in the light of data limitations described above. Additional data and monitoring may allow for better predictions that can more easily be weighed against the annual cost of augmenting sediment. Alternatives that allow for sediment replenishment without annual mechanical augmentation may offer a longer-term solution, though their effectiveness, when compared to recent mechanical augmentation efforts, is unknown.

# DATA SUMMARY

The following section provides detailed information on the various types and sources of data used in this report.

## D.1 Topographic and Bathymetric Elevation Data

D.1.1 Light Detection and Ranging (LiDAR) Data

The Program has collected high-resolution LiDAR data across the study area each year since 2009. The minimum specifications require LiDAR to be collected at a 2.3ft average ground sample distance (GSD) with greater than 2 pulses/m$^2$. Actual post spacing was often 4-8 pulses/m$^2$. Vertical topographic accuracy requirements for these acquisitions were less than 0.3 ft (3.6 inches), though delivered accuracies often achieved better (Table D.1). Prior to 2016, LiDAR was only collected over dry portions of the banks and riverbed. Wetted areas were "hydroflattened" to smooth and approximate the water surface elevation.

Starting in 2016, topo-bathymetric LiDAR was deployed which allowed for the collection of both topographic and bathymetric data. These acquisitions use near-infrared-wavelength lasers to collect topographic data in non-water areas and use water-penetrating green-wavelength lasers to collect bathymetry. Between 2016 and 2021 LiDAR elevation data were collected by Quantum Spatial Inc. (QSI) in either October or November (QSI, 2016- 2021). Annual survey and ground control points are used to calibrate new LiDAR surfaces and ensure consistency with past years. Bathymetric accuracy of the calibrated LiDAR surface is evaluated with check points captured in submerged areas of the channel at the time of LiDAR flights. Data is processed by QSI and delivered as 3-foot resolution elevation rasters. Tested accuracies for those rasters are shown in Table D.1. The accuracy values in Table D.1 represent the 95% confidence interval, as derived from the population of differences between field-measured and DEM values. Accuracy assessments are designed to meet the guidelines of the Federal Geographic Data Committee National Standard for Spatial Data Accuracy (FGDC, 1998). From 2016–2021 the accuracy assessment data indicate elevation values in wet areas had consistently higher uncertainty than dry areas across all years due to inherent differences in bathymetric and topographic LiDAR data acquisition and processing (Szafarczyk and Toś, 2022). As a result of deeper and more turbid water during the period of data collection, wet areas in 2019 had a higher vertical uncertainty value at 9 inches (Table D.1).

**Table D.1.** Vertical accuracy estimates for the LiDAR DEM surfaces from each year for wet and dry areas. Accuracy values represent 95% confidence in the estimate.

| Year | Dry, Unvegetated Accuracy (in) | Wet Accuracy (in) |
|------|-------------------------------|-------------------|
| 2009 | 3.0 | NA |
| 2012 | 1.6 | NA |
| 2016 | 1.7 | 3.1 |
| 2017 | 2.2 | 4.6 |
| 2018 | 1.2 | 4.2 |
| 2019 | 1.2 | 9.0 |
| 2020 | 2.2 | 3.1 |
| 2021 | 1.7 | 2.1 |

To enable evaluation of the pre-augmentation period, this report uses two years (2009 and 2012) of topographic-only LiDAR data and all years (2016-2021) of topo-bathymetric LiDAR. In 2009 and 2012, LiDAR collection occurred when river flows were low (see Table D.2) and water covered a small portion (~25%) of the active channel area, allowing for ~75% LiDAR coverage. The uncertainty in thalweg elevation and volume change created by these missing channel elevations will be discussed in Chapters 2 and 4.

**Table D.2.** Summary of LiDAR data used in analyses

| | **2009 and 2012** | | **2016 - 2021** | |
|---|---|---|---|---|
| LiDAR date, resolution | March 2009, November 2012, 2.3 ft GSD Topographic only | | Fall (Oct or Nov), 2.3 ft GSD Topo-bathymetric | |
| Flow rate during LiDAR collection (cfs) | **J2 Return** | **Overton** | **J2 Return** | **Overton** |
| | 0–134 | 200–400 | 90–2,000 | 250–2,400 |

D.1.2 Uncertainty Evaluation for Rasters of Difference
Several methods exist in literature for quantifying uncertainty from difference rasters including the use of fuzzy inference systems (Wheaton et al., 2010; Bangen et al., 2016) for systematic error and the use of probability thresholds to limit noise when quantifying total erosion or total deposition (Lane et. al., 2003). After careful analysis of our LiDAR data, we found that the distribution of error over the active channel approximates a normal distribution and does not portray evidence of systematic biases that would lead to significant over or under-estimation of changes in difference rasters. Given this finding, we elected to follow the example of Anderson, 2019 in which normally distributed positive and negative errors are assumed to cancel one another out, removing the need for thresholding.

To verify the absence of systematic error in topographic LiDAR as reported by the contractors, we extracted elevations from each DEM between 2016 and 2021 along roads within the study area (Figure D.1). These locations are stable and paved and expected to stay consistent such that any measured difference in DEM surface should represent error and not an actual change in elevation. Differences between the highest and lowest elevation extracted along the line are generally between 0.05 and 0.15 feet (0.6 to 1.8 inches) and standard deviations calculated for all years are around 0.05 feet (0.6 inches). These values represent the variability among surfaces due to LiDAR accuracy and DEM production methods. We can therefore confirm that the difference associated with acquisition and production accuracy and error between any two years' DEMs are generally less than 0.2 ft (2.5 inches) and in line with the accuracy as assessed by the contractor. We can also conclude there is no systematic bias to elevation error because at any given linear extraction location there is no consistency to the year that is the lowest or highest elevation (Figure D.1). For example, the 2021 survey (Figure D.1, orange line in Panels B-D) is the lowest elevation at Location 10, is around the average elevations at Location 1, and is relatively high in elevation at Location 15.
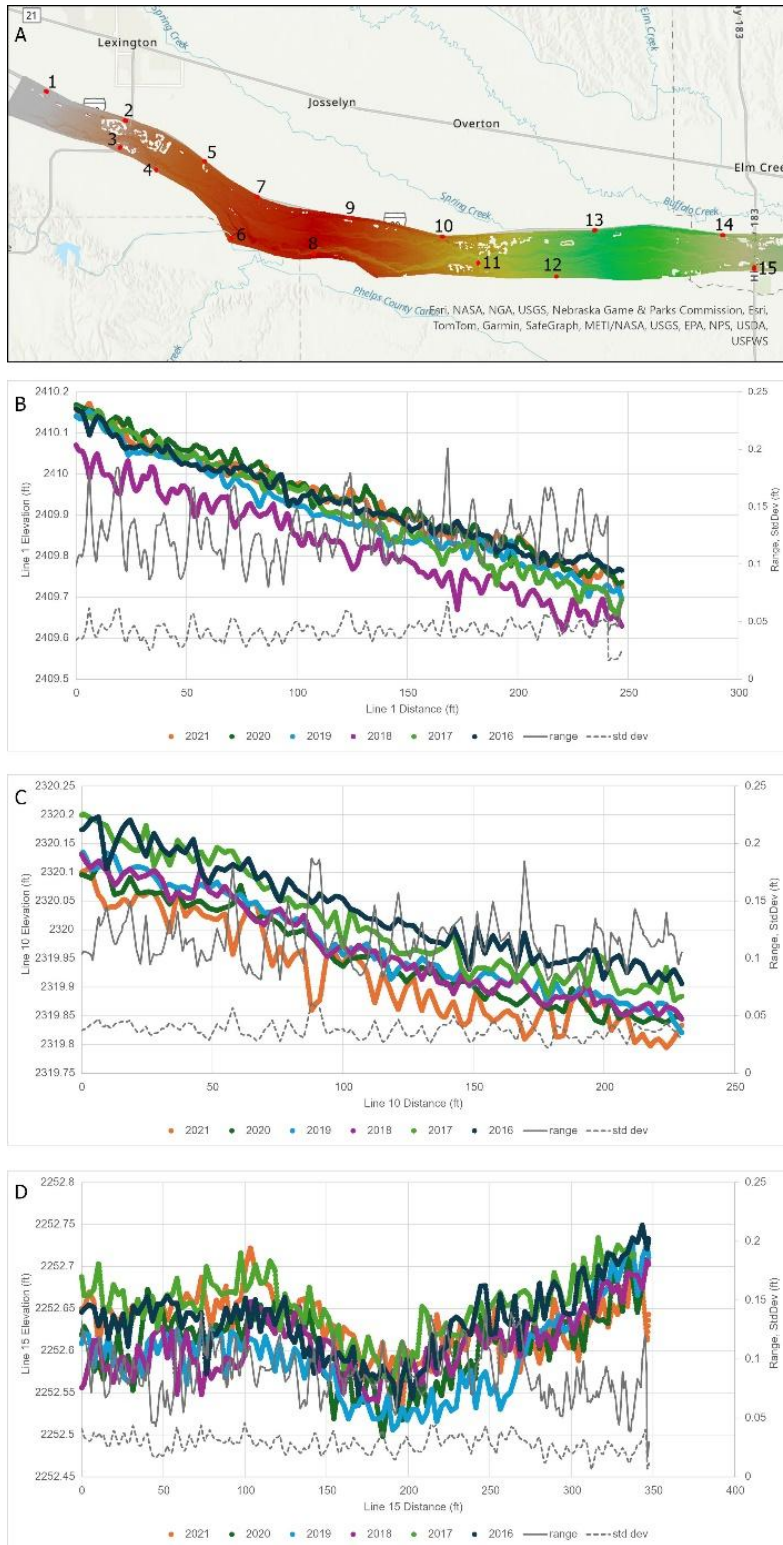
**Figure D.1**. Linear elevation extractions from three example paved surfaces (Location 1, Panel B; Location 10; Panel C, and Location 15, Panel D) in the study area (Panel A).

To verify the absence of systematic error in bathymetric LiDAR we examined the median average difference between bathymetric checkpoints and the DEM provided by the contractor. As shown in Table D.3, the median differences vary from slightly positive to slightly negative each year and remain within 1.5 inches of zero every year. This indicates that while the magnitude of LiDAR error is larger in inundated areas (Table D.1), there is no evidence of systematic error that would not average to zero.

**Table D.3** Median difference of bathymetric checkpoints and LiDAR DEM.

| Year | Number of Points | Median vertical error of bathymetric LiDAR (ft) |
|------|------------------|-------------------------------------------------|
| 2016 | 140 | -0.049 |
| 2017 | 288 | 0.03 |
| 2018 | 58 | 0.043 |
| 2019 | 128 | -0.115 |
| 2020 | 251 | 0.013 |
| 2021 | 340 | -0.036 |

We did observe systematic error due to vegetation changes in areas that experience plowing, tree clearing, mowing or haying vs. rest years for grasslands, or other major changes to vegetation height and cover that may be near or within typical accuracy estimates. These typical problem areas are rarely located within our area of interest for erosion and deposition (active channel), so by clipping the difference rasters to the active channel these areas are removed from our calculations. The full difference rasters presented in Appendix A demonstrate this vegetation bias and show where the active channel was clipped each year.

Following this post-processing effort to remove systematic error, and with the given reported accuracies, we believe it is reasonable to quantify change without using thresholds or other methods that may exclude data. Given the accuracy reports provided by the LiDAR contractor and our independent analysis of the DEM surfaces, we conclude that DEM elevation errors are small (< 0.2 ft or 2.5 inches). These results and reports thus suggest that it is reasonable to include the entire dataset in plots and calculations and that positive and negative errors should be canceled out (Anderson, 2019).

D.1.2 Pre-2016 Bathymetric Data
The primary data source for pre-2016 elevation data in the wetted portion of the channel was 2009–2016 systematic surveys of channel cross-section elevations conducted for the system-scale channel geomorphology and vegetation monitoring project (Tetra Tech, 2017). Prior to 2009 limited bathymetric survey data is available.

Repeat cross section data were collected by the United States Bureau of Reclamation (USBR) in 1989 and DJ&A consultants in 2002 (Holburn et al. 2006). These entities surveyed a total of 11 cross sections in 1989 between the J2 Return and KCD. Ten were repeated in 2002. A map of these cross section locations can be found in Chapter 2, Figure 2.7.

### D.2 Hydrologic Data

Three sources of discharge data were used in our analyses. The furthest downstream, approximately 4.5 miles above the Kearney Canal Diversion (KCD) is the United States Geological Survey (USGS) Cottonwood Ranch Mid-Channel Gage (06768035) which measures stage and discharge of part of the river and was used solely for specific gage analysis (Section 2.5). A second USGS gage is located at the Overton Bridge (06768000) seven miles downstream of the J2 Return and ten miles upstream of the KCD. This gage captures the total flow immediately downstream of the confluence of the J2 Return Channel and the North Channel of the Platte. The period of record for the Overton stream gage extends from October 1, 1930, to present. However, the gage has been relocated several times and was moved to the present location on October 10, 1986. At the current location, operation has been continuous with one major datum adjustment (lowered by 2.0 ft) on September 30, 2004.

The third source data used in our analyses were records of discharge released from the Tri-County Supply Canal (Supply Canal) into the J2 Return Channel via the J2 Return. These records are provided by the Central Nebraska Public Power and Irrigation District (CNPPID). Typically, J2 Return releases represent the majority of total flow in the J2 Return Channel except for 100-300 cfs of baseflow. The exception to this is when high flows (~3,000 cfs) on the North Channel activate a channel that runs between the North and J2 Return Channels (the breakthrough channel, see Figure D.2). When the breakthrough channel is activated, an unknown but substantial quantity of flow is added to the J2 Return Channel. The breakthrough channel has periodically been blocked to prevent flow from entering and endangering a gas pipeline, however permanent closure of the channel is not currently allowed.
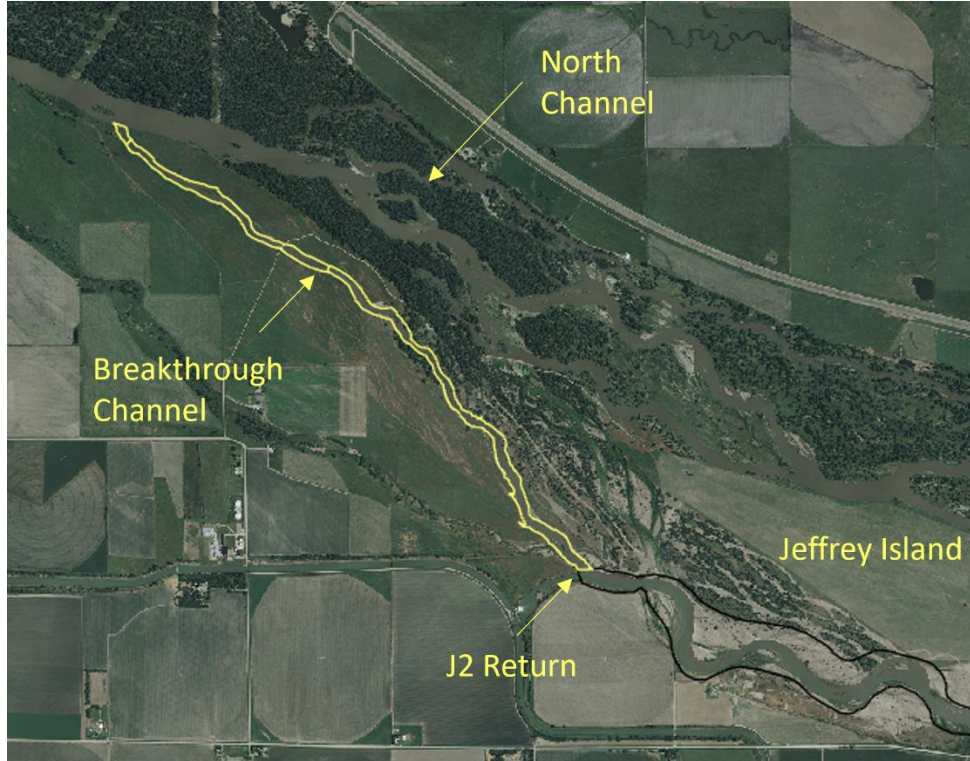
**Figure D.2** Breakthrough channel connecting the North Channel to the J2 Return Channel during high flow conditions.

Figure D.3 presents 2009–2021 flow at the Overton Bridge (blue) alongside J2 Return releases (orange). J2 Return flows never exceeded 2,025 cfs during this period, whereas the Overton gage shows that there were several months in which mean flow was above 6,000 cfs. The peak daily flow of 15,300 cfs at Overton occurred in June of 2015. This flood had large geomorphic effects downstream of Overton such as high lateral erosion and channel widening (Section 3.6). As a result of the controlled hydrology from the J2 Return (except for occasional breakthrough channel activation), the J2 Return Channel does not experience floods as the North Channel does.  This limits the ability of the channel to convey augmented sediment that is placed within the J2 Return Channel.
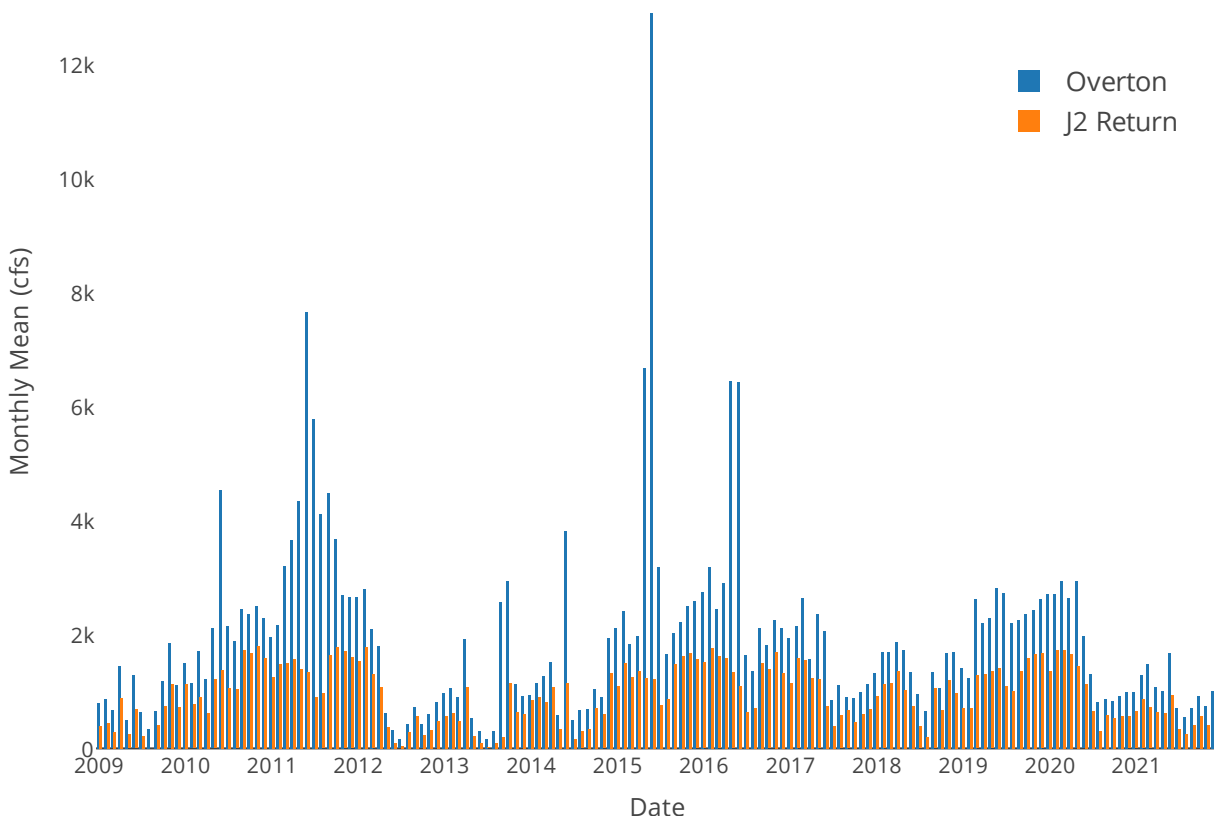
Figure D.3 Monthly mean discharge from CNPPID to the J2 Return Channel and at the USGS Overton gage from 2009 to 2021.

### *D.3 Hydraulic Models*

D.3.1 Two-Dimensional Modeling

Since 2016, annual topo-bathymetric data has been used to update an SRH-2D (Lai, 2008) hydraulic model of the Associated Habitat Reach (AHR) that computes depth, velocity, and shear stress at each two-dimensional (2D) node over a range of in-channel flows (500 to 5,000 cfs). Each of the five model reaches has been calibrated, adjusting Manning's n to better match known data, and validated by comparing model results to measured water surface elevations. Water surface elevations were measured through field survey or LiDAR each year. Approximately 20 known water surface elevation points were collected each year at various flows and locations along the AHR. As shown in Table D.4, validated models predict water surface elevations with typical accuracies within one to two tenths of a foot.

**Table D.4**. Average difference between modeled and measured water surface elevation (ft) at sampled locations within SRH-2D model domains at various flows.

| Model Reach | 2016 | 2017 | 2018 | 2019 | 2020 | 2021 |
|---|---|---|---|---|---|---|
| Grand Island to Chapman | 0.01 | NA | NA | 0.18 | -0.07 | 0.21 |
| Shelton to Grand Island | 0.02 | -0.07 | -0.09 | 0.09 | -0.01 | -0.11 |
| Kearney to Shelton | -0.06 | 0.17 | -0.04 | -0.1 | -0.06 | 0.01 |
| Odessa to Kearney | NA | 0.23 | -0.07 | 0.13 | -0.06 | 0.26 |
| Overton to Odessa | -0.28 | NA | -0.15 | 0.11 | 0.1 | 0.15 |
| Lexington to Overton | NA | NA | 0.14 | 0.06 | -0.02 | 0.30 |

D.3.2 One-Dimensional Modeling

Prior to 2016, two one-dimensional (1D) hydraulic models were created, the first using 2009 LiDAR and survey data, the second using 2012 LiDAR and survey data. Both models were created using HEC-RAS with 78 cross-sections (PRRIP 2022a, HEC-RAS 2008) spaced an average of 1,165 ft apart through the study area. These models pre-dated topo-bathymetric LiDAR and relied on a combination of terrestrial LiDAR and supplemental field surveys. The models were calibrated using USGS rating curves at gage locations and LiDAR-measured water surface elevations at various locations along the AHR. The differences between published gage rating curves and modeled results were found to be within two tenths of a foot at all six gage locations and the average difference between LiDAR and modeled water surface elevations were found to be 0.04 feet (HDR, 2011).

***D.4 Sediment Data***

Detailed sediment analyses were conducted between 2009 and 2016 to estimate sediment deficits and desired augmentation volumes (The Flatwater Group 2010; Tetra Tech 2017). These included suspended and bedload monitoring and sieve grain size analysis. The sediment found in the Platte River is typically coarse to very coarse sand with a D50 of 0.5 to 2 mm. Sediment is coarser at the upstream end of the J2 Return Channel than it is on the North Channel or downstream of the North/J2 Return Channel confluence. At the time of this report, bed armoring has been observed but not measured on the upstream end of J2 (see Figure D.4.  For a more thorough description of monitoring activities and results, see section 1.4.

**Figure D.4.** Visual comparison of coarse armor layer overlaying finer sand on the channel bed approximately 500 feet downstream from the J2 Return

### D.5 Aerial Imagery

High resolution (sub-1-meter pixel) aerial imagery collection has been commissioned by the Program annually or semi-annually since 2009. Products from these collections have typically included true-color as well as color-infrared (CIR) rasters. For this report we also made use of publicly available aerial imagery products pre-dating 2009. Sources for these images include the National Aerial Photography Program (NAPP), the United States Fish and Wildlife Service (USFWS), the Central Platte Natural Resources District (CPNRD), and the National Agricultural Imagery Program (NAIP). Table D.5 summarizes the year of collection, flow at the time of collection at the USGS Overton Gage, and the source of the imagery for each product used in this report.

**Table D.5.** Summary of aerial imagery sources and river flow at time of imagery capture.

|        | **Average Overton Gage Flow on Collection Date (cfs)** | **Source** |
|--------|--------------------------------------------------------|------------|
| **1988** | 2550 | NAPP |
| **1998** | 400 | USFWS |
| **2004** | 240 | CPNRD |
| **2007** | 285 | NAIP |
| **2009** | 1000 | PRRIP |
| **2010** | 310 | PRRIP |
| **2011** | 2800 | PRRIP |
| **2013** | 429 | PRRIP |
| **2014** | 264 | PRRIP |
| **2016** | 1120 | PRRIP |
| **2018** | 1550 | PRRIP |
| **2019** | 2400 | PRRIP |
| **2022** | 330 | PRRIP |

*References*

Anderson, S. (2019). Uncertainty in quantitative analyses of topographic change: error propagation and the role of thresholding. *Earth Surface Processes and Landforms, 44*, 1015-1033.

Bangen, S., Hensleigh, J., McHugh, P., & Wheaton, J. (2016). . Error modeling of DEMS from topographic surveys of rivers using fuzzy inference systems. *Water Resources Research, 52*, 1176– 1193.

Dewberry. (2010). *LiDAR Quality Assurance (QA) Final Report Sub-Project 1: Platte River Corridor Nebraska/Kansas LiDAR.*

Federal Geographic Data Committee (FGDC). (1998). *National Standard for Spatial Data Accuracy.*

HDR. (2011). *1-D Hydraulic and Sediment Transport Model Final Hydraulic Modeling Technical Memorandum.*

HEC-RAS. (2008). *Hydraulic Reference Manual.* U.S. Army Corps of Engineers, Hydrologic Engineering Center.

Holburn, E.R., Fotherby, L.M, Randle, and D.E. Carlson. (2006). Trends of Aggradation and Degradation along the Central Platte River: 1985 to 2005. United States Bureau of Reclamation.

Lai, Y. (2008). *SRH-2D Version 2: Theory and User's Manual.* Bureau of Reclamation Technical Service Center Sedimentation and River Hydraulics Group.

Lane, S., Westaway, R., & Hicks, M. (2003). Estimation of erosion and deposition volumes in a large, gravel-bed, braided river using synoptic remote sensing. *Earth Surface Processes and Landforms, 28*, 249-271.

Platte River Recovery Implementation Program (PRRIP) Executive Director's Office (EDO). (2022). *First Increment Extension Science Plan.*

Quantum Spatial Inc. (QSI). (2016). *Platte River, Nebraska – Fall 2016: Topobathymetric LiDAR Technical Data Report.*

Quantum Spatial Inc. (QSI). (2017). *Platte River, Nebraska – Fall 2017: Topobathymetric LiDAR Technical Data Report.*

Quantum Spatial Inc. (QSI). (2018). *Platte River, Nebraska – Fall 2018, Nebraska: Topobathymetric LiDAR Technical Data Report.*

Quantum Spatial Inc. (QSI). (2019). *Platte River Fall 2019, Nebraska: Topobathymetric LiDAR Technical Data Report.*

Quantum Spatial Inc. (QSI). (2020). *Platte River Fall 2020, Nebraska: Topobathymetric LiDAR Technical Data Report.*

Quantum Spatial Inc. (QSI). (2020). *RE: Platte River Recovery Implementation Program, Update of baseline data for 2018 and 2017.*

Quantum Spatial Inc. (QSI). (2021). *Platte River Fall 2021, Nebraska: Topobathymetric LiDAR Technical Data Report.*

Szafarczyk, A., & Toś, C. (2022). The use of green laser in LiDAR bathymetry: State of the art and recent advancements. Sensors, 23(1), 292.

The Flatwater Group, in association with Tetra Tech and HDR (2010). Sediment Augmentation Experiment Alternatives Screening Study Summary Report, prepared for the Platte River Recovery Implementation Program, 266 p.

Tetra Tech. (2017). Final Data Analysis Report Channel Geomorphology and In-Channel Vegetation, prepared for the Platte River Recovery Implementation Program, 305 p.

Wheaton, J., Brasington, J., Darby, S., & Sear, D. (2010). Accounting for uncertainty in DEMs from repeat topographic surveys: improved sediment budgets. *Earth Surface Processes and Landforms, 35*, 136-156.

**CHAPTER 1 Sediment augmentation: History and Context**

## *1.1    Abstract*

Prior to implementation of a full-scale sediment augmentation experiment in 2017, the Platte River Recovery Implementation Program (PRRIP) and others have undertaken multiple monitoring, modeling and small-scale augmentation experiments to describe, quantify, and predict channel response to clearwater releases from the Johnson No. 2 Hydropower Return (J2 Return) near Lexington, NE. Since construction in the 1940s, the J2 Return has released sediment-free water into the south channel of the Platte River resulting in significant channel incision and planform change. This chapter summarizes findings from five decades of investigations leading up to full-scale augmentation. It also describes implementation of full-scale augmentation operations, with a focus on the location and volume of sediment augmentation.

## *1.2    Introduction*

Water infrastructure often leads to longitudinal discontinuity of water and sediment in rivers (Wohl et al., 2015; Schmidt and Wilcock, 2008; Poff et al.; 1997, Kondolf 1997; Ligon et al., 1995). In response, rivers adjust toward new states of equilibrium after infrastructure-related disturbances to water and sediment supply (Howard, 1982). Adjustments to river planform, slope, width, and longitudinal profile occur abruptly at the sites of dams (Ward and Stanford, 1995), or in the case of our study area, the J2 Return. The J2 Return releases clear, sediment-free water into the south channel of the Platte River near Lexington, NE. River adjustments to lack of sediment supply extend and dissipate downstream for significant distances and tend to incise the upper portion of channel toward a convex profile (Smith and Mohrig, 2017; Graf, 2006; Williams, 1978). Over time, effects of the disturbance can propagate for large distances downstream (Smith and Mohrig, 2017). As a management strategy to balance the needs for human water use with river ecosystem function, sediment augmentation can help mitigate sediment imbalance that causes channel incision (Mortl and Cesare, 2021).

The Platte River Recovery Implementation Program (Program or PRRIP) is responsible for implementing certain aspects of the recovery plans for three threatened and endangered species including the highly endangered whooping crane (*Grus americana*). More specifically, the Program has a management objective to improve survival of whooping cranes during migration through increased use of the Associated Habitat Reach (AHR) of the Platte River in central Nebraska (PRRIP 2006a). This ninety-mile reach extends from Lexington, NE downstream to Chapman, NE and includes the Platte River channel and off-channel habitats within three and a half miles of the river (Figure 1.1).

**Figure 1.1.** Associated Habitat Reach (AHR) of the central Platte River in Nebraska extending from Lexington downstream to Chapman.

The Program has invested fourteen years implementing an adaptive management program to test strategies for increasing suitability of whooping crane habitat in the AHR. One area of focus has been the impact of a sediment deficit at the upstream end of the AHR on channel morphology. More specifically, channel incision and narrowing has occurred downstream of a clearwater hydropower return and Program stakeholders are concerned those impacts could progress downstream through time, impeding our ability to maintain the wide, unvegetated, braided river morphology that is suitable for whooping crane roosting. Concerns about incision emerged in the 1980s, approximately 40 years after the Johnson No. 2 Hydropower Return (J2 Return) began operations. Several investigations were conducted in the late 1990s and early 2000s to evaluate the magnitude of the deficit and develop the concept of sediment augmentation into a management action to be implemented during the First Increment of the Program (2007-2019).

During the First Increment of the Program, Adaptive Management Plan (AMP; PRRIP 2007) activities included additional monitoring, modeling, and evaluation of the feasibility and performance of various strategies to augment sediment. By 2016, Program decision makers advised by the Independent Science Advisory Committee (ISAC) concluded the best way to evaluate the performance of sediment augmentation was to initiate a full-scale sediment augmentation management experiment designed to offset the total sediment deficit downstream of the J2 Return. Implementation began in 2017 and annual augmentation continued through 2022.[6] Subsequent chapters of this document present analyses and interpretation of data collected prior to and during the sediment augmentation experiment. The objective of this introductory chapter is to provide an overview of the body of research and monitoring that led to implementation of full-scale augmentation. This begins with work leading up to Program initiation in 2007, including efforts to quantify the magnitude of the sediment deficit in the AHR

---

[6] This analysis focuses on the period of 2017-2021 due to the lag time in remote sensing data processing.

and devise a sediment augmentation concept to be implemented under the AMP. We then transition to a description of adaptive management implementation efforts during the First Increment leading up to the full-scale augmentation experiment. The chapter concludes with an overview of full-scale augmentation including the location, timing, and magnitude of augmentation operations.

## 1.3    Pre-Program monitoring, modeling, and research 1978-2006

The first known discussion of sediment as a potential driver in morphologic change in the central Platte River occurs in Williams (1978). In that Geological Survey (USGS) Circular (781), Williams describes changes in width, braiding, sinuosity and bed aggradation/degradation in the North Platte and Platte Rivers in Nebraska over historical timeframes. Much of the publication focuses on large reductions in channel width that occurred in the decades following the initiation of reservoir construction in the North Platte River basin in the early 1900s. Williams focuses much of the publication on correlations between declining discharge and width metrics. However, he also included a specific gage analysis, noting that observed fluctuations in bed elevations at stream gage locations reflected complex regulation of both water and sediment delivery to the river.

In 1981, the USGS published a series of open-file reports describing sediment transport, channel morphology and other physical characteristics of various segments of the Platte River. Kircher (1981a) collected bedload and suspended sediment samples from segments of the South Platte, North Platte, and central Platte Rivers and used them to develop estimates of sediment transport and effective discharge for each segment (Kircher 1981b). Karlinger et al. (1981) explored the relationship between discharge, sediment, and channel width in the Central Platte, providing theoretical predictions of channel width adjustment to changes in sediment and flow. Finally, Crowley (1981) produced a detailed investigation of bedforms downstream of Grand Island, NE, characterizing the geometry and movement of macroforms as well as their relationship to channel narrowing.

In the late 1980s, O'Brien & Currier (1987) produced a report that explored changes in the morphology and vegetation in the Big Bend Reach of the Central Platte River.[7] The authors attempted to quantify magnitude of incision through comparison of historical quadrangle maps, concluding the channel had degraded three to ten feet from the late 1890s to the 1960s. Finally, the authors referenced several published works on empirical threshold relationships in alluvial channels (regime theory) and expressed concern that the reductions in flow and sediment supply in the Big Bend Reach could cause the channel to shift from a braided to meandering morphology. The authors concluded by recommending a complete analysis of sediment supply and transport capacity of the Central Platte.

In the early 1990s, basin stakeholders began the negotiations that ultimately led to the authorization of the Program in 2007. As part of those negotiations, a number of different investigations were initiated by the Platte River Environmental Impact Statement (EIS) Office and were published in the early 2000s. The first was a comprehensive evaluation of the physical history of the Central Platte River conducted by Simons and Associates (2000) which focused on

---

[7] The Big Bend Reach roughly encompasses the 90-mile Associated Habitat Reach of the central Platte from Lexington, NE to Chapman, NE.

drivers of vegetation expansion into the channel in the 20th century. The authors noted that the bed of the Central Platte has coarsened over time and limited bed degradation has been observed. They ultimately concluded that sediment transport played a secondary role in channel narrowing, and that the channel bed was generally in a condition of dynamic equilibrium. Despite relegating sediment supply to a secondary factor in channel narrowing, the authors did (for the first time) introduce the concept of augmenting sediment to reduce bed degradation where it occurs. They recommended further analysis of potential relationships between augmentation, sediment transport, and riparian vegetation with a combined sediment transport and vegetation model developed by the United States Bureau of Reclamation (USBR).

Randle and Samad (2003) produced the first detailed evaluation of historical changes in sediment transport, reporting trends for the period of 1895-1999. Near the end of that report, the authors note that the main source of sediment between the J2 Return Channel and Overton was the bed and banks of the channel. They also noted that the thalweg was approximately 20 feet below the top of the right bank and had eroded six feet vertically between 1989 and 2002. These incision estimates were developed as part of a separate aggradation/degradation analysis by EIS Team published in 2006 (Holburn et. al. 2006). That work analyzed repeat channel cross section surveys to identify spatial and temporal trends in channel aggradation and degradation. The authors found a clear trend of degradation in a 25-mile reach from the J2 Return to Odessa. The most pronounced degradation occurred at the upstream end and gradually diminished until the difference in average annual change in cross-sectional area declined below 10 ft$^2$ which was assessed to be stable.

The major publication presenting the EIS Team's analysis and proposed restoration strategy was published in 2004. As with prior comprehensive assessments, Platte River Channel: History and Restoration (Murphy et al. 2004) discusses sediment along with other potential drivers of planform change. The authors discuss the theoretical progression of incision below the J2 Return, describing the process of winnowing of fine material from the riverbed, causing bed material in the reach that is incising to become significantly coarser through time. This process gradually results in armoring that limits the depth of channel incision at that location (assuming enough coarse material is available). Critically, the authors assessed that the process of incision would progress downstream until it was arrested by a combination of armoring and a decrease in local river slope.

Murphy et al. (2004) cited Graf (1998) and de Vries et.al. (1973) to predict how quickly channel incision would expand both vertically and downstream from the J2 Return under the theoretical assumption of steady flow and a channel bed of uniform sand. The figure of predicted incision through time is reproduced below as Figure 1.2. The figure predicts the progression of incision through the AHR and the authors note it could take centuries for the channel to reach equilibrium.
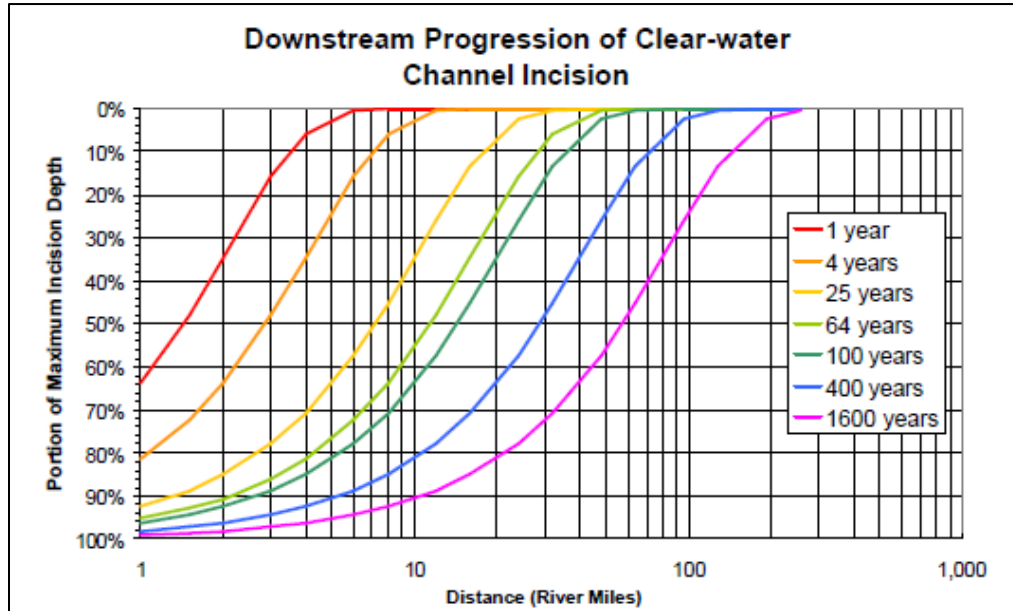
**Figure 1.2**. Reproduction of Figure 4.16 from Murphy et al (2004). Figure shows estimated progression of incision over time below the J2 Return.

As with prior EIS Team reports, the authors concluded that increased sediment supply is necessary to offset the deficit due to clearwater returns and to bring sediment supply into balance with cumulative sediment transport capacity of the river. The proposed solution was sand augmentation via mechanical pushing of island and bank material into the channel. This would have the effect of 1) increasing sediment supply and reducing median grain size of the riverbed, increasing bed mobility, and 2) widening the channel in augmentation reaches. Murphy et al. provided the hypothetical example of mechanically pushing 500 tons per day, or 100,000[8] yd$^3$ per year, requiring 20 acres of islands be leveled over the course of a year.

The EIS Team's final estimates of sediment deficit in the AHR and proposed volume of sediment augmentation were developed using an integrated hydraulic, sediment transport, and vegetation model called the Platte River Sediment Transport and Riparian Vegetation Model or SED-VEG model (Murphy et al. 2006). Model results indicated 85,000 to 175,000 tons (57,000 to 120,000 yd$^3$) of sediment were eroded annually from the bed and banks of J2 Return Channel, another 50,000 to 100,000 tons (35,000 to 70,000 yd$^3$) eroded annually from the bed and banks between the confluence with the North Channel and the Overton Bridge, and 180,000 tons (120,000 yd$^3$) eroded annually from the bed and banks of the river between Overton and Wood River 56 miles downstream.

Within the Program's AMP is the culmination of the EIS Team research described above. The AMP prescribes sediment augmentation as a management action to be tested under an adaptive management framework during the First Increment of the Program (2007-2019). Priority hypothesis Sediment 1 (reproduced as Figure 1.3) provides an overview of the magnitude and

---

[8] Murphy et al. used a different volume to mass conversion factor.

hypothesized benefits of sediment augmentation. Specifically, annual mechanical augmentation of 185,000 tons (125,000 yd$^3$) of sediment near Overton under existing flow regime and 225,000 tons (150,000 yd$^3$) of sediment under the proposed flow regime[9] achieves sediment balance, eliminating the sediment deficit due to clearwater hydropower returns. Subsequent hypotheses (Sediment 2-4) predict increases in braiding and channel width due to augmentation.
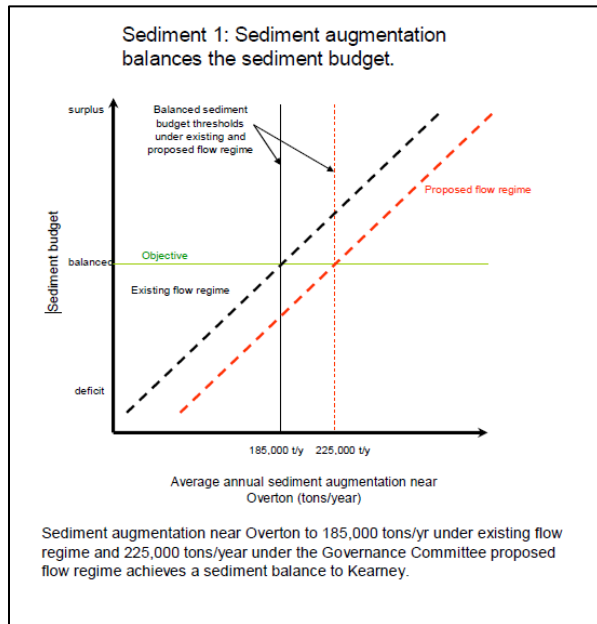


**Figure 1.3** Priority hypothesis Sediment 1 reproduced from the Program Adaptive Management Plan (PRRIP 2006).

### *1.4    Sediment augmentation research during the First Increment (2007-2016)*

Following Program authorization in 2007, a team of consultants was retained to evaluate the feasibility of implementing sediment augmentation (The Flatwater Group 2010). The scope of work included development of an updated sediment transport model for the AHR[10] and evaluation of alternative methods and locations to implement the experiment. A baseline mobile bed sediment transport model was developed using the U.S. Army Corps of Engineers HEC-RAS program (HEC-RAS, 2008). It was then modified to represent and evaluate a range of sediment augmentation alternatives. Figure 1.4 is a recreation of baseline (no augmentation) sediment transport modeling results from the study. The modeled annual sediment deficit for the 12.5-year simulation period was 152,000 tons (100,000 yd$^3$).

---

[9] Proposed flow regime refers to implementation of the Program's Water Action Plan designed to reduce deficits to United States Fish and Wildlife Service (USFWS) target flows by 130,000 – 150,000 acre-feet annually. Implementation of the Plan began in 2007. As of 2024, water projects are credited with reducing deficits by approximately 110,000 acre-feet annually. Water has been used to increase flow during whooping crane migration, during the summer to enhance baseflows, and to conduct vegetation scour/management experiments.

[10] The SED-VEG model was abandoned after Program authorization due to concerns about accuracy of model results and the custom/proprietary nature of the code which made it difficult to use.

**Table 4-1 Total Sediment Deficit and Surplus Volumes in Each Reach**

| Subreach | Upstream Limit | Downstream Limit | Specific Location | Aggradational/ Degradational | Deficit (-)/ Surplus (+) (t/y) |
|---|---|---|---|---|---|
| 1 | Lexington Bridge | Overton Bridge | North Channel | Slightly to moderately aggradational | +66,400 |
| 2 | J-2 Return | Overton Bridge | South Channel | Degradational | -96,700 |
| 3 | Overton Bridge | Elm Creek Bridge | Cottonwood Ranch Reach | Degradational | -108,500 |
| 4 | Elm Creek Bridge | Kearney Canal diversion structure | Immediately Upstream of Kearney Diversion | Slightly to moderately aggradational | +32,700 |
| 5 | Kearney Canal diversion structure | Odessa Bridge | Immediately Downstream of Kearney Diversion | Degradational | -46,100 |
| **Total Reach** | | | | | **-152,200[1]** |

Note:
[1] For the purpose of the Study, the sediment deficit for the entire Project reach has been rounded to 152,000 t/y.

**Figure 1.4** Reproduction of Table 4-1 from The Flatwater Group (2010) providing baseline HEC-RAS sediment transport model results for the reach from Lexington, NE downstream to Odessa, NE.

Augmentation material gradations, sediment sources, methods of introducing sediment into the channel and augmentation locations were evaluated in the feasibility study. The report recommended two augmentation alternatives be implemented as part of a pilot-scale management experiment. The first alternative was similar to augmentation as proposed in the AMP. Bulldozers would push sediment from banks and islands (median grain size of 1.2 mm) into the channel, spreading the material across the width of channel to be mobilized by flow. This method had the benefit of widening the channel while augmenting sediment. The second alternative involved hydraulic mining of sediment from an existing gravel mine adjacent to the channel and screening it to produce a median grain size of 0.5mm. The screened sand and water slurry would then be pumped/piped directly into the channel. This alternative was similar to typical gravel mining operations with the expectation that unusable fines are discharged back into the mine.

Both augmentation alternatives were designed, permitted, and implemented in 2012–2013. Analysis of the alternatives concluded a year later (The Flatwater Group 2014). During the experiment, approximately 82,000 tons (55,000 yd$^3$) of hydraulically mined sand (D50 0.5 mm) were pumped into the lower end of the J2 Return Channel upstream of the confluence with the North Channel. Over 100,000 tons (70,000 yd$^3$) of overbank material (D50 of 1.2 mm) were bulldozed into the main channel downstream of the Overton Bridge at the upper end of the Cottonwood Ranch Habitat Complex. Monitoring was conducted during the experiment and used to assess the feasibility of augmentation methods as well as update sediment transport modeling and augmentation volume targets.

Implementation of mining/pumping and bulldozer augmentation revealed pros and cons for each augmentation method. Sand pumping maximized the volume of source material per surface area disturbed (material can be hydraulically mined to a depth of at least 40 ft) and allowed control of the gradation of the augmentation material. On the other hand, sand pumping had a much higher unit cost, low spatial flexibility due to the point source nature of the method, and it was difficult to match the augmentation rate to the channel transport capacity during low flows. Augmentation by bulldozer had a much lower unit cost and provided more flexibility in both location and placement of sediment, maximizing mobilization. Cons included low material volume per surface area disturbed and inability to control the sediment gradation.

The project team concluded that an annual average of 60,000 tons (40,000 yd$^3$) of annual augmentation (D50 of 1.2 mm) could be sustained in the lower portion of the J2 Return Channel without excess sediment accumulation. However, actual transport would range from 11,000 tons (7,000 yd$^3$) in dry years to 135,000 tons (90,000 yd$^3$) in wet years and rates would increase or decrease depending on material gradation. The volume of augmentation that could be sustained without excess sediment accumulation was lower than the model-derived annual sediment deficit between Overton and Elm Creek, which averaged 109,000 tons (73,000 yd$^3$) and ranged from 25,000 tons to 220,000 tons (17,000 to 150,000 yd$^3$).

The feasibility study team also modeled over-augmentation in the J2 Return Channel. Pumping 150,000 tons (100,000 yd$^3$) of sediment (D50 ~ 0.5 mm) annually into the J2 Return Channel was estimated to reduce the downstream deficit to approximately 43,000 tons (30,000 yd$^3$) on average. Using larger material from riverbanks (D50 ~ 1.2 mm), the deficit was reduced to 73,000 tons (50,000 yd$^3$) on average.

The Program paused sediment augmentation following completion of the pilot-scale management experiment while two other sediment-related efforts were concluded. The first was an update of sediment transport modeling to estimate the sediment deficit caused specifically by J2 Return flows (Tetra Tech 2015). This was accomplished by comparing sediment transport model results with and without J2 Return flows. The model indicated a relatively strong correlation between the volume of J2 releases and the sediment deficit downstream of the Overton Bridge. The reach was generally near balance during years when J2 releases were less than about 300,000 acre-feet, and the deficit increased to approximately 100,000 tons (70,000 yd$^3$) in years when J2 releases were in the range of 1,000,000 acre-feet. Eliminating J2 releases from the model reduced the average annual deficit downstream of Overton from 92,000 tons to 61,000 tons (60,000 to 40,000 yd$^3$), a reduction of 31,000 tons (20,000 yd$^3$) per year. Most of the remaining incision in the model occurred in the Cottonwood Ranch reach.

The second effort was the conclusion of an eight-year field-based monitoring program to assess system-scale changes in geomorphology and vegetation in the AHR (Tetra Tech 2017). Monitoring included repeat transect surveys of the channel, bed and bank material sampling, sediment transport measurements, and vegetation monitoring. Analyses of that data led to the conclusion that the annual sediment deficit in the Overton to Kearney reach was most likely in the range of 50,000 tons to 75,000 tons (30,000 to 50,000 yd$^3$). However, estimates of the deficit from cross section surveys and sediment transport estimates were highly variable with large confidence intervals, leading to low confidence in conclusions.

The ISAC provided feedback in 2014 and 2015 (ISAC 2014 and ISAC 2015) recommending that the Program implement large-scale augmentation in the reach immediately downstream of the J2 Return and intensively monitor channel response using multiple lines of evidence. The committee specifically mentioned application of geomorphic change detection techniques with Topo-bathymetric Light Detection and Ranging (LiDAR) data, analysis of trends in cross-sections and other geomorphic metrics through time, evaluation of the magnitude of change in the longitudinal profile, and specific gage analyses.

The Program's policy-making Governance Committee (GC) concurred with this advice and authorized the Executive Directors Office to design and implement a full-scale sediment augmentation experiment. That experiment commenced in 2017 with partial scale augmentation in that year[11] and full-scale augmentation in 2018-2021. The next section of Chapter 1 provides an overview of sediment augmentation implementation over the course of the management experiment.

---

[11] More than the full-scale augmentation volume was moved during 2017, but the majority of that material was used to eliminate a meander bend and restore farmland that had been eroded. A berm was constructed to prevent the channel from continuing to migrate south towards a road and farmstead.

### *1.5    Full-scale sediment augmentation management experiment (2017-2021)*

1.5.1    Sediment augmentation area

The Sediment augmentation sites are located in the J2 Return Channel, beginning approximately 0.75 miles downstream of the J2 Return and extending one mile east. This one-mile section includes three augmentation sites (Figure 1.5) that Central Nebraska Public Power and Irrigation District (CNPPID) has designated as available source sites for augmentation. These sites are bounded by the black, red, and yellow polygons in Figure 1.5. Since 2017, only two have been used for source material. Pending evaluation of results, augmentation may continue in a downstream direction with one more major grading site targeted in this upstream reach (Site 3 in Figure 1.5) before moving downstream to the Plum Creek Complex, approximately 4 miles further downstream.
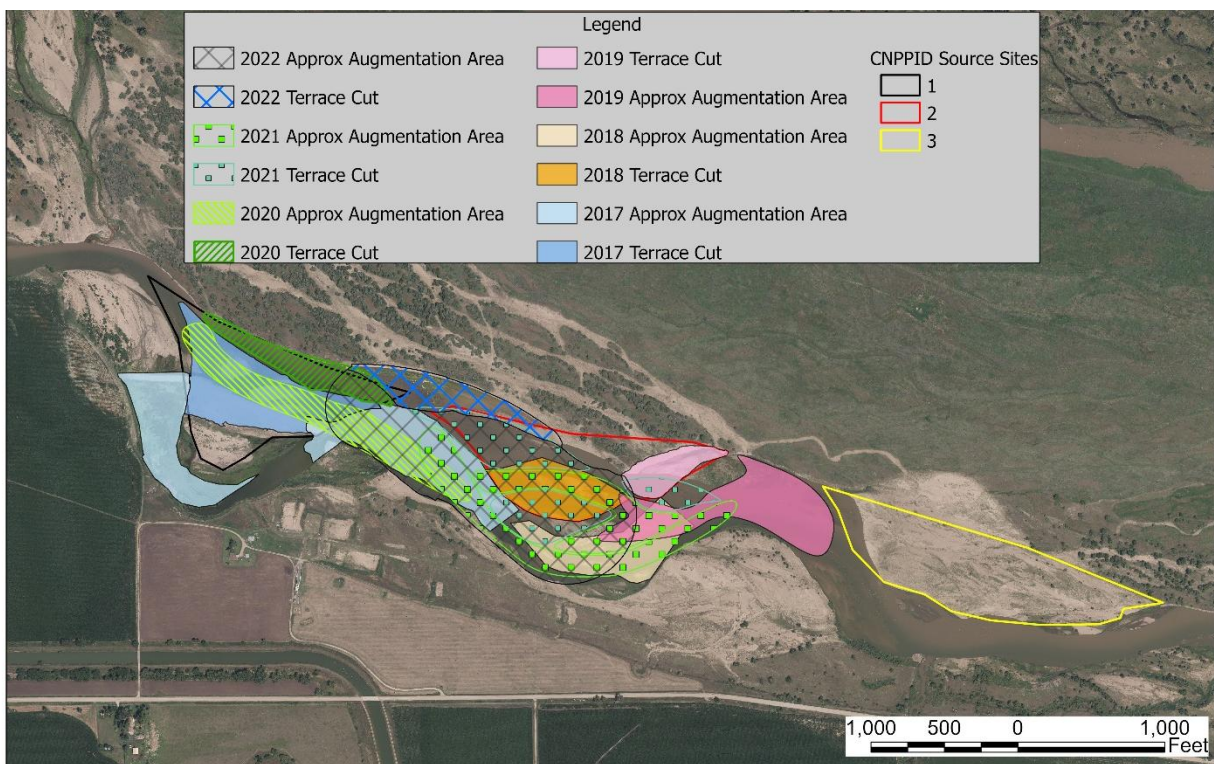


**Figure 1.5** 2017-2022 Augmentation Project Boundaries.

1.5.2    Timing

Sediment augmentation is implemented in the late summer/early fall each year to coincide with conducive flows out of the J2 Return. Summer low flows allow sediment to be staged, whereas long, high flow releases beginning in mid-September transport material away from the site. Due to CNPPID's hydropower production schedule, these high flow releases are interrupted by intermittent low flows. During these low flows, contractors can operate heavy equipment such as bulldozers and scrapers within the channel and stage more sediment for transport.

### 1.5.3   Design considerations

Alluvial material augmented to the riverbed is intended for transport downstream to mitigate sediment deficits. A full-scale sediment augmentation target was set between 60,000 to 80,000 tons (40,000–55,000 yd$^3$) per year over a design-life of 18 years of augmentation beginning along the high banks below the J2 Return (Figure 1.5).

To begin the design process, the existing stage range elevations within the chosen area must be calculated. These elevations are calculated by running hydraulic models at peak and low flows (1650 cfs and 300 cfs, respectively) typical for CNPPID hydrocycling during late summer/early fall. These values are used to guide excavation (cut) and augmentation area elevation targets.

To encourage natural erosion of high terraces on the north bank, an elevation near the average of the stage range is chosen as the final grade for the excavation area (terrace cut areas in Figure 1.5 from which the sediment is excavated). This allows occasional inundation during high flow events, during which some bank material will be removed. To prevent nominal stage increase within the reach, the augmentation area of the project is designed at an elevation near or below the lowest end of the stage range.

Given those elevation targets, the design volume of the project must be determined. System-scale monitoring data collected from 2009 to 2014 demonstrated that trends in aggradation-degradation are highly dependent on hydrology (Tetra Tech 2014). Knowing this, it is important to consider the hydrologic condition for the given design year. If it appears that there is a dry trend, CNPPID may operate in a conservation mode, releasing less flow into the J2 Return Channel. Under these conditions, design volume tends to be lower to match expected lower flows for sediment distribution. If it is a wet year, flow releases may be higher, allowing for the distribution of more material pushed into the channel.

Knowing elevation and volume targets, the last piece of the design equation is choosing an excavation area. Loading LiDAR data from the previous year into AutoCAD Civil3D (Autodesk, San Francisco, CA) provides an existing grade against which the design surfaces can be compared. By creating an approximate design surface set to the final grade elevation, volume differencing calculations can be run. Due to the variability of elevation along the existing grade surface, an iterative approach is necessary to adjust the excavation area until the "Cut" volume is approximately equal to the target value.

Given the possibility that flows may be too low for sediment transport during construction, it is important that there is enough area within the channel for the augmented material to be placed at the lowest stage elevation. An approximate design surface is created within the channel at the lowest stage elevation. This surface is compared to the existing grade and its area adjusted until "Fill" volume is approximately equal to "Cut" volume.

### 1.5.4   Sediment augmentation summaries

The design approach for 2017 and 2018 targeted 60,000 tons (40,000 yd$^3$) of immediate augmentation (Table 1.1), while encouraging the channel to continue to erode material out of the high terrace (north bank) on Jeffrey Island (PRRIP 2018). In fall of 2017, the upstream-most meander in the channel was cut off by excavating a pilot channel through an abandoned terrace and constructing a berm to shift the river to the north and mobilize sediment.  23,000 yd$^3$ were

augmented to the main channel and 13,500 yd$^3$ of sediment were placed into the abandoned meander.

In fall of 2018, efforts moved downstream with the same target of 40,000 yd$^3$ and a more passive approach. By cutting down the next downstream bar, we were able to keep the sediment source on the adjacent high terraces on the left bank and encourage some deposition from upstream sources. The passive approach from 2018 was maintained in 2019, again with a target of 40,000 yd$^3$. This excavation was completed just downstream of the 2018 site. Construction can be seen in Figure 1.6. The 2020 design moved upstream, overlapping some of the original 2017 site. Due to Normal-to-Wet hydrologic conditions and high terraces on the site, the augmentation target was higher at 50,000 yd$^3$. The fall 2021 design also had a higher volume at 53,000 yd$^3$. This was due to the spread-out nature of the design, with 3 separate excavation sites being augmented into the channel. Augmentation in 2022 was designed in the same area as 2017 and 2020 since the high terraces of the area provided ample material for augmentation. With flows lower in 2022, the design volume was reduced to 45,000 yd$^3$.

**Table 1.1** Sediment augmentation as-built volumes 2017-2022.

| Year | Augmented (tons) | Sediment Augmentation Volume (yd$^3$) | Volume Leaving Sed Aug Area (yd$^3$)* |
|------|------------------|---------------------------------------|----------------------------------------|
| 2017 | 34,500 | 23,000 | 34,500 |
| 2018 | 64,305 | 42,900 | 73,100 |
| 2019 | 63,500 | 42,300 | 116,500 |
| 2020 | 86,475 | 57,700 | 42,200 |
| 2021 | 76,982 | 51,300 | 60,600 |
| 2022 | 65,789 | 43,900 | |

*Volume change in augmentation area measured by differencing LiDAR elevations

**Figure 1.6** Construction of 2019 Sediment Augmentation Project (42,300 yd$^3$ ).

### *1.6    First increment extension – Big Question #3*
In 2015, Program stakeholders concluded that it was not possible to meet all Program Milestones prior to the end of the First Increment in 2019. This led to a negotiated 13-year extension of the Program referred to as First Increment Extension or just Extension. The first science priority in the Extension was an overhaul of the AMP to reflect current learning priorities, called the First Increment Extension Science Plan (PRRIP 2022). Extension Big Question #3 (Figure 1.7) and related management hypotheses focus on the sediment deficit below the J2 Return, progression of impacts due to the deficit, and potential consequences for whooping crane habitat downstream of Overton. The following chapters of this data synthesis present multiple lines of evidence to address this Big Question. Chapter 2 is a retrospective analysis of the magnitude and progression of incision through time, Chapter 3 evaluates longitudinal response to sediment augmentation, and Chapter 4 expands that evaluation into three-dimensions, exploring both vertical and lateral channel evolution in the periods before and after initiation of the full-scale augmentation management experiment.

> **Extension Big Question #3: Is sediment augmentation necessary to create and/or maintain suitable whooping crane habitat?**
>
> *Channels with ≥ 650 ft maximum width unobstructed by dense vegetation (MUCW) are highly suitable for whooping crane roosting.*

**Management Hypothesis: Sediment augmentation is necessary to halt narrowing and incision in the south channel downstream of the J-2 Return.**

**X-Y Graph**
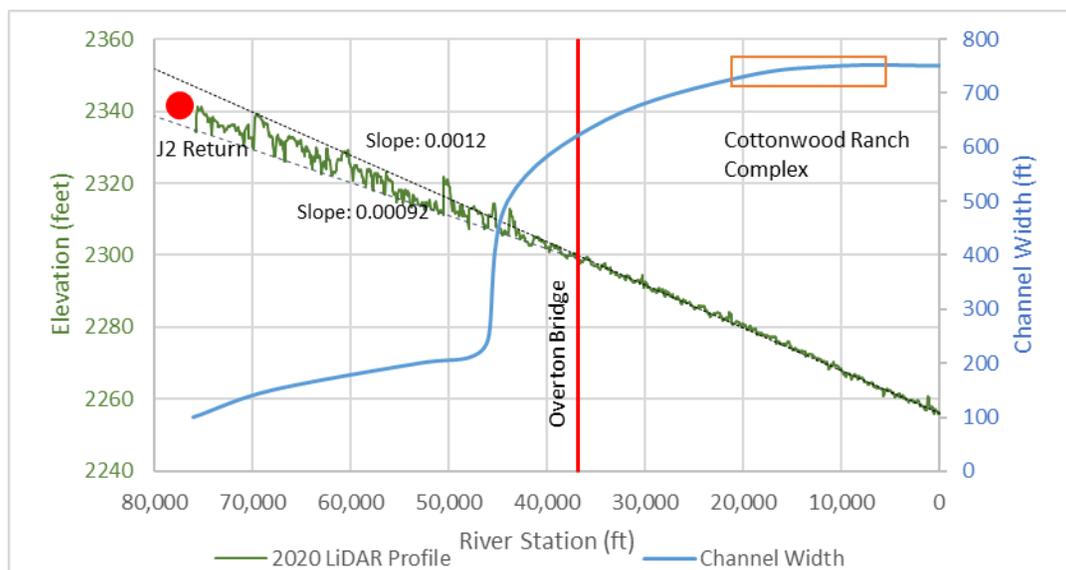


Full scale sediment augmentation (60,000–80,000 tons annually in the south channel below J2 Return) is necessary to offset the sediment deficit and halt narrowing and incision that has caused the upper portion of the south channel to transition to a narrow meandering planform, which is much less suitable for WC roosting. If incision is not halted, the affected reach will continue to expand downstream past the Overton Bridge, reducing habitat suitability at the Cottonwood Ranch complex.

**Alternative Hypotheses:**

- More or less sediment must be augmented to offset the south channel deficit.
- Augmentation at alternative locations will halt narrowing and incision.
- Full scale augmentation is not feasible over the long term – not enough supply.
- Incision and narrowing progresses downstream so slowly that augmentation is not necessary.
- Mechanical channel widening will halt narrowing and incision at habitat complexes.

**Figure 1.7** Extension Big Question #3. South channel refers to the J2 Return Channel.

## References

Crowley, K.D. (1981). Large-scale bedforms in the Platte River downstream from Grand Island, Nebraska; structure, process, and relationship to channel narrowing (No. 81-1059). US Geological Survey,.

de Vries, M. (1973). "River-bed Variations–- Aggradation and Degradation," Delft Hydraulic Laboratory Publication No. 107, Delft, Netherlands.

Graf, W.L., (2006). Downstream hydrologic and geomorphic effects of large dams on American rivers. Geomorphology, 79(3-4), pp.336-360.

Graf, W. (1998). Fluvial Hydraulics, Flow and Transport Processes in Channels of Simple Geometry, John Wiley & Sons, New York, New York, 681 pp.

HEC-RAS. (2008). Hydraulic Reference Manual. U.S. Army Corps of Engineers, Hydrologic Engineering Center.

Holburn, E.R., Fotherby, L.M, Randle, and D.E. Carlson. (2006). Trends of Aggradation and Degradation along the Central Platte River: 1985 to 2005. United States Bureau of Reclamation.

Howard, A.D., (1982). Equilibrium and time scales in geomorphology: Application to sand-bed alluvial streams. Earth Surface Processes and Landforms, 7(4), pp.303-325.

ISAC. (2014). Responses to Questions Posed by the Platte River Recovery Implementation Program (PRRIP) in October 2014, prepared for the Platte River Recovery Implementation Program, 18 p.

ISAC. (2015). Responses to Questions Posed by the Platte River Recovery Implementation Program (PRRIP) in July 2015, prepared for the Platte River Recovery Implementation Program, 13 p.

Karlinger, M.R., Mengis, R.C., Kircher, J.E. and Eschner, T. (1981). Application of theoretical equations to estimate the discharge needed to maintain channel width in a reach of the Platte River near Lexington, Nebraska. US Geol. Surv. Open File Rep, pp.81-697.

Kircher, J.E. (1981a). Sediment analyses for selected sites on the South Platte River in Colorado and Nebraska, and the North Platte and Platte Rivers in Nebraska; Suspended sediment, bedload, and bed material (No. 81-207).

Kircher, J.E. (1981b). Sediment transport and effective discharge of the North Platte, South Platte, and Platte Rivers in Nebraska (No. 81-53). US Geological Survey.

Kondolf, G. M. (1997). Hungry water: Effects of dams and gravel mining on river channels. Environmental Management 21 (4): 533–551. https://doi.org/10 .1007/s002679900048.

Ligon, F.K., Dietrich, W.E. and Trush, W.J., (1995). Downstream ecological effects of dams. BioScience, 45(3), pp.183-192.

Mörtl, C. and De Cesare, G., (2021). Sediment Augmentation for River Rehabilitation and Management—A Review. Land, 10(12), p.1309.

Murphy, P.J., T.J. Randle, L.M. Fotherby, and J.A. Daraio. (2004)."Platte River channel: history and restoration". Bureau of Reclamation, Technical Service Center, Sedimentation and River Hydraulics Group, Denver, Colorado.

Murphy, P.J., T.J. Randle, L.M. Fotherby, and R.K. Simons. (2006). Platte River sediment transport and vegetation model. Bureau of Reclamation, Technical Service Center. Denver, Colorado.

O'Brien, J.S. and P.J. Currier. (1987). Channel morphology, channel maintenance, and riparian vegetation changes in the big bend reach of the Platte River in Nebraska. Unpublished report.

Platte River Recovery Implementation Program (PRRIP). (2006). Final Platte River Recovery Implementation Program Adaptive Management Plan.  U.S. Department of the Interior, State of Wyoming, State of Nebraska, State of Colorado.

Platte River Recovery Implementation Program (PRRIP). (2018). Sediment Augmentation Monitoring Brief.

Platte River Recovery Implementation Program (PRRIP). (2022). First Increment Extension Science Plan.

Poff, N. LeRoy, J. David Allan, Mark B. Bain, James R. Karr, Karen L. Prestegaard, Brian D. Richter, Richard E. Sparks, and Julie C. Stromberg (1997). The natural flow regime. BioScience 47 (11): 769-784.

Randle, T.J., Samad, M.A. (2003). Platte River Flow and Sediment Transport Between North Platte and Grand Island, Nebraska (1895 – 1999).

North Platte and Grand Island, Nebraska (1895-1999). U.S. Dept. of Int., Bur. Of Reclamation report, Denver, CO. 60 pp. Avail. online at: http://www.usbr.gov/pmts/ sediment/projects/index.html.

Schmidt, J. C., & Wilcock, P. R. (2008). Metrics for assessing the downstream effects of dams. Water Resources Research, 44(4).

Smith, V.B. and Mohrig, D., (2017). Geomorphic signature of a dammed Sandy River: the lower Trinity River downstream of Livingston Dam in Texas, USA. Geomorphology, 297, pp.122-136.

Simons & Associates, Inc. and URS Greiner Woodward Clyde. (2000). Physical history of the Platte River in Nebraska: Focusing upon flow, sediment transport, geomorphology, and vegetation. Prepared for Bureau of Reclamation and Fish and Wildlife Service Platte River EIS Office, dated August 2000.

Tetra Tech. (2014). Final 2013 Platte River Data Analysis Report Channel Geomorphology and In Channel Vegetation. Prepared for the Platte River Recovery Implementation Program.

Tetra Tech. (2015). Draft Model Results, Platte River Sediment-transport Modeling, South Channel at Jeffrey Island, prepared for the Platte River Recovery Implementation Program, 19 p.

Tetra Tech. (2017). Final Data Analysis Report Channel Geomorphology and In-Channel Vegetation, prepared for the Platte River Recovery Implementation Program, 305 p.

The Flatwater Group, in association with Tetra Tech and HDR (2010). Sediment Augmentation Experiment Alternatives Screening Study Summary Report, prepared for the Platte River Recovery Implementation Program, 266 p.

The Flatwater Group, in association with Tetra Tech and HDR (2014). Sediment Augmentation Final Pilot Study Report, prepared for the Platte River Recovery Implementation Program, 123 p.

Ward, J.V. and Stanford, J.A., (1995). The serial discontinuity concept: extending the model to floodplain rivers. Regulated rivers: research & management, 10(2-4), pp.159-168.

Williams, Garnett P. (1978). The case of the shrinking channels: the North Platte and Platte Rivers in Nebraska. M.S. Thesis. University of Wyoming, Laramie. In U.S. Geological Survey Circular 781. 48 pp.

Wohl, E., Bledsoe, B. P., Jacobson, R. B., Poff, N. L., Rathburn, S. L., Walters, D. M., & Wilcox, A. C. (2015). The natural sediment regime in rivers: Broadening the foundation for ecosystem management. BioScience, 65(4), 358-371.

**CHAPTER 2   Evaluation of trends in incision prior to full-scale sediment augmentation**

## *2.1   Abstract*

The Platte River Recovery Implementation Program (PRRIP or Program) is concerned that incision and narrowing downstream of the J2 Return may continue to progress downstream, negatively impacting the suitability of roosting habitat for the highly endangered whooping crane (*Grus americana*). Evaluating historical patterns and rates of incision provides insight into the potential magnitude of future impacts in absence of long-term augmentation of sediment supply. We conducted retrospective analyses to evaluate spatial and temporal patterns of incision. This included comparing current channel topography to the historical channel elevation (relative elevation model), evaluation of incision trends at repeat transect survey locations, development of specific gage analyses at the Overton Bridge and Cottonwood Ranch mid-channel stream gages, and estimation of changes in channel sinuosity through time using aerial imagery. These analyses indicated a wave of vertical incision propagated down through the study area after J2 Return began operations in the early 1940s. In the early 2000s, the primary mechanism of channel degradation shifted from incision to lateral migration, with the highest intensity of migration occurring in upper half of the J2 Return Channel.

## *2.2   Introduction*

As discussed in Chapter 1 of this data synthesis, since the 1980s, stakeholders of the Platte River Recovery Implementation Program (PRRIP or Program) have been concerned about channel degradation due to clearwater hydropower returns near Lexington, NE. During the First Increment of the Program, the Governance Committee (GC) initiated monitoring, modeling, and research projects to explore the magnitude and extent of the problem. Those efforts resulted in three major conclusions:

1) There is a persistent sediment deficit downstream of the J2 Return that has resulted in incision and narrowing of the segment of channel that extends from the J2 Return to the Overton Bridge (J2 Return Channel).
2) Downstream of the Overton Bridge, there was no discernable degradational trend during the period of 2009-2016.
3) Over time, the degradation (incision and narrowing) observed in the J2 Return Channel could progress downstream beyond the Overton Bridge, decreasing the proportion of the central Platte River suitable as habitat for whooping crane roosting.

In response to these findings, the Program initiated a full-scale sediment augmentation experiment in 2017 to test the hypothesis that offsetting the sediment deficit downstream of the J2 Return is necessary to halt downstream progression of channel degradation (Extension Big Question 3). Implicit in this hypothesis is an unquantified level of risk relating to the rate that degradation is progressing downstream absent augmentation as well as the relationship between incision magnitude and degradation of habitat suitability. The objective of this chapter is to evaluate the magnitude and rate of channel degradation in the decades prior to augmentation and compare to stakeholder predictions. This is accomplished through four retrospective analyses that rely on historical aerial imagery, stream gaging data, repeat channel transect surveys, and remote sensing topographic data collected prior to implementation of full-scale augmentation.

2.2.1    Study area

The focus area for this study encompasses the western portion of the Program's Associated Habitat Reach (AHR) extending from Lexington, NE downstream to the Kearney Canal Diversion (KCD), located two miles downstream of Elm Creek, NE. Figure 2.1 provides an overview of the study area including channel segments, stream gage locations, and landmarks referenced in this chapter.
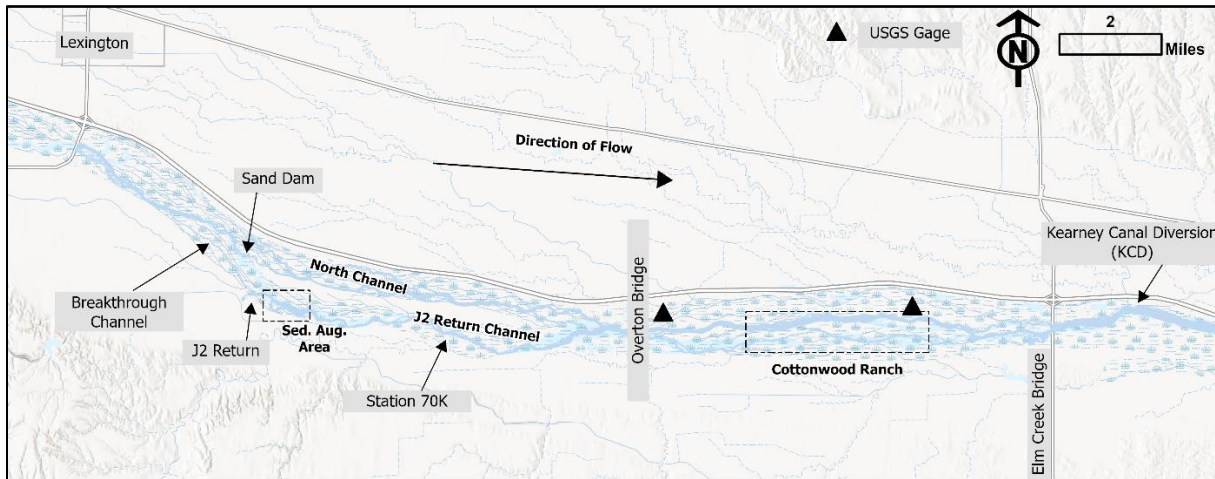


**Figure 2.1**. Map of the sediment augmentation study area including stream gage locations and landmarks of interest.

To provide consistent spatial referencing (stationing) for all longitudinal analyses, we delineated the approximate centerline of the floodplain from the KCD upstream to the Lexington bridge (Figure 2.2) and cut transects across the entire floodplain perpendicular to centerline at five-foot intervals.  Stationing starts at 0 at KCD and ends at station 113,780 at the Lexington bridge. Stationing for important landmarks is provided in Table 2.1.
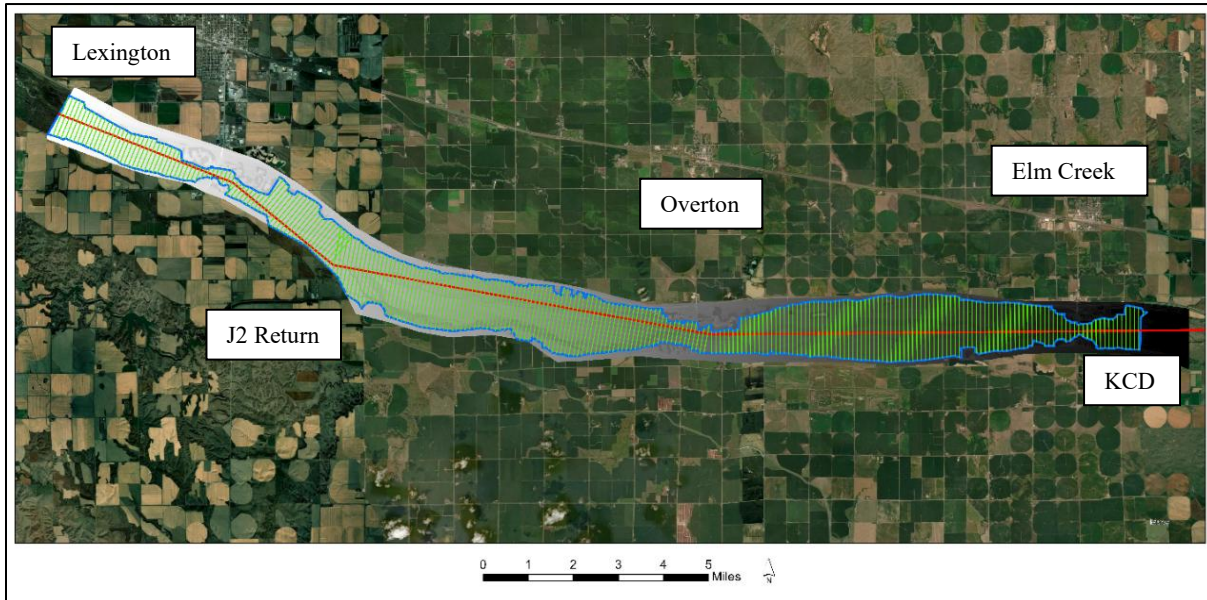
**Figure 2.2**. Floodplain centerline (red) and transects (green) through study area. Transects were generated perpendicular to centerline at five-foot intervals with example transects plotted at 500 ft spacing in this figure.

**Table 2.1.** Landmarks in the study area and associated stations.

| Landmark | Station (ft) |
|---|---|
| Lexington Bridge | 113,780 |
| Berm at upstream North/J2 Return Channel split | 101,890 |
| J2 Return (Sand Dam is roughly same stationing) | 91,955 |
| Upstream extent of sediment augmentation area | 89,360 |
| Downstream extent of sediment augmentation area | 84,000 |
| North Channel/J2 Return Channel confluence | 55,290 |
| Overton Bridge | 52,600 |
| Cottonwood Ranch, upstream extent | 39,925 |
| Cottonwood Ranch, mid channel stream gage | 25,120 |
| Cottonwood Ranch, downstream extent | 23,665 |
| Elm Creek Bridge | 8,395 |
| Kearney Canal Diversion (KCD) | 0 |

### 2.2.2   Overview of analyses

As stated in the introduction, the objective of this chapter is to explore historical incision and planform change downstream of the J2 Return prior to the initiation of full-scale sediment augmentation in the fall of 2017. The J2 Return began operations in the early 1940s but there was little focus on channel incision in this reach until the 1980s. Consequently, historical data is limited primarily to historical aerial photography, limited repeat cross section surveys collected in the late 1980s and early 2000s, and stream gaging records. In this chapter we utilized these

data in combination with contemporary remote sensing to explore patterns of channel incision through time. Specific analyses include:

1) development of a Geomorphic Grade Line and relative elevation model for 2016 to provide a snapshot of historical channel incision (relative to floodplain elevation) prior to implementation of full-scale augmentation,
2) analysis of historical repeat transect surveys and LiDAR data to evaluate spatial and temporal patterns of incision relative to those predicted in Murphy et al. (2004),
3) specific gage analyses at the Overton and Cottonwood Ranch Mid-Channel stream gages to identify temporal patterns of incision at those locations, and
4) estimation of channel sinuosity from aerial photography to quantify changes in channel length in the J2 Return Channel through time.

The results of these analyses are interpreted together to provide our assessment of spatial and temporal patterns of channel change prior to the implementation of the full-scale sediment augmentation management experiment and predict potential future patterns of incision in absence of augmentation.

## *2.3  Geomorphic Grade Line and relative elevation model*

### 2.3.1  Methods

We utilized methods presented by Powers et al. (2019) to generate a Geomorphic Grade Line (GGL), or linear regression of valley slope. We found this approach to be appropriate in our context because the reach of interest consists of a single river that has fairly unrestricted flow and sediment transport. The Overton Bridge and KCD structures cause only small discontinuities in a localized area which were not significant enough to cause the GGL to deviate from a linear pattern. To create the GGL, we used 2021 Light Detection and Ranging (LiDAR) derived topography. First, we hand delineated the geographical extent of the existing floodplain.  Mid-channel islands were not removed but human-made features like gravel mines, road embankments, and other development-related topographic features were clipped from the boundary. The fall 2021 LiDAR digital elevation model (DEM) was then sampled along transects at five-foot intervals within the floodplain, and we calculated average elevation for each transect (station). Mean transect elevations were regressed against station to establish the GGL for the study area. The GGL was used as the reference plane for development of a relative elevation model (REM) of the study area.

Relative elevation models (REMs) provide a way to visualize and quantify channel elevations without influence of the overall valley slope and are commonly used in river restoration to determine areas of cut and fill when regrading the valley bottom (Powers et al., 2019). To develop a REM, we first generated a raster of the GGL for the study area. We then differenced the fall 2016 LiDAR DEM and GGL (DEM – GGL) to calculate the elevation of each raster cell relative to the GGL.

The physical location or alignment of the thalweg was identified for each year (2016–2021) using the Hydrology Toolbox in ArcGIS Pro 2.9.3 to generate flow direction and flow accumulation rasters from annual DEMs derived from topo-bathymetric LiDAR.  We delineated a stream network of connected flow paths in the channel and filtered the flow paths to select the

highest stream order flow path through the study area to designate as the channel thalweg. Visual inspection of aerial imagery validated the use of these accumulated flow paths as reasonable thalweg lines except for 2018 and 2021, where thalwegs were originally routed in secondary channels. To maintain consistency with other years, we manually confined the alignment of the 2018 and 2021 thalwegs to the main channel using the highest order streamline in that fell within the main channel. The resulting thalweg lines were simplified to reduce extraneous vertices using the ArcGIS Pro 2.9.3 Simplify Line tool, the Douglas-Peucker algorithm, and a tolerance of 5 ft.

Thalweg lines were processed into longitudinal profiles by sampling DEM elevations at the intersection of the thalweg lines and stationed transects spaced every 5 ft perpendicular to the stationing centerline (transect methods are described in Chapter 2). We calculated at-a-station change in thalweg elevation between consecutive years and for the study period as a whole (2016–2021).

### 2.3.2 Results

The regression of average elevation versus river station (numbered downstream to upstream), or GGL, can be found in Figure 2.3. The slope of the GGL in the study area is 0.001276. Because stationing is from downstream to upstream, slope appears positive in the equation. The slope of the GGL is consistent with previous analyses of channel slope in the AHR (Murphy et al., 2004).
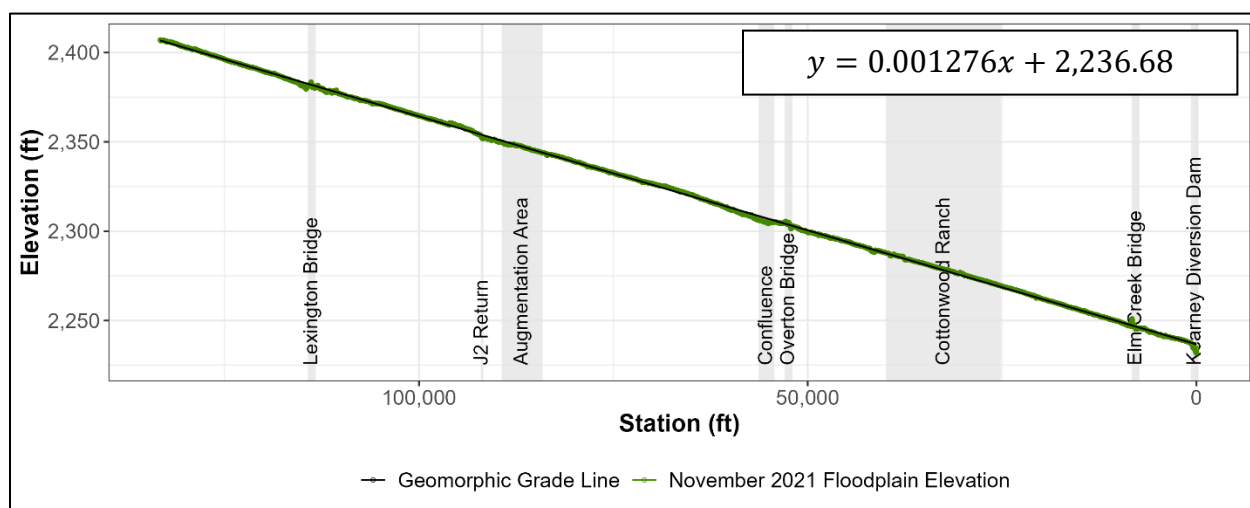


$$y = 0.001276x + 2{,}236.68$$

**Figure 2.3.** Geomorphic Grade Line (GGL) (black) of historical channel footprint in study area sensu Powers et al. (2019). Equation of the GGL presented in top right. Average elevation data sampled from 2021 LiDAR data (green).

The REM for 2016 is presented in Figure 2.5. A profile plot of REM elevations at lowest point in the channel (thalweg) is provided in Figure 2.6. The REM and REM thalweg profile provide a quantitative visualization of cumulative channel change downstream of the J2 Return to the extent that the GGL provides a good representation of pre-development channel elevations. As demonstrated in Figure 2.5, elevation deviation from GGL (incision) is greatest immediately downstream of the J2 Return (see field photos in Figure 2.4). Channel elevation in that segment in 2016 was on the order of 15–20 ft below GGL. In comparison, the relative elevation of the North Channel in that same area, which is not affected by hydropower return flows, was only 2–

4 ft below GGL. In the highly incised upper half of the J2 Return Channel, the REM also indicates a change in planform to a narrower channel with high sinuosity that is visible in relative elevations ranging from 10 ft to 22 ft below GGL. This pattern becomes less obvious as the magnitude of J2 Return Channel incision decreases in a downstream direction. At the confluence of the North Channel and J2 Return Channels 6.5 miles downstream of the return, most of the channel is 4–6 ft below GGL and braiding is apparent with a limited amount of incision progressing back up the North Channel. Downstream of the North and J2 Return Channel confluence, a limited amount of incision can be observed in the mile of channel downstream of the Overton Bridge. Beyond that, the REM indicates channel elevations are generally consistent relative to the GGL.



**Figure 2.4.** Field photos from July, 2024 depicting high eroding banks in the J2 Return Channel.
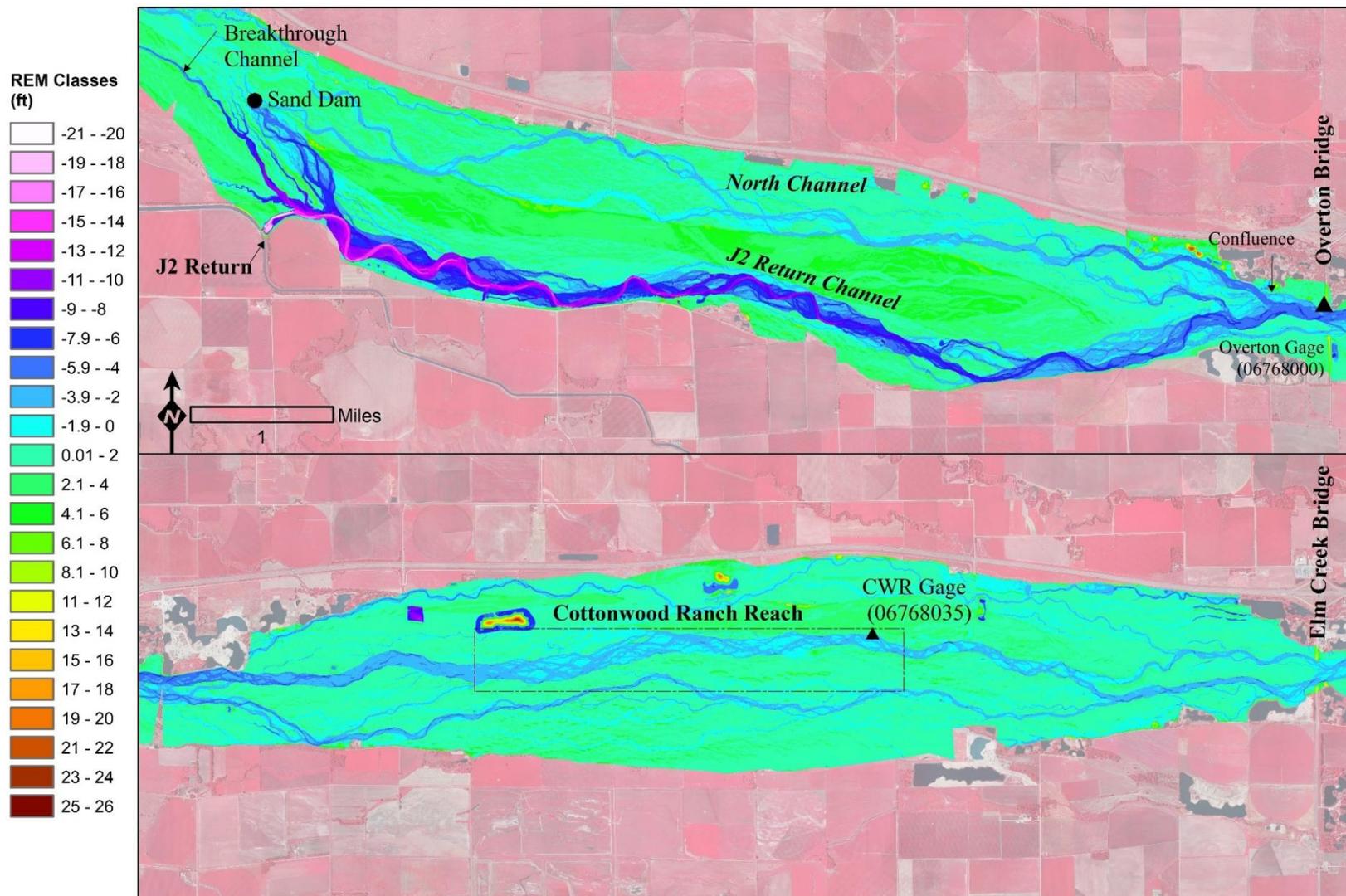
**Figure 2.5.** Relative elevation model (REM) of 2016 topo-bathymetry compared to the average elevation of the historical channel (GGL). The figure is split into J2 Return to Overton Bridge (top) and Overton Bridge to Elm Creek Bridge (bottom). Edges appear irregular due to clipping of ponds and other human-manipulated surfaces. Deviations from the GGL are much larger (10-20 ft below the floodplain) near the J2 Return and decrease to 1-6 ft below the floodplain toward the downstream extent of the study area.
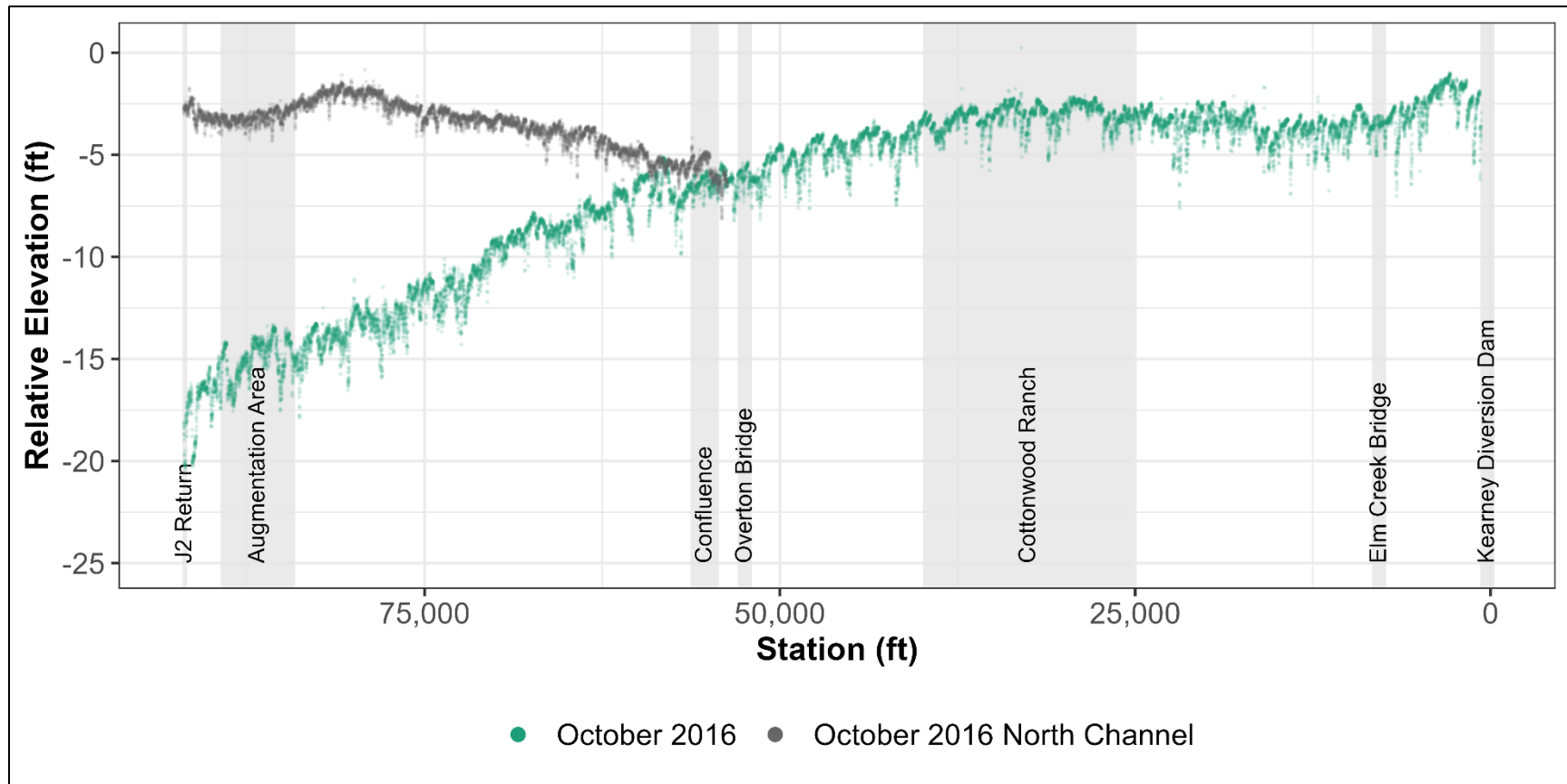
**Figure 2.6.** Elevation of deepest point (thalweg) in the North Channel (gray) and J2 Return/Main Channel (green) relative to Geomorphic Grade Line (GGL). The segment of channel immediately downstream of the J2 Return is incised on the order of 15–20 feet lower than the North Channel at the same station. Magnitude of incision decreases in a downstream direction with the thalweg becoming roughly parallel to GGL (GGL has a value of 0) near the upper end of the Cottonwood Ranch habitat complex. North Channel incision is also apparent upstream of the confluence of the North and J2 Return Channels.

## 2.4    Analysis of spatial and temporal trends in incision 1989-2016 relative to predictions

### 2.4.1    Methods

Murphy et al. (2004) included predictions of incision downstream of the J2 Return over time based on an incision wave propagation model (de Vries 1973), later referenced in Graf (1998). The model predicted downstream propagation of incision through time based on a ratio of incision downstream of the J2 Return relative to maximum incision at the return. According to Murphy et al. (2004), the maximum incision relative to the North Channel thalweg elevation in 2002 was 13.3 ft. We compared to the Murphy et al. (2004) predictions of downstream spread of incision by plotting incision as the difference in elevation from modified GGLs that match the elevations of the 2002 North Channel thalweg and mean cross-sectional elevations. We used 1989 and 2002 channel cross sections and 2016 LiDAR data to compare observed and predicted incision patterns (Figure 2.9).

Repeat cross section data used in this analysis were collected by the United States Bureau of Reclamation (USBR) in 1989 and DJ&A consultants in 2002 (Holburn et al. 2006). These entities surveyed a total of 11 cross sections in 1989 between the J2 Return and KCD (Figure 2.7.). Ten were repeated in 2002. We clipped the cross sections in ArcGIS to the extent of the active channel (5,000 cfs flow boundary) and calculated the minimum (thalweg) elevation and mean channel elevation at each survey cross section. The 2016 LiDAR DEM was also clipped and sampled to calculate thalweg and mean channel elevations at 5-foot intervals throughout the reach. Both mean and thalweg elevations were calculated and used in the analysis to evaluate maximum (thalweg) incision as well as general channel incision (mean). We used cubic (third order polynomial) regression to model full longitudinal profiles for thalweg and mean channel elevations from 1989 and 2002 with cross section data from 11 points in 1989 and 10 points in 2002 (Figure 2.8). Third order regression provided the best fit to the limited transect data and was consistent with the general shape of the 2016 LiDAR-derived profiles for mean cross-sectional elevation. We used a generalized additive mixed model (GAMM) for the 2016 thalweg elevations rather than a polynomial regression due to a more accurate fit. The methods for the GAMM are further described in Section 3.4.1. Note that this analysis is based on limited historical data and no uncertainty estimate is available for the 1989 or 2002 surveys.
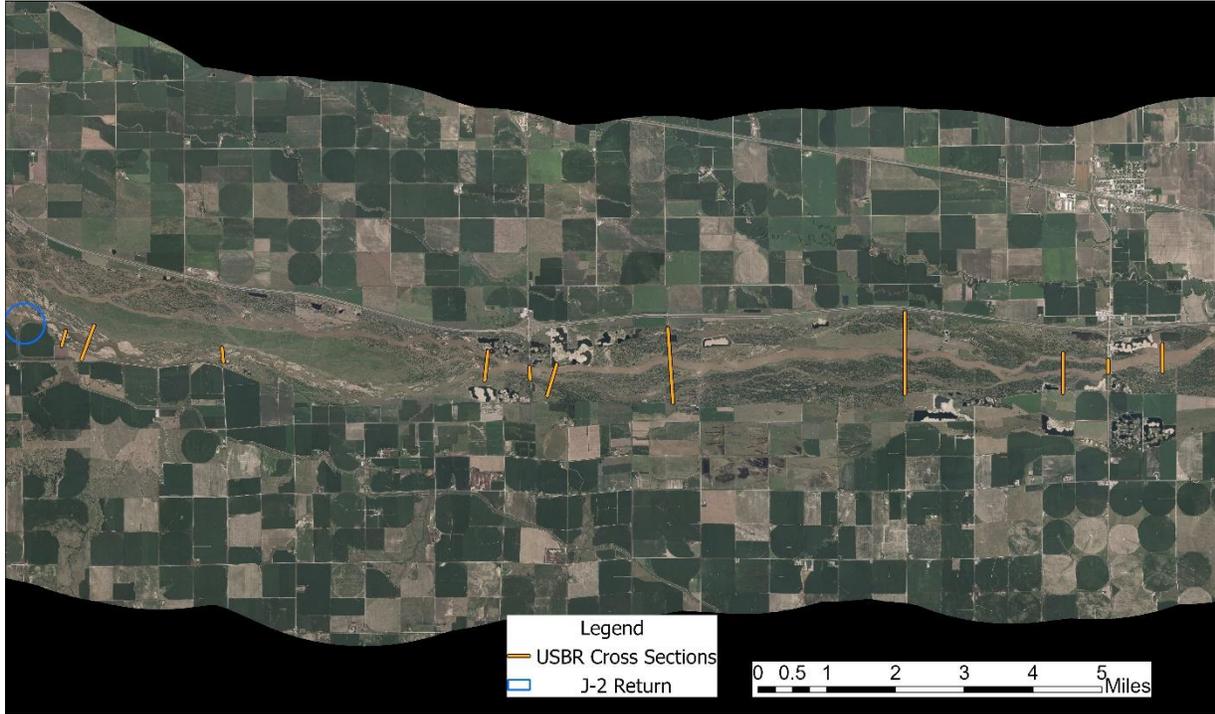
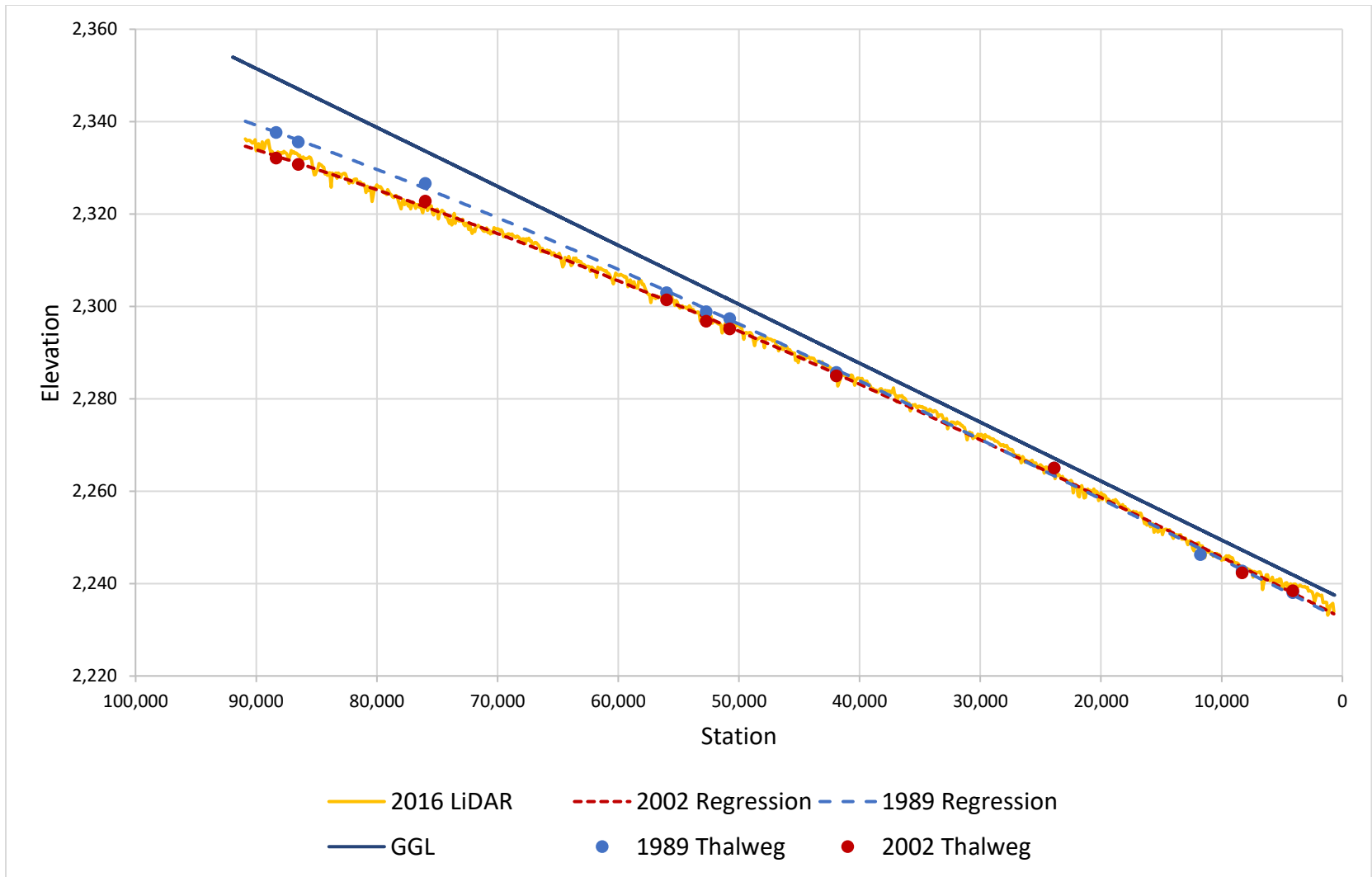**Figure 2.7**. Locations of USBR 1989 and 2002 survey cross-sections.

**Figure 2.8.** Modeled longitudinal profiles (cubic regression) of thalweg from 1989, 2002 cross section data. Profiles plotted with Geomorphic Grade Line (GGL) and thalweg profile from 2016 LiDAR data. Deviation from the GGL is evident between Stations 50,000 and 90,000 and increases between 1989 and 2002. No additional increase in deviation is observed between 2002 and 2016. Note that these findings are based on limited historical data and error estimates are not available.

Incision was calculated at 100 ft intervals by differencing profile elevation from modified GGLs for both the thalweg profile and the mean channel elevation profile. We used Murphy et al.'s (2004) maximum incision value of 13.3 ft below the 2002 North Channel thalweg for our maximum potential thalweg incision. To validate the use of this value, we confirmed that 2016 channel elevations remained approximately 13 ft below the original 2002 North Channel thalweg elevation at the original USBR transect location. Mean channel elevations from 2016 did not match the minimum mean channel elevation in 2002, so we used the 2016 minimum mean cross-sectional elevation for our maximum possible incision of mean channel elevation. The modified GGLs were based on the original GGL, but reduced in elevation by 3.59 ft to meet the 2002 North Channel thalweg elevation for thalweg comparisons, and reduced by 0.59 ft for mean elevations. The final step in recreating Murphy et al.'s incision plot was calculating proportion of maximum incision depth by dividing profile incision depth by maximum incision depth at each station.

### 2.4.2   Results

Comparisons of observed incision relative to Murphy et al. (2004) predictions are provided in Figure 2.9. The top panel (panel a) presents thalweg (minimum channel elevation) incision relative to Murphy et al.'s predictions. The bottom panel (panel b) presents mean channel incision relative to predictions. Both panels begin one mile downstream of the J2 Return and end at the KCD. The number of years in both plots reference years since J2 Return was constructed.

When observed incision is plotted on top of predictions, the observed extent of thalweg and mean channel incision propagation over the course of the 80 years since J2 Return operations began both fall between the 4-year and 25-year predictions for years 2002 and 2016. This indicates downstream propagation of incision has occurred substantially more slowly than predicted. Beyond the similarity in slower rate of observed progression of incision relative to predictions, the temporal incision patterns differ substantially.

The thalweg incision plot (panel a) indicates that approximately 55% of thalweg incision immediately downstream of the J2 Return occurred prior to 1989 and the remainder occurred prior to 2002. Between 2002 and 2016, the thalweg was stable, with little vertical incision occurring during that period. The mean channel elevation plot (panel b) indicates that mean channel incision did not stabilize after 2002, especially in the three-mile segment below the J2 Return, where mean channel elevation continued to decrease despite thalweg stability. Taken together, the panels indicate a shift from incision to erosion through lateral channel movement (lateral erosion) after 2002.

The 1989, 2002, and 2016 incision plots all terminate slightly less than 20 miles downstream of the J2 Return at the KCD. The plotted portion of maximum incision depth between approximately 10 and 20 miles downstream of the diversion is highly variable indicating inconsistent trends in that reach. This may be due to differing patterns of sediment accumulation and transport upstream or through KCD during wet and dry periods. A longer monitoring period may help to distinguish patterns of river dynamics from variability.
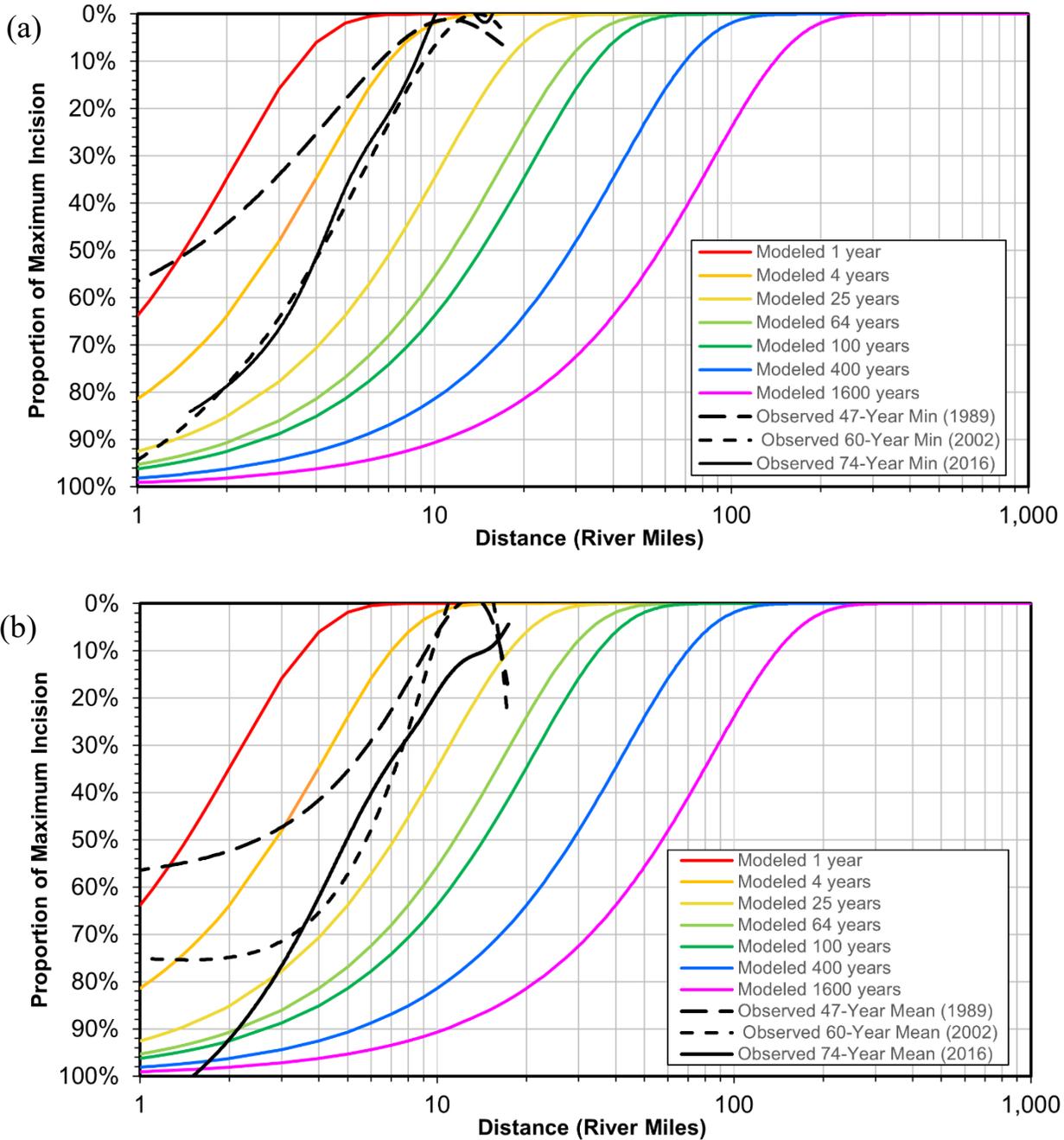
**Figure 2.9.** Channel incision estimates below J2 Return plotted on top of incision propagation estimates from Murphy et al. (2004). Minimum cross section elevation (thalweg) incision is shown in (a) and the mean channel elevation incision is shown in (b). Number of years represents years since operation started at J2 Return. Observed values from 1989 and 2002 were estimated with a 3rd order polynomial model through 10 transect locations, while 2016 observed

values are based on a Generalized Additive Mixed Model made with LiDAR data (thalweg) and a 3rd order polynomial through LiDAR data (mean).

Our use of Murphy et al.'s estimate of 13.3 ft for maximum thalweg incision below the North Channel allows for calculation of estimated thalweg elevation after 74 years (1942 to 2016) and subsequent comparison to 2016 LiDAR data (Figure 2.10). The model-predicted and measured thalweg elevation values diverge in the J2 Return Channel. The incision propagation model does not account for changes in channel slope, sinuosity, or sediment discharge through time, limiting its ability to predict the range of responses observed due to clearwater release from the J2 Return.
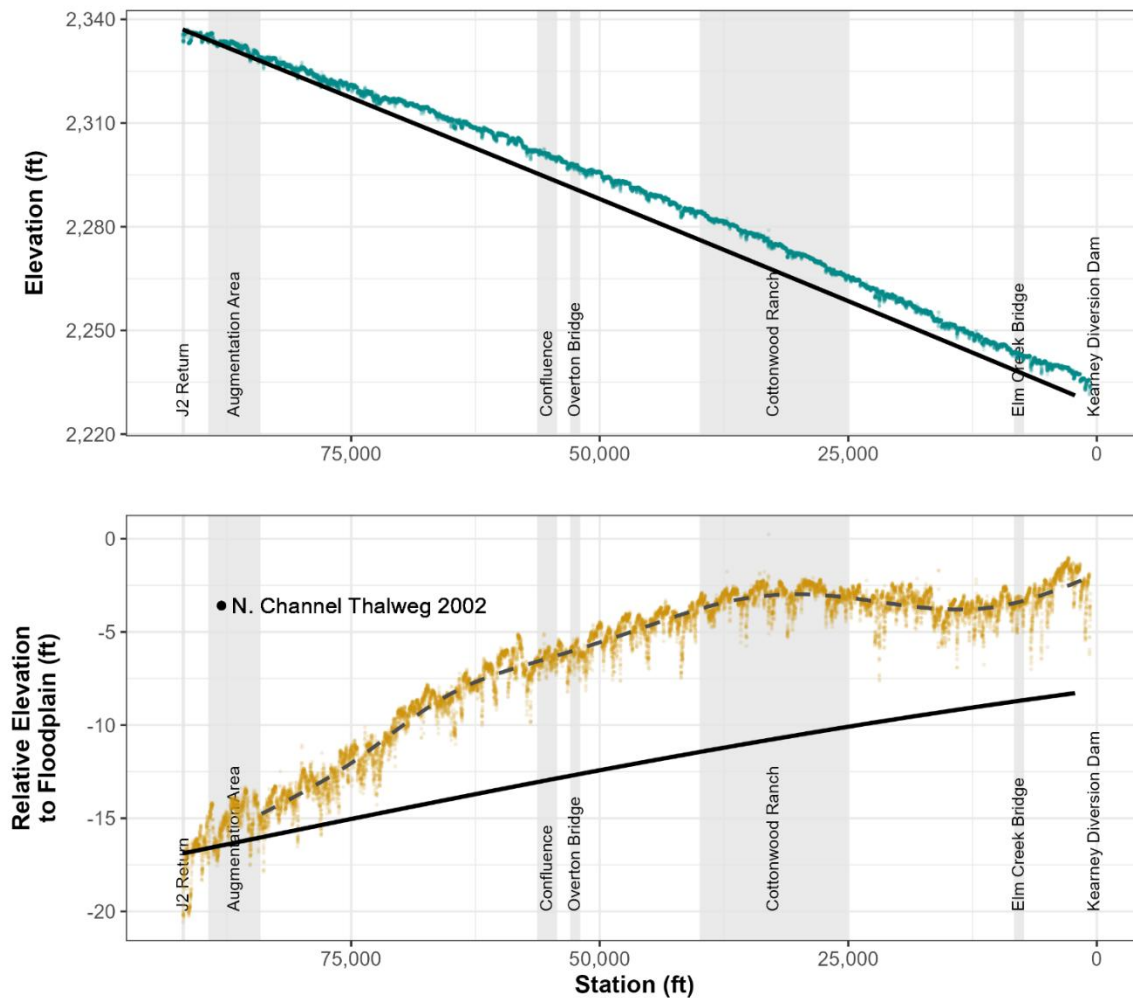


**Figure 2.10.** Observed and predicted channel thalweg elevations (a) and relative elevations to the floodplain (b) according to incision models presented in Murphy et al. (2004). The bold black lines in both plots show predicted elevations, while the dashed line in (b) is a modeled thalweg from a generalized additive mixed model (GAMM). We used a maximum potential thalweg incision value of 13.3 ft below the 2002 North Channel thalweg to be consistent with historical estimates.

## *2.5    Specific gage analysis*

### 2.5.1    Methods

The presence of USGS stream gages at the Overton Bridge and the downstream end of Cottonwood Ranch (see location Figure 2.1) provide an opportunity to assess incision patterns through time at those locations via a specific gage analysis. Trends of increasing or decreasing water surface elevation at a constant discharge can be linked to a variety of complex processes and can be associated with geomorphic change, bridge/site modification, changes in sediment supply, and changes in roughness (vegetation dynamics). Increasing water surface elevation at a constant discharge through time is an indication that the channel at that location is aggradational, whether width changes or remains static. Declining water surface elevation could indicate several channel responses, including channel degradation alone or channel widening. In this study, we interpret decline in water surface elevations to be generally indicative of channel degradation.

Specific gage analyses can be conducted using either stage-discharge records or physical measurements that are used to develop and adjust stage-discharge rating curves. This analysis relies solely on physical measurement data to eliminate potential biasing related to stages that are estimated from rating curves (Samaranayake 2009, Biedenharn et al. 2017). Physical measurements include an unknown but low uncertainty in stage. Discharge at stage is estimated using current-meters or acoustic doppler current profilers (ADCP). USGS rates measurements as excellent, good, fair or poor, which correspond to potential errors of less than 2%, 5%, 8%, and greater than 8% respectively (Turnipseed and Sauer 2010). For the purpose of this analysis we filtered physical measurement data to remove measurements with poor ratings as well as all measurements in the months of December through February, which are often ice-affected.

Specific gage analyses examine trends in water surface elevation through time at a discharge. We chose to evaluate three discharges at each gage including the 10th and 50th percentile of mean daily discharge and median of instantaneous annual peak discharge during the period when physical measurements were available. These three discharges allowed us to evaluate trends in stage at low flows, normal flows, and at approximate bankfull discharge.

Most specific gage analyses involve development of simple linear regressions of stage through time for a range of discharges around a target discharge (Chen et al. 1999, Biedenharn et al. 2017). This is done to obtain a sufficient sample size to meet linear regression assumptions. For example, a specific gage analysis at 1,000 cfs would generally include all measurements collected from 800 to 1,200 cfs. If actual discharges are skewed above/below target through time, this approach can provide a biased estimate of stage change. Using simple linear regression also has other limitations including inability to model non-linear relationships and lack of meaningful estimates of uncertainty.

To address these issues, we developed generalized additive models (GAMs) for all physical measurement data at each gage with smoothed relationships limited to five degrees of freedom (Hastie and Tibshirani 1990). GAMs allowed us to estimate possible non-linear relationships of stage-discharge relationships using all appropriate physical measurement data. We then plotted the estimated relationships of stage-discharge for the three discharges described above with 95% confidence intervals.

## 2.5.2   Results

### 2.5.2.1   Overton Gage (06768000)

The period of record for the Overton stream gage extends from October 1, 1930, to present. However, the gage has been relocated several times and was moved to the present location on October 10, 1986. At the current location, operation has been continuous with one major datum adjustment (lowered by 2.0 ft) on September 30, 2004. Specific gage analysis results cover the period from October 1986 to present with an adjustment to bring the entire period of record onto a single datum. Figures 2.11 through 2.13 provide a time series of aerial imagery at the gage location.
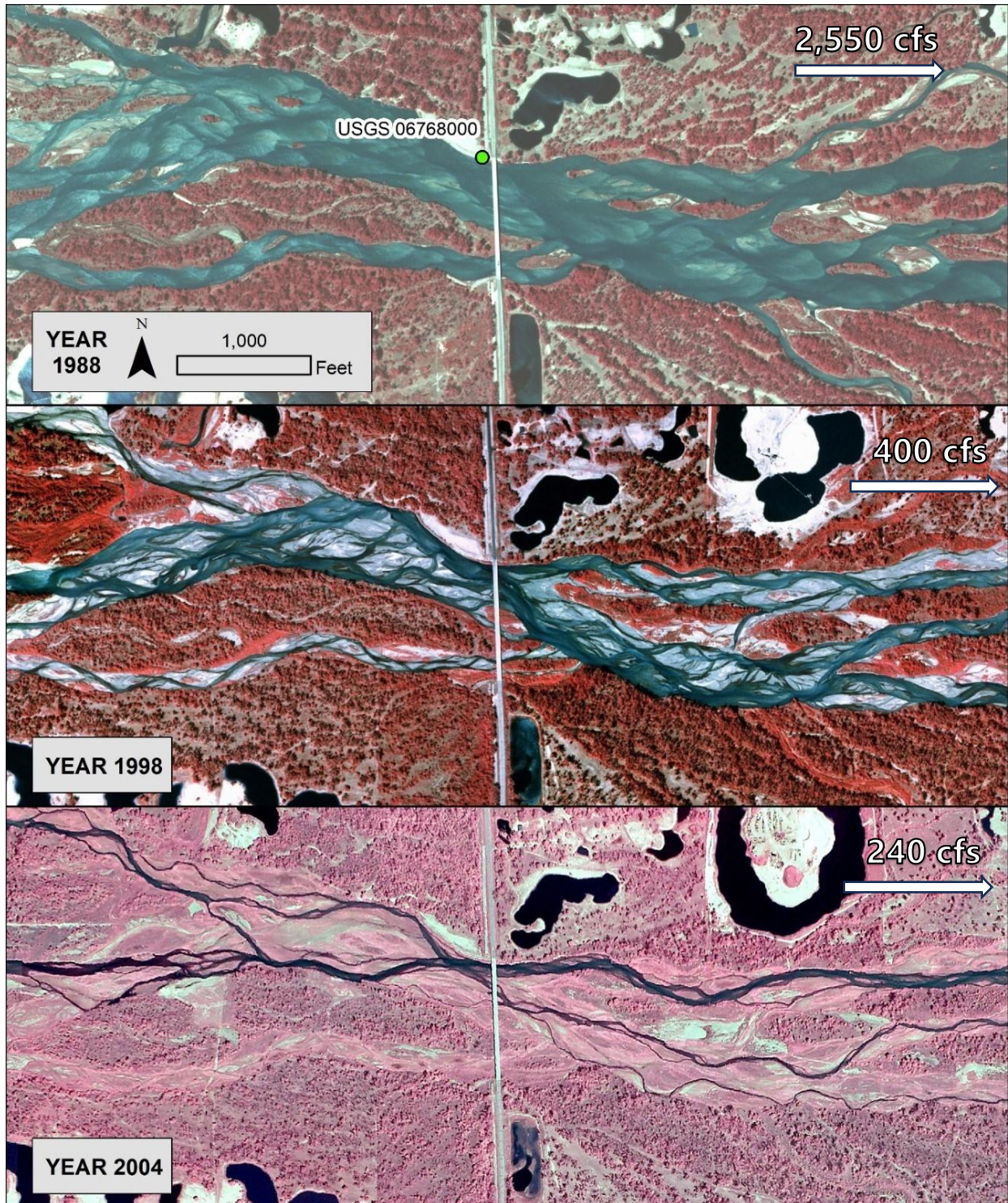
**Figure 2.11.** Imagery at Overton Gage (USGS 06768000) 1998 through 2004.
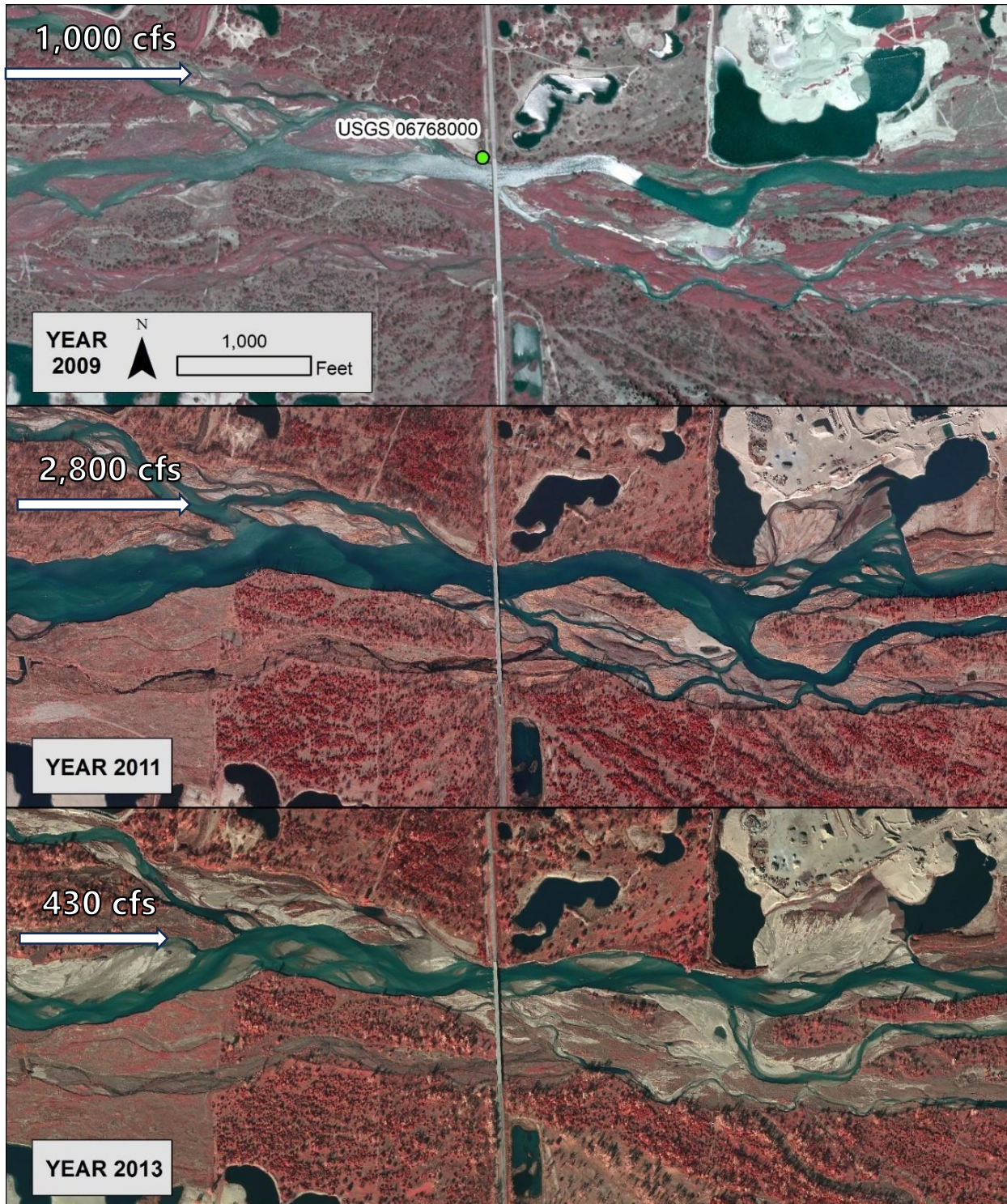
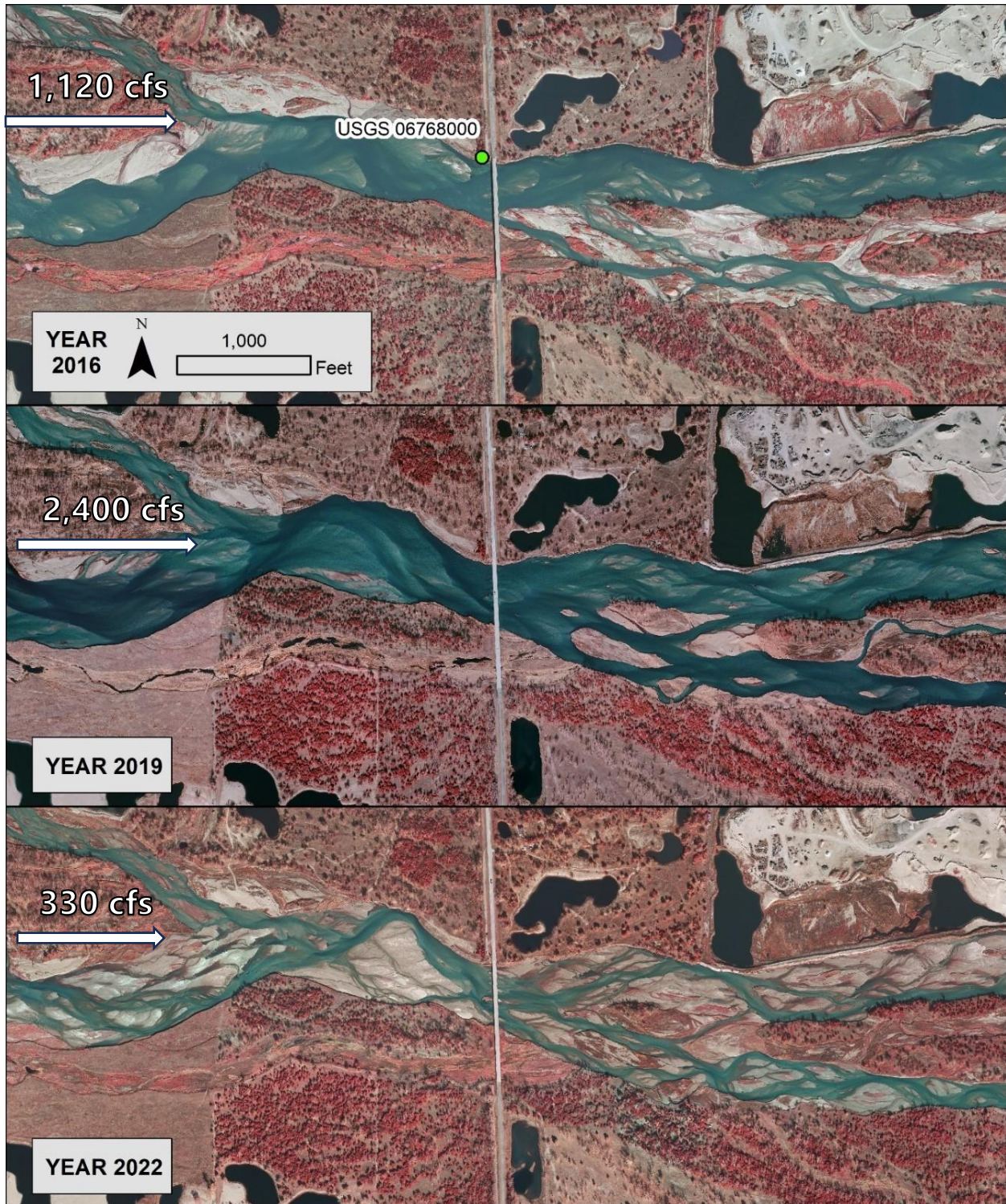**Figure 2.12.** Imagery at Overton Gage (USGS 06768000) 2009 through 2013.

**Figure 2.13.** Imagery at Overton Gage (USGS 06768000) 2016 through 2022.

Figure 2.14 provides physical stage measurement data for the study period at the current Overton gage location along with trailing 30-day mean discharge. In the figure, stages are binned by discharge. The measurement data indicates slight decline in stage for discharges below 3,000 cfs until the late 1990s when the decline began to accelerate, especially at lower discharges. The trend of declining stage continued through approximately 2013 when it reversed and stage began to increase at low discharges (<1,000 cfs). Stage trends at higher discharges are less clear but appear to indicate a long term decline.
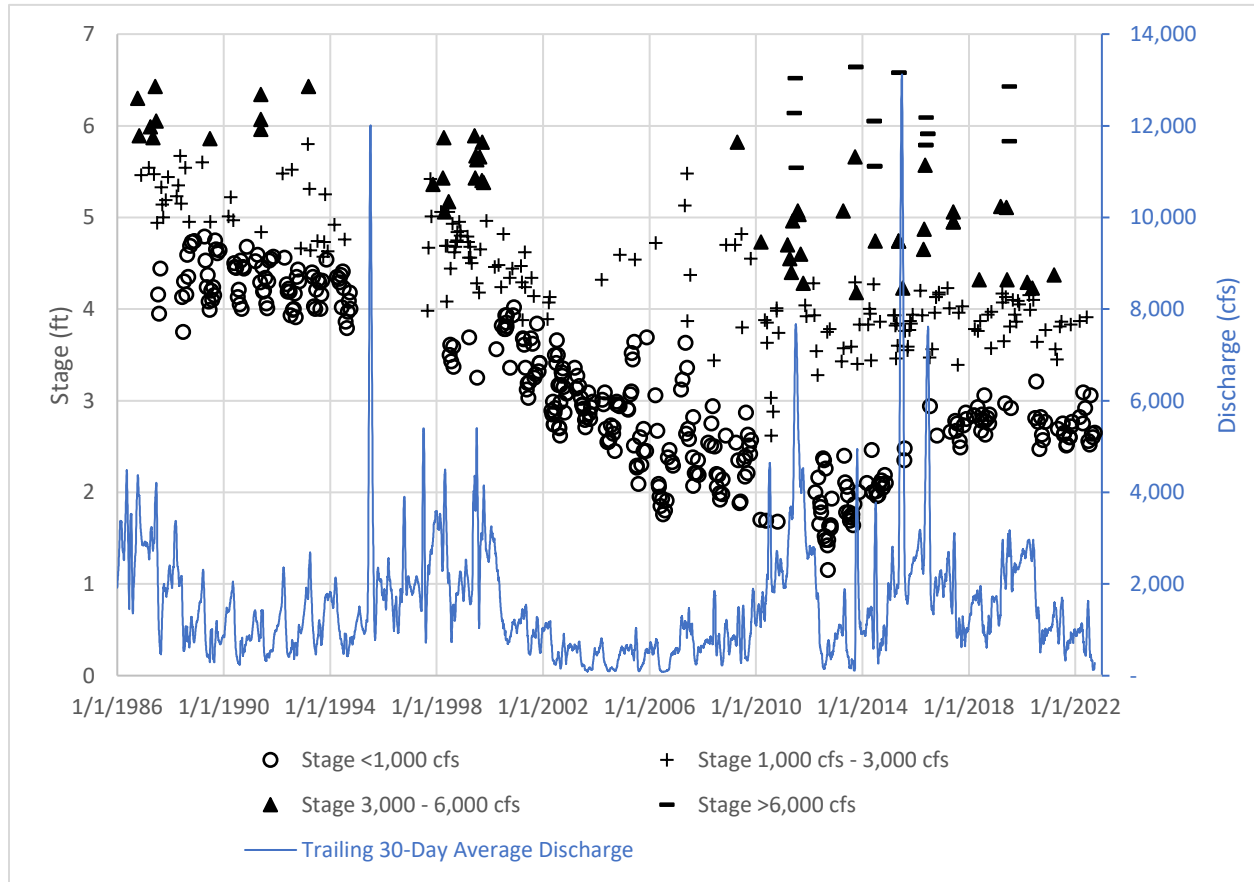


**Figure 2.14.** Physical measurement stage data at Overton Gage (USGS 06768000) and trailing 30-day average discharge. Presence of stage measurements in flow ranges above corresponding discharge on this figure reflect use of 30-day average trailing discharge.

Figure 2.15 provides specific gage analysis results. The specific gage analysis indicates decreasing stage at the Overton Bridge at low and median discharges from 1986-2013 with a total magnitude of approximately two feet. That trend is reversed in 2014 with stage increasing, especially at the 10th percentile discharge. Stage at the median annual peak discharge has declined throughout the period of record. This indicates that approximately two feet of incision occurred at the bridge between 1990 to 2014 with the greatest rate of change in the 2000s.
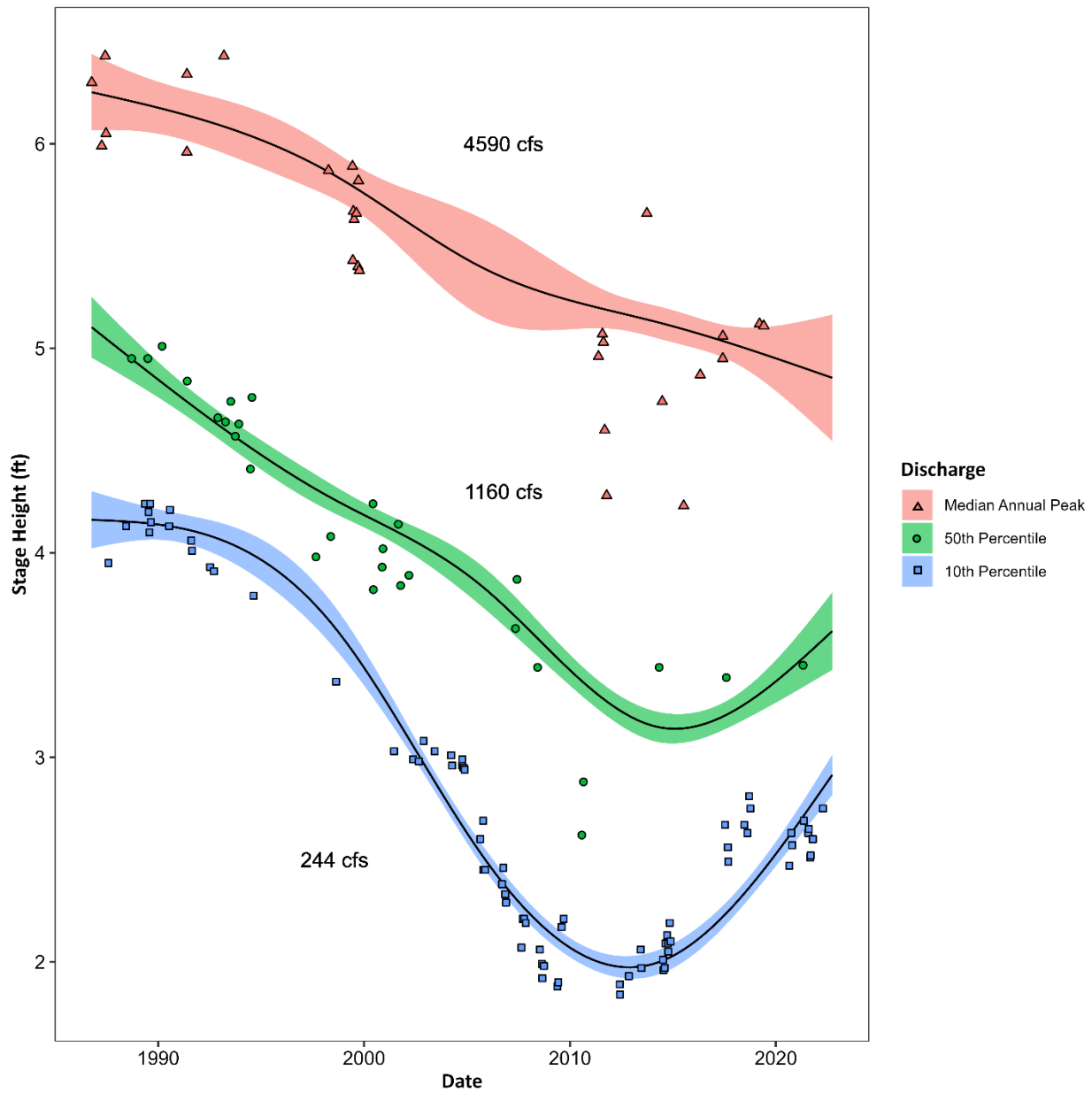
**Figure 2.15.** Specific Gage analysis for Overton Gage (USGS 06768000) at 10th percentile discharge of 244 cfs, median discharge of 1,160 cfs, and median annual peak discharge of 4,590 cfs. Shaded regions represent 95% confidence intervals for each discharge. Results indicate that elevations at this gage have decreased since 1986, though a rebound may be occurring beginning in 2013.

### 2.5.2.2 Cottonwood Ranch Mid-Channel Gage (06768035)

The period of record for the Cottonwood Ranch Mid-Channel stream gage extends from October 1, 2001 to present. The gage has operated at the current location through that entire period and there have been no datum adjustments. Figures 2.16 and 2.17 provide a time series of aerial imagery at the gage location.
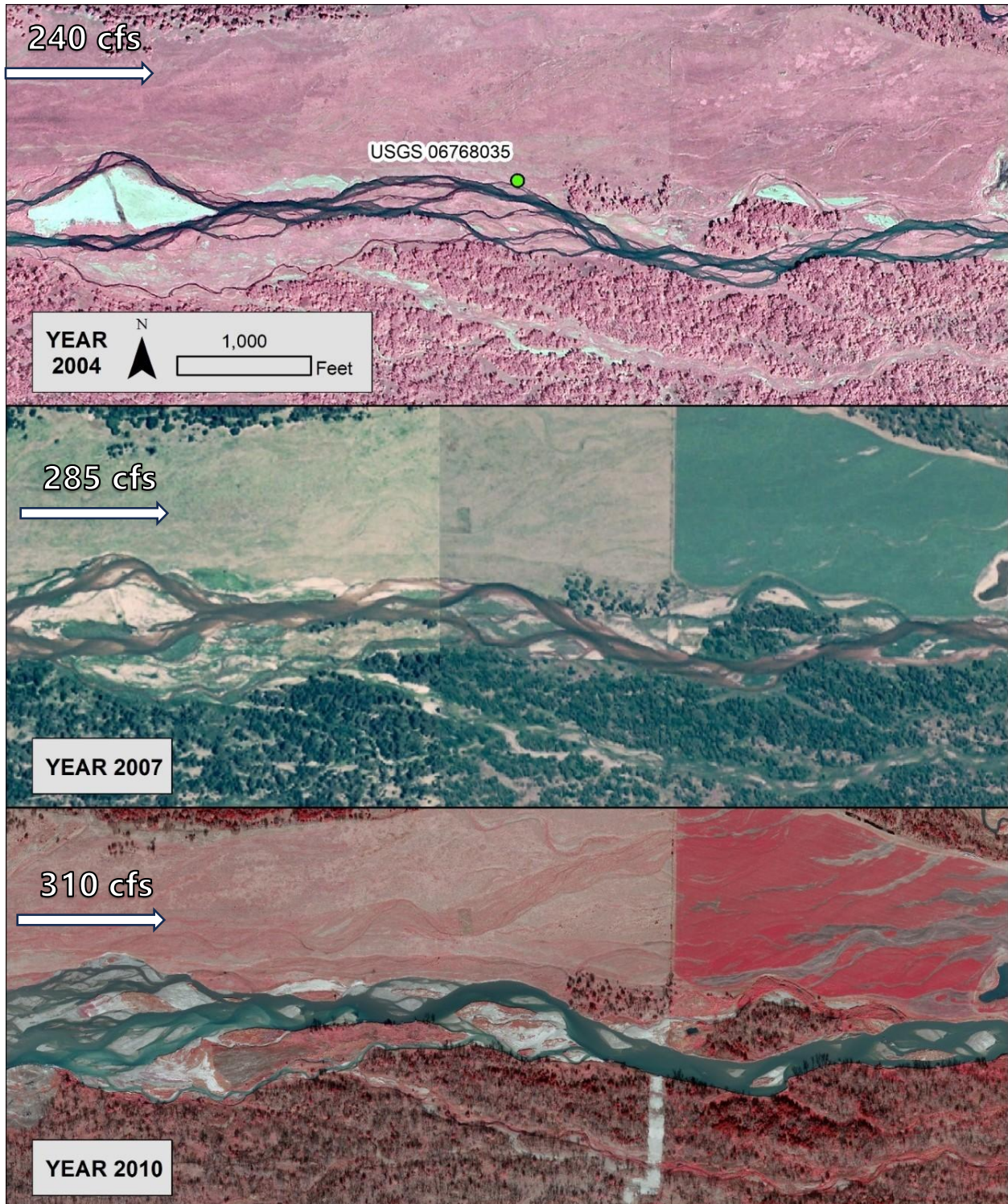
**Figure 2.16.** Imagery at Cottonwood Ranch Mid-Channel Gage (USGS 06768035) 2004 through 2010.
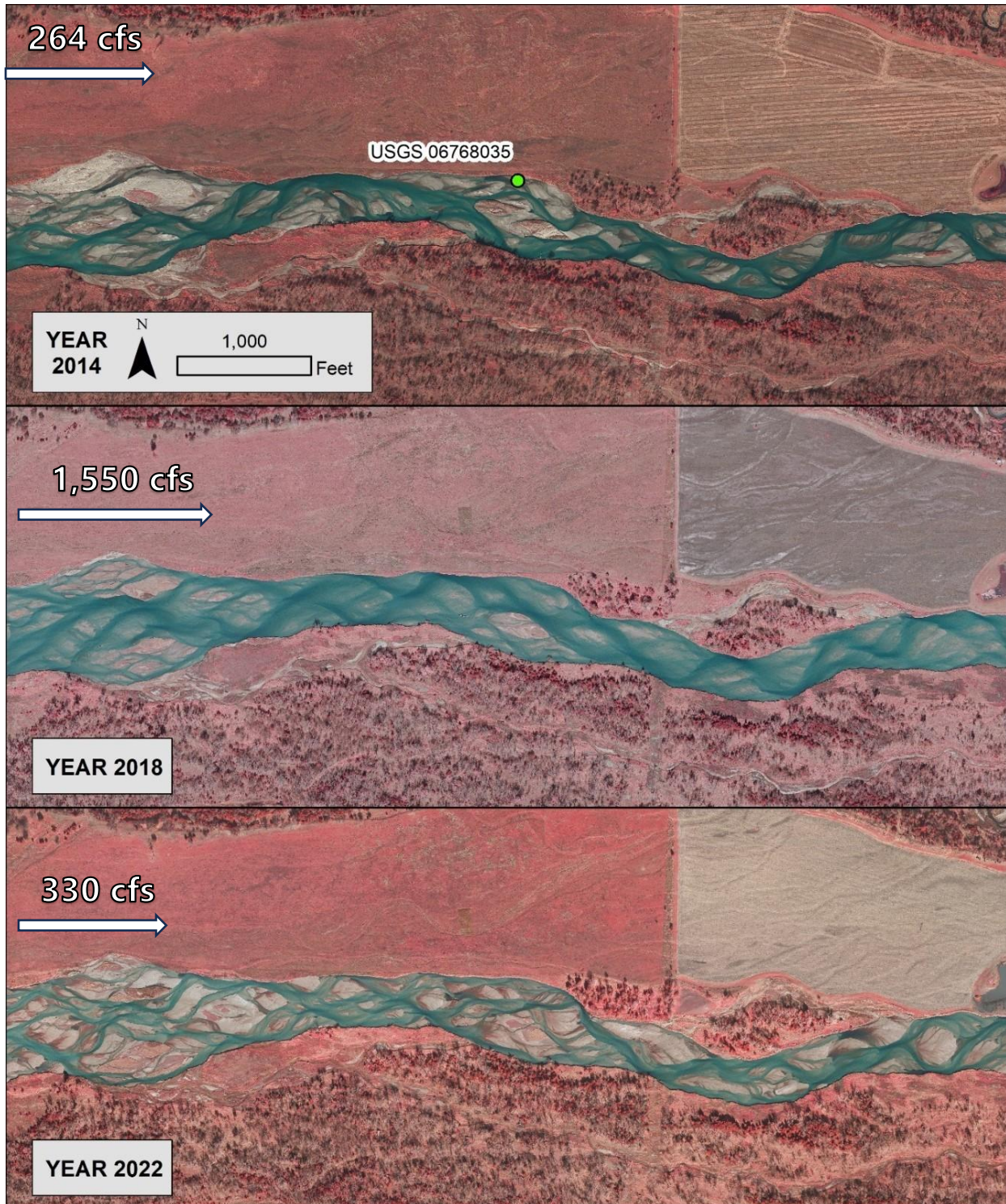
 **Figure 2.17.** Imagery at Cottonwood Ranch Mid-Channel Gage (USGS 06768035) 2014 through 2022.

Figure 2.18 provides physical stage measurement data for the period of record at Cottonwood Ranch Mid-Channel gage along with trailing 30-day mean discharge. The raw stage measurements indicate relative stability at low discharges (<1,000 cfs) until 2007, increasing stage from 2007 to 2011, and stability since 2012. The lack of stage measurements at discharges exceeding 3,000 cfs limit ability to interpret trends in stage for peak flows.
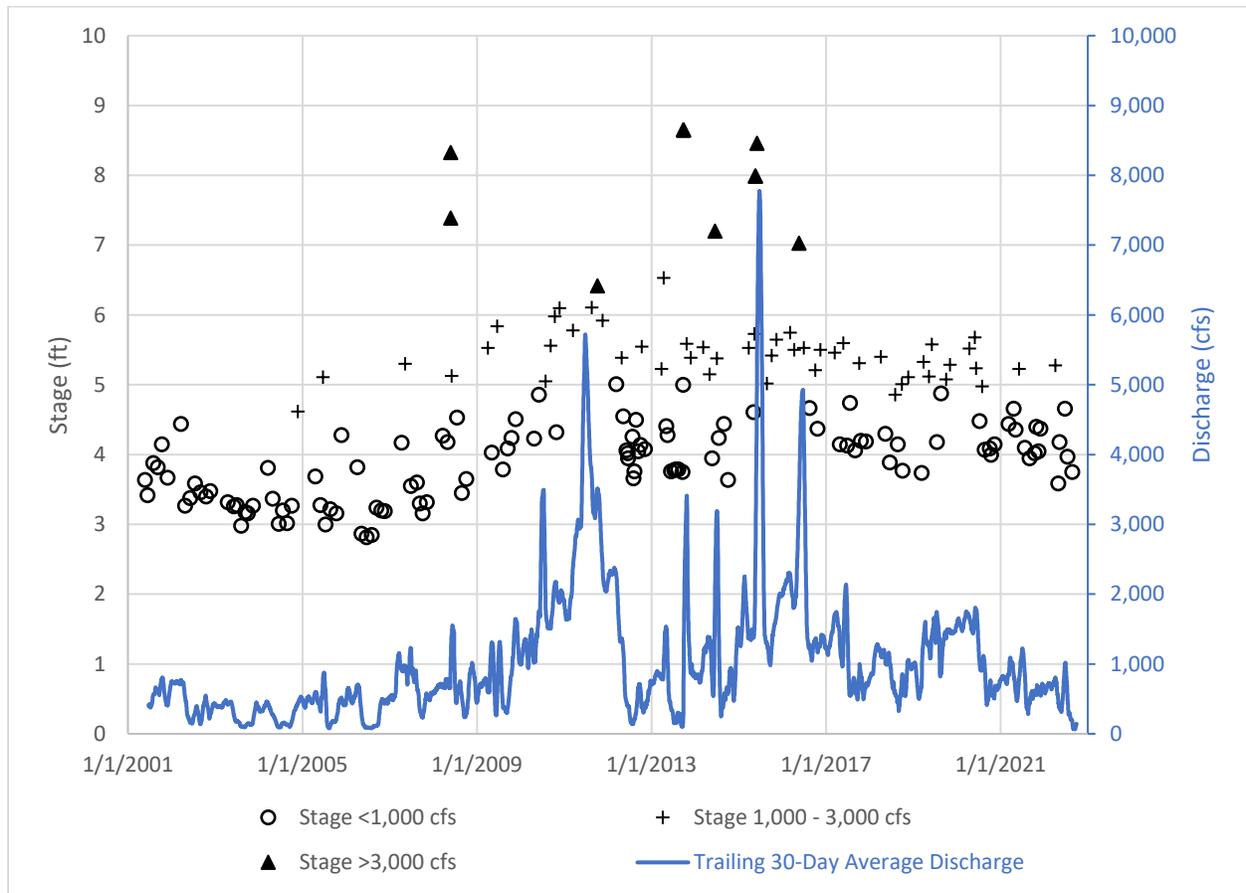


**Figure 2.18.** Physical measurement stage data at Cottonwood Ranch Mid-Channel gage (06768035) and trailing 30-day average discharge.

Figure 2.19 provides specific gage analysis results. The specific gage analysis indicates stable to slightly increasing stage at low and median discharges during the period of record. There are an inadequate number of stage measurements at the median annual peak discharge to establish any trends in stage at approximate bankfull discharges.
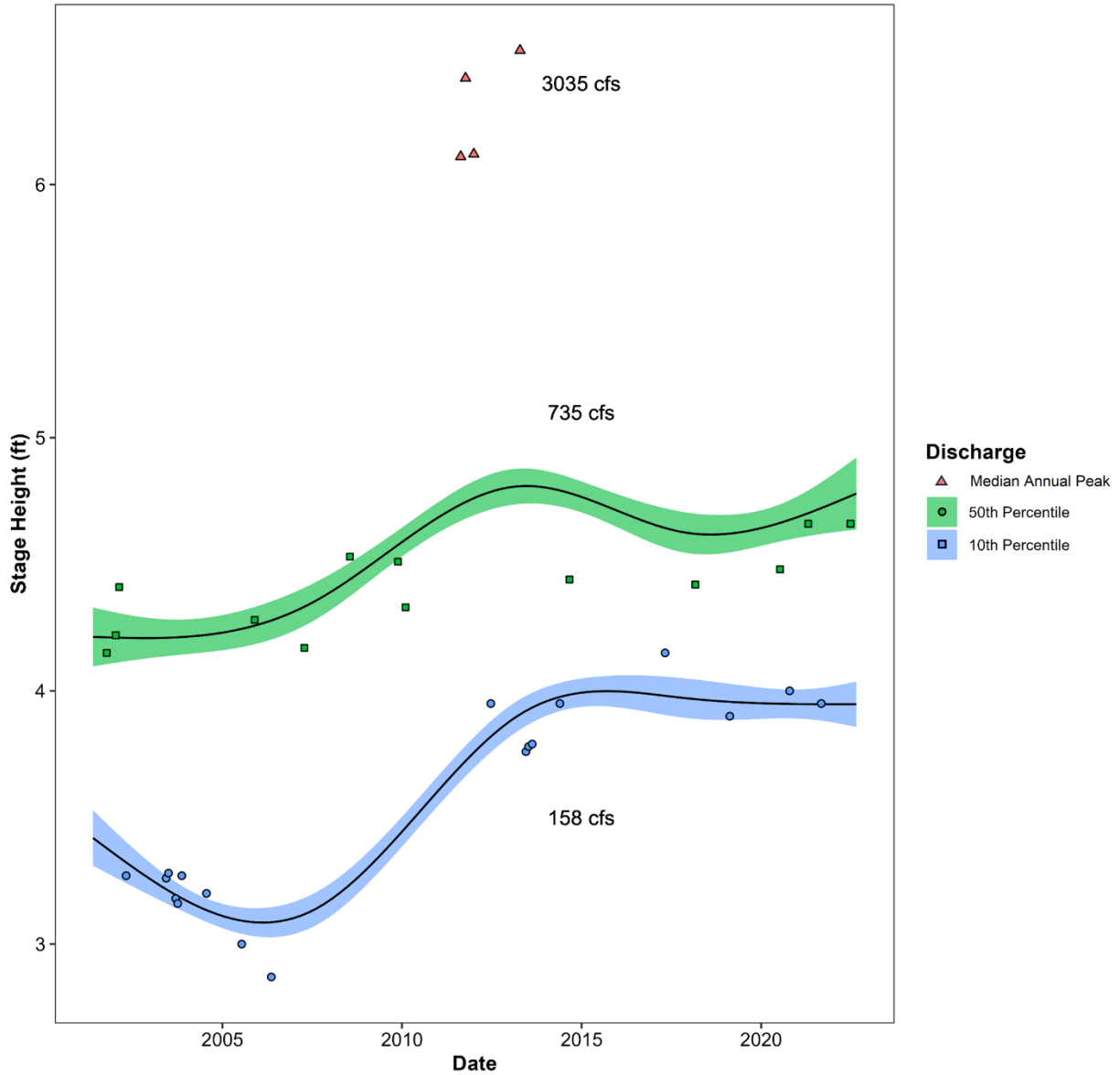
**Figure 2.19.** Specific Gage analysis for Cottonwood Ranch Mid-Channel Gage (USGS 06768035) at 10th percentile discharge of 158 cfs, median discharge of 735 cfs, and median annual peak discharge 3,035 cfs. Shaded regions represent 95% confidence intervals for each discharge. Results indicate that elevation at this gage increased slightly until approximately 2012 and 2015 for median and 10th percentile discharge, respectively, and remained relatively stable afterward.

## 2.6    Channel sinuosity upstream of the Overton Bridge

### 2.6.1    Methods

As discussed in Section 2.3, the REM appears to show a shift in channel geometry upstream of the Overton Bridge, especially in the upper half of the J2 Return Channel. In that section, the channel shifted from a braided planform (historically) to narrower and more sinuous wandering form. The results of the incision analysis presented in Section 2.4 indicated minimal vertical incision after 2002 with continuing decline in mean channel elevation in the upper portion of the reach. Taken together, these findings indicate that after 2002 the channel adjustment is occurring primarily through lateral channel movement with increasing meander intensity.

We quantified this increase in meandering by estimating annual sinuosity in the reach between the J2 Return and Overton Bridge using aerial imagery. The first step in this analysis involved hand-delineating channel length by tracing the thalweg from the Overton Bridge to the J2 Return in a series of primarily color-infrared imagery spanning the period of 1969 to 2016. Imagery series captured at high discharge were not included as the thalweg could not be identified. We then calculated straight-line distances between the starting and ending points of each year's thalweg and divided total thalweg channel length by the straight-line distance producing an estimate of sinuosity for each year/image.

### 2.6.2    Results

Sinuosity analysis results are presented in Figure 2.20. Sinuosity ranged from 1.1 – 1.15 during the late 1960s through the late 1990s. Sinuosity began to increase in the early 2000s with that trend continuing up to the initiation of full-scale sediment augmentation in 2017. Many systems of stream classification (Leopold and Wolman, 1957; Rosgen, 1994; Fryirs, K. & Brierley, G, 2005) include measures of sinuosity as part of their distinction between braided and meandering streams or rivers. In these systems, threshold sinuosity to transition from a braided to meandering channel ranges from 1.2 -1.5. By 2016, mean sinuosity in the J2 Return Channel had increased to the lower end of this threshold, consistent with a transition toward a meandering planform.
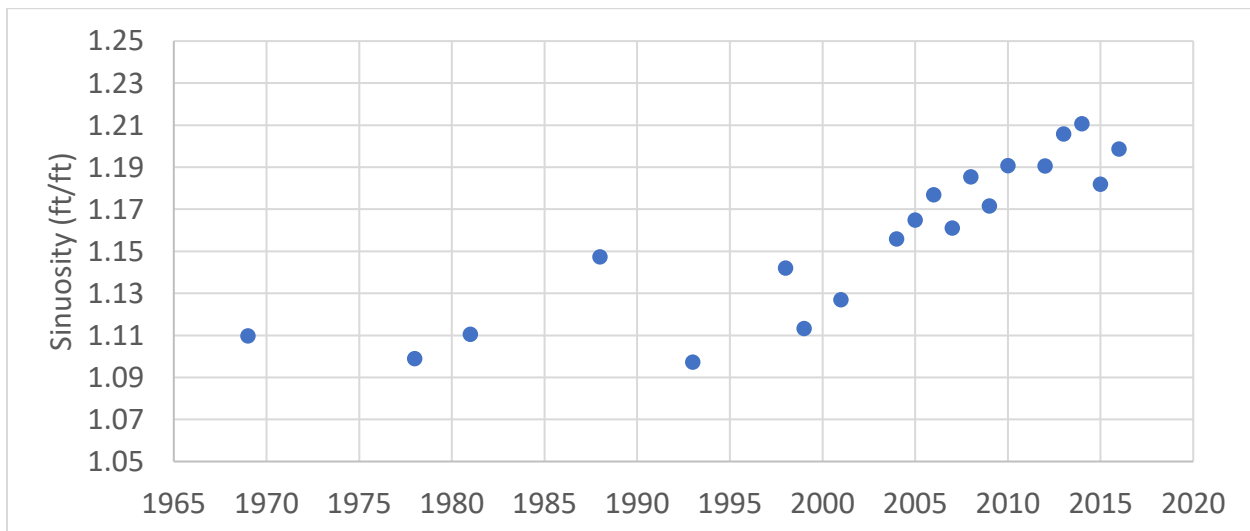


**Figure 2.20.** Ratio of total channel length to straight-line length (sinuosity) between the J2

Return and the Overton Bridge 1969 to 2016. Figure shows an increase in sinuosity starting in the early 2000s.

## *2.7    Discussion*

The Program's Extension Big Question 3 asks whether augmentation is necessary to keep incision and narrowing from progressing downstream past the Overton Bridge and negatively impacting the suitability of habitat for whooping cranes. The retrospective analyses presented above provide information about historical incision patterns in the study area. The first analysis (2016 REM) indicates there has been approximately 16 ft of incision immediately downstream of the J2 Return. The magnitude of incision declines to about four ft at the confluence of the North and J2 Return Channels near the Overton Bridge and is negligible at the upper end of the Cottonwood Ranch habitat complex. Patterns of incision that can be observed in the REM also indicate the most incised segment in the J2 Return Channel (upper half) has transitioned from braided to a wandering planform that is narrower with higher sinuosity.

Thalweg and mean channel elevation profiles created from 1989 and 2002 repeat cross section surveys, along with 2016 LiDAR profiles, indicate that incision stabilized by the early 2000s. The 2016 and 2002 channel thalweg profiles are topographically similar along the interpolated profile between the ten available thalweg points from 2002. However, comparison of mean channel profiles indicates mean channel elevation continued to decline in the reach downstream of the J2 Return, signaling a shift from a pattern of vertical incision to lateral migration. This is consistent with the trend of increasing sinuosity upstream of the Overton Bridge starting in the early 2000s.

The specific gage analysis at the Overton Bridge indicated approximately two ft of incision occurred at the bridge between 1990 to 2014 with the greatest rate of change in the 2000s. After 2014, stage increased somewhat at the 10th percentile flow (low flow) increasing back to early 2000s levels by 2016. The similarity in low flow stage in early 2000s and 2016 is consistent with the similarity in 2002 and 2016 thalweg profiles but it should be noted that the profile analysis misses the cycle of incision followed by deposition that was observed in the gage data. The specific gage at Cottonwood Ranch indicates that reach has been stable to slightly aggradational since the mid-2000s. However, it should be noted that pilot-scale sediment augmentation occurred one mile upstream of the Overton gage in late 2012 and early 2013 and a considerable amount of channel widening though mechanical augmentation occurred upstream of that gage on Cottonwood Ranch during the period of 2005-2013. Those actions likely affected trends in stage at the gage locations.

Beyond documenting incision rates and patterns, the Program is interested in the rate of incision progression. How long until incision and narrowing progress downstream of Overton and that segment begins to transition to the wandering channel observed below the J2 Return? A change from braided to wandering or even meandering planform could indicate the system is in disequilibrium, or could be a normal, equilibrium response to shifts in sediment supply as meandering rivers are usually associated with less bedload transport than braided or wandering rivers of equal size. These analyses indicate that vertical incision slowed dramatically by 2002 with the channel continuing to evolve via increasing meandering (lateral migration) in the three-mile reach below the J2 Return. This shift from vertical to lateral change was likely caused by a

number of factors, including but not limited to: a decrease in channel slope, armoring of the channel bed in the J2 Return Channel that limited vertical incision, and degradation of the channel below the root depth of bank vegetation which increased bank erodibility.

Overall, the retrospective analyses indicated the first wave of channel degradation (vertical incision) appears to have propagated down through the study area by 2002 with a total magnitude of incision of 16 feet at the J2 Return, four ft at the Overton Bridge and negligible incision at the upper end of Cottonwood Ranch. The second wave of channel degradation via lateral migration has been dominant since the early 2000s. The second wave relationships between incision, channel slope, and planform evolution are explored further in Chapters 3 and 4.

## *2.8    References*

Biedenharn, D. S., Allison, M. A., Little Jr, C. D., Thorne, C. R., & Watson, C. C. (2017). *Large-scale geomorphic change in the Mississippi River from St. Louis, MO, to Donaldsonville, LA, as revealed by specific gage records*. US Army Corps of Engineers, Mississippi Valley Division, Engineer Research and Development Center.

Chen, A.H., D.L. Rus, and C.P. Stanton (1999). Trends in Channel Gradation in Nebraska Streams, 1913-95. (Vol. 99, No. 4103). US Department of the Interior, US Geological Survey.

de Vries, M. (1973). "River-bed Variations - Aggradation and Degradation," Delft Hydraulic Laboratory Publication No. 107, Delft, Netherlands.

Fryirs, K. A., Brierley, G. J. (2005). Geomorphology and River Management: Applications of the River Styles Framework. Germany: Wiley

Graf, W. (1998). *Fluvial Hydraulics, Flow and Transport Processes in Channels of Simple Geometry*, John Wiley & Sons, New York, New York, 681 pp.

Hastie, T., and Tibshirani, R. (1990). Exploring the nature of covariate effects in the proportional hazards model. *Biometrics*, 1005-1016.

Holburn, E.R., Fotherby, L.M, Randle, and D.E. Carlson. (2006). Trends of Aggradation and Degradation Along the Central Platte River: 1985 to 2005. United States Bureau of Reclamation.

Leopold, L. B., & Wolman, M. G. (1957). *River channel patterns: braided, meandering, and straight*. US Government Printing Office.

Murphy, P.J., T.J. Randle, L.M. Fotherby, and J.A. Daraio. (2004). "Platte River channel: history and restoration". Bureau of Reclamation, Technical Service Center, Sedimentation and River Hydraulics Group, Denver, Colorado.

Powers, P.D., Helstab, M. & Niezgoda, S.L. (2019). A process-based approach to restoring depositional river valleys to Stage 0, an anastomosing channel network. River Research and Applications, 35(1), 3– 13. Available from: https://doi.org/10.1002/rra.3378

Rosgen, D. L. (1994). A classification of natural rivers. *Catena*, *22*(3), 169-199.

Samaranayake, V. A. (2009). The statistical review of three papers on specific gage analysis. *Rep., US Army Corps of Engineers*.

Turnipseed, D.P., and Sauer, V.B. (2010). Discharge measurements at gaging stations: U.S. Geological Survey Techniques and Methods book 3, chap. A8, 87 p. (Also available at http://pubs.usgs.gov/tm/tm3-a8/.)

**CHAPTER 3    Evaluation of longitudinal change after sediment augmentation in the Central Platte River, NE, USA**

### 3.1    Abstract

In this chapter we evaluated changes from a two-dimensional perspective with planform and profile analyses. This approach allowed us to target specific variables that are either hydrologically important or offer direct comparison with historical data. Implementation of annual REMs highlighted areas of aggradation and incision, and led to the identification of Station 70,000 as an area of active transition from braided to wandering planforms. Using changepoint analysis we found that average channel aggradation may be negatively correlated with flow in the J2 Return Channel and positively correlated with flow downstream of Overton Bridge. We compared wetted width and sinuosity to pre-augmentation data and found that both have increased over the past decades. Sinuosity appears to be continuing to increase gradually, while wetted width appears stable in more recent years. The spatial pattern of wetted width increasing in the downstream direction closely mirrors the spatial pattern of thalweg slope.

### 3.2    Introduction

In this chapter, our objective is to examine changes in our reach of interest since augmentation began from a two-dimensional perspective and evaluate the role of sediment augmentation in relation to these changes. This involved analysis of planform and profile data during the first five years of sediment augmentation implementation, (2017–2021), and the year prior to beginning augmentation (2016) during which topo-bathymetric data was also collected. Planform analyses made use of this data and pre-augmentation topographic-only LiDAR and aerial imagery. In the following sections, we present methods and results for analysis of annual relative elevation models (REMs), longitudinal analyses of thalweg elevation and mean channel elevation, and planform analyses of wetted width and sinuosity. We follow with a more detailed evaluation of channel incision and planform change near the midpoint between augmentation and the Overton Bridge (Station 70,000).

### 3.3    Relative elevation model

In Chapter 2, we introduced the relative elevation model (REM) as a tool to visualize channel planform and incision relative to the elevation of the floodplain. That chapter discussed incision patterns prior to augmentation. In this chapter, we extended the REM analysis through the augmentation experiment to evaluate change during augmentation.

#### 3.3.1    Methods

We developed annual (2016–2021) REMs of channel topography relative to average floodplain elevation using the methods described in Chapter 2 derived from Powers et al. (2019). REMs were generated by differencing annual LiDAR from the Geomorphic Grade Line (GGL) surface that approximates the elevation of the valley-scale floodplain in the reach. The resulting REM rasters were classified into two-foot intervals to observe topographic changes during the sediment augmentation experiment.

#### 3.3.2    Results

The 2016 and 2021 REMs for the segments of the study area upstream and downstream of the Overton Bridge are included in Figure 3.1 and Figure 3.2. In general, the pattern of incision

downstream of the J2 Return extends the length of the J2 Return Channel to the Overton Bridge (Figure 3.1). Headcutting (incision) is present in the lower section of the North Channel, in the breakthrough channel upstream of the J2 Return, and in the sand-dammed channel that was formerly connected to the North Channel (Figure E.1). This headcutting is due to the elevation of the affected channel segments adjusting to match the base level of the incising J2 Return Channel.
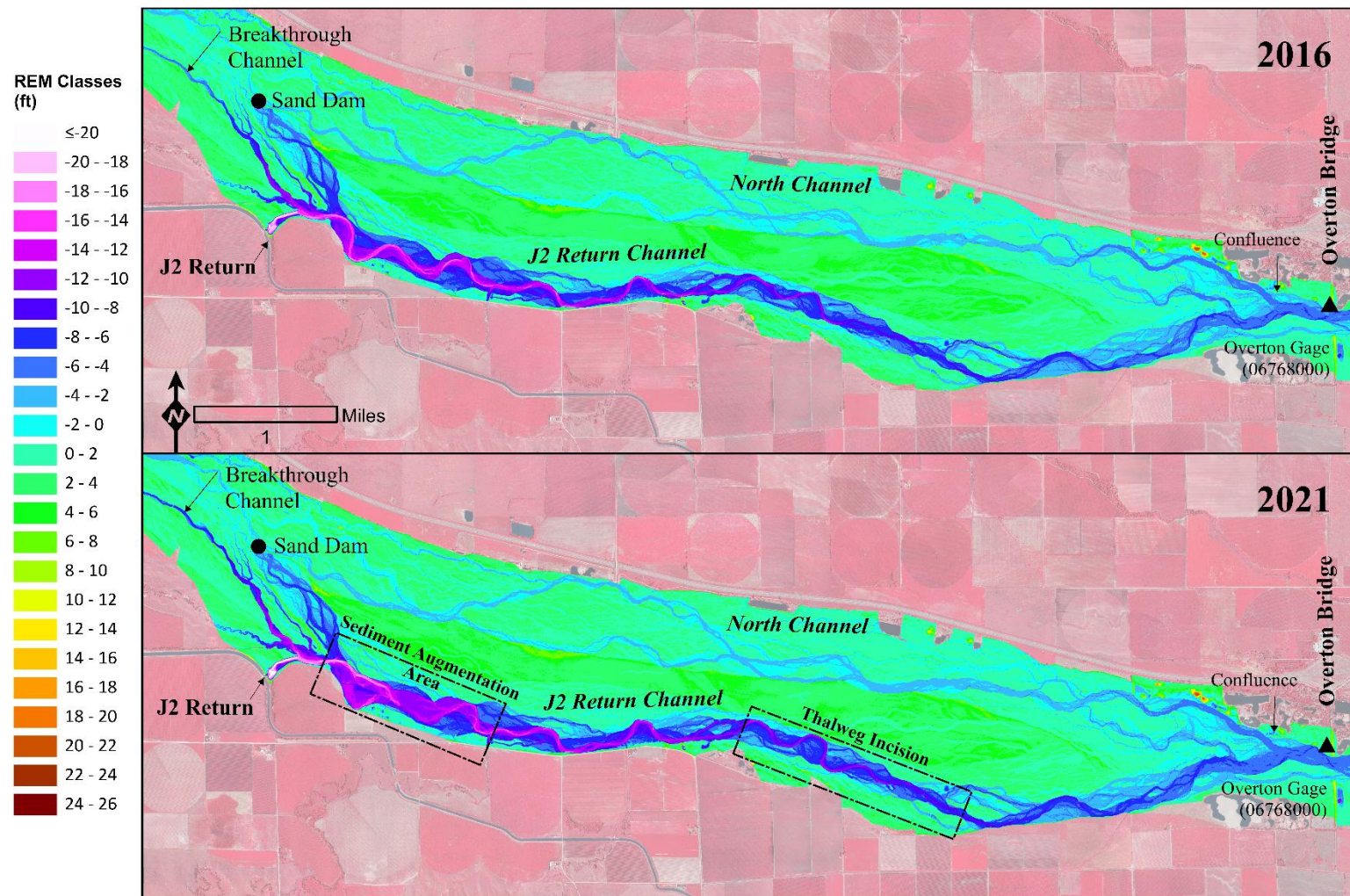
**Figure 3.1.** Relative elevation models (REMs) of the portion of the study area upstream of Overton in 2016 (top) and 2021 (bottom). The topographic signature of sediment augmentation is apparent in the 2021 REM as is a segment of thalweg incision midway between the J2 Return and Overton Bridge. More change occurred from 2016-2021 upstream of Overton Bridge than downstream (comparing Figure 3.1 to Figure 3.2 below).
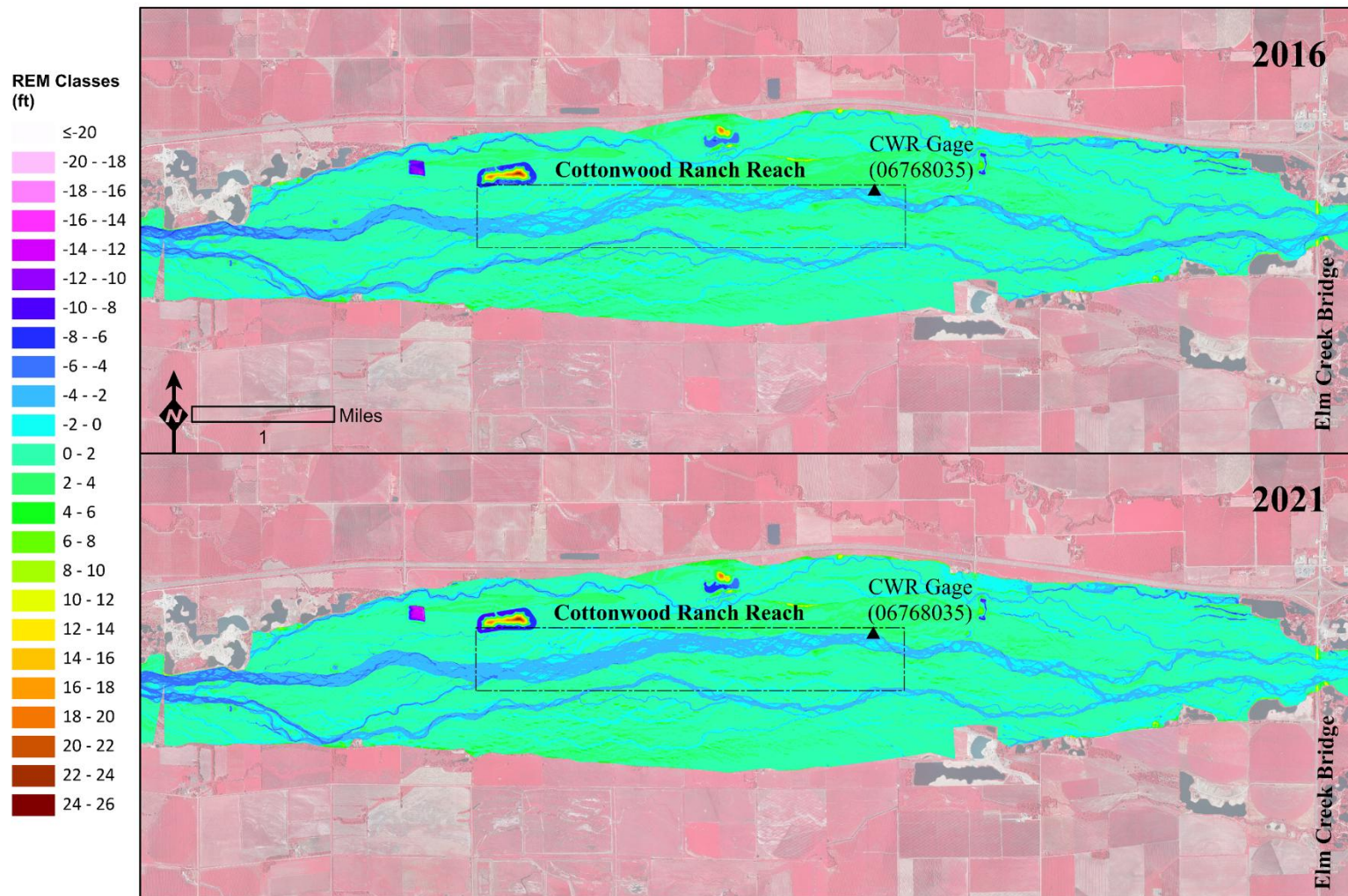
**Figure 3.2.** Relative elevation models (REMs) of the portion of the study area downstream of Overton to the Elm Creek Bridge in 2016 and 2021. Large changes to relative elevation are not apparent in this reach.
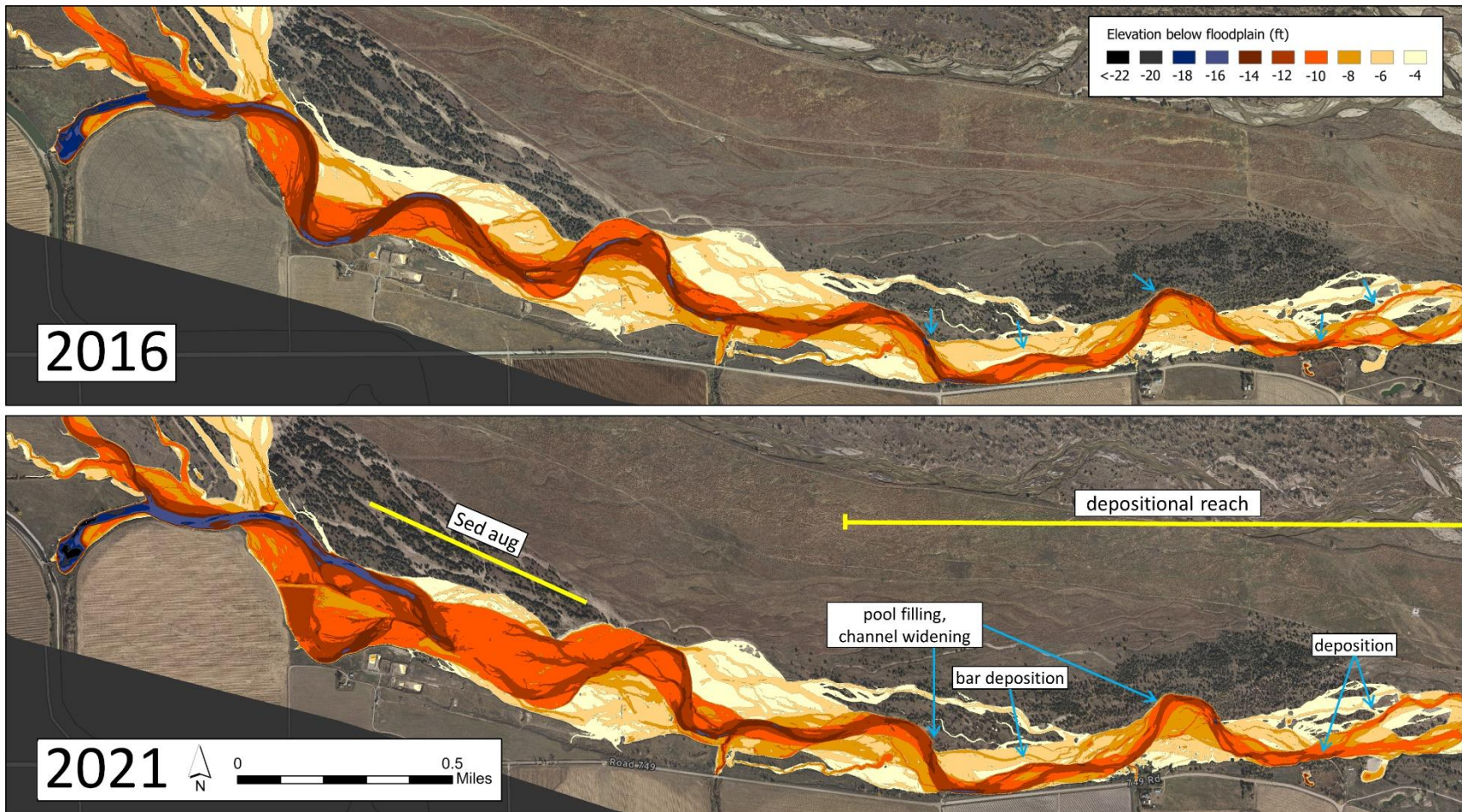
**Figure 3.3.** Annotated relative elevation model of the sediment augmentation area and downstream. The color scale illustrates four feet or more below the average floodplain and omits higher elevations. Incision occurred upstream of augmentation (blue) and deposition occurred downstream of augmentation.

When comparing 2016 and 2021 REMs upstream of Overton, changes are apparent in the J2 Return Channel. The scars of sediment augmentation projects are visible in the farthest upstream area, most notably the 2017 project which blocked a meander to protect private property, shifting the thalweg north (see Section 1.5.4). This shortening of the thalweg caused local erosion that is abruptly arrested by deposition from augmentation projects that occurred just downstream (Figure 3.3).  Downstream of the augmentation area, deposition occurred in the form of pool filling, channel widening, and bar deposition (Figure 3.3). Midway through the J2 Return Channel, an area of thalweg incision extends toward the Overton Bridge (Figure 3.1).

Below Overton Bridge (Figure 3.2), a small amount of pronounced incision is present downstream of the bridge but subsides near the upstream boundary of Cottonwood Ranch with thalweg elevation stabilizing at approximately 3 ft below the GGL. Despite year-by-year variations in the REMs of this reach, there is no signature of prolonged substantial change in relative elevations.

Given most channel change during the sediment augmentation experiment occurred in the segment upstream of the Overton Bridge, all annual REMs for that area are plotted together in Figure 3.4 with a continuous color scale ranging from -1 ft to -29 ft below GGL. In the sediment augmentation area, the sediment source locations for annual augmentation operations along the left (North) bank are apparent starting near the upper end of the augmentation area in 2017 and moving downstream through 2019. Augmentation operations subsequently moved back upstream in 2020 and 2021. Downstream, the area of channel incision and planform transition is located near Station 70,000 (Figure 3.4, outlined in yellow). Meandering intensity progressively increased in that area from 2016–2021.
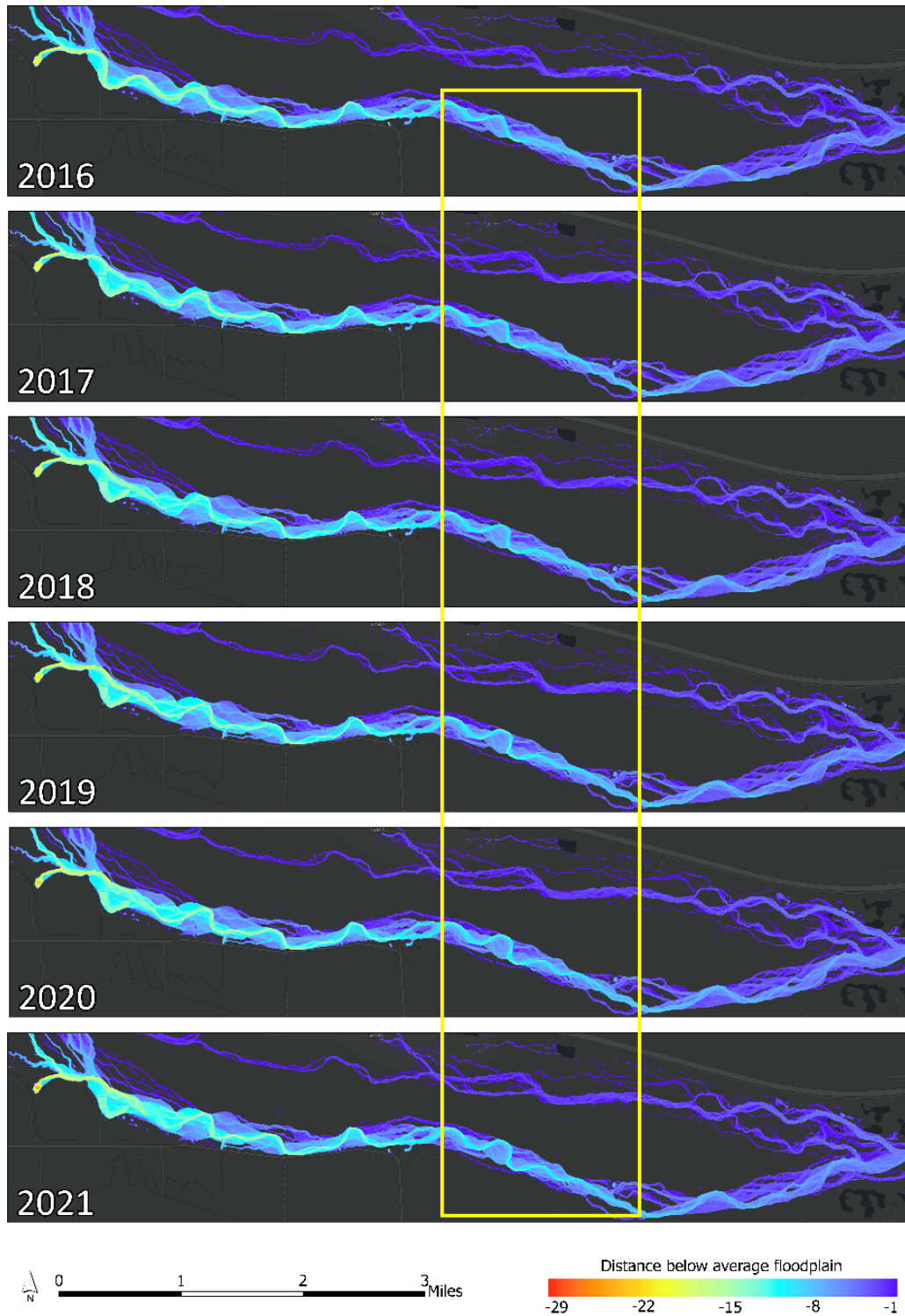
**Figure 3.4.** Annual relative elevation models (REMs) of the J2 Return Channel (2016 to 2021). Meander development and thalweg incision can be observed near Station 70,000 (yellow box).

### 3.4    Longitudinal profile of channel thalweg 2016–2021

While visual comparison of REMs is useful for identification of areas of changes during sediment augmentation, longitudinal profiles of the deepest point of the channel (thalweg) provide a more specific numerical measure of spatial and temporal patterns of aggradation or degradation during the sediment augmentation experiment. As discussed in Section D.1, LiDAR elevations in wet areas such as the channel thalweg are less accurate than LiDAR over dry areas (< 0.2 ft). Typical wet error was found to be within 0.3 ft of checkpoints and within 0.75 ft of checkpoints in 2019 due to higher flow and turbidity in that year. This error should be born in mind, however, we believe our conclusions are still valid despite the additional uncertainty.

#### 3.4.1    Methods

Annual thalwegs were delineated for each year of analysis using methods described in Section 2.3.1.

Changepoint analysis, a method of detecting statistically similar segments, was used to identify patterns in measured changes in mean thalweg elevations for the reach extending from the downstream end of the sediment augmentation area (Station 84,000) to Station 15,000[12]. Changepoints were calculated using the changepoint package in R version 4.2.2 (Killick et al., 2022; R Core Team 2022; Killick & Eckley 2014). We used the Pruned Exact Linear Time (PELT) method to detect multiple changepoints of sample mean, and the Changepoints for a Range of Penalties (CROPS) process to determine a manual penalty value of 200 on the log likelihood scale with diagnostic plots (Haynes et al., 2017 Killick et al., 2012). PELT is a dynamic programming technique that sequentially and iteratively optimizes changepoint locations, and CROPS automatically calculates all changepoint locations according to a variety of penalty values to assist with optimal penalty selection.

#### 3.4.2    Results

Figure 3.5 provides annual thalweg alignments for 2016–2021. Annual alignments in the upper half of the J2 Return Channel were consistent, except for several expanding meanders and the sediment augmentation area where thalweg location has been manipulated. The planform transition from single thread wandering (upstream) to braided (downstream) is also apparent in Figure 3.5. Approximately two miles upstream of the Overton Bridge, annual alignments begin to diverge with annual differences increasing spatially with channel width and braiding intensity. Annual differences are most apparent in the Cottonwood Ranch Reach in the Overton to Elm Creek Bridge segment and in the reach immediately upstream of the KCD (below the Elm Creek Bridge).

The longitudinal profiles for 2016 and 2021 are plotted in Figure 3.6 along with the Geomorphic Grade Line (GGL) for the study area. Both longitudinal profiles are convex in shape, with slope increasing in a downstream direction, away from the area of maximum incision immediately below the J2 Return. Differences in 2016 and 2021 thalweg profiles are apparent in the sediment augmentation area (upstream of Station 84,000) where the 2021 thalweg is higher than 2016 because of augmentation operations. Downstream in the J2 Return Channel, a segment between Stations 72,000 and 66,000 shows incision relative to the rest of the channel. Below the Overton

---

[12] Analysis ended at Station 15,000 to eliminate backwater effects from the Kearney Canal Diversion.

Bridge, thalweg elevations appear to have been stable through Cottonwood Ranch and increased upstream of the Elm Creek Bridge (Station 25,000 to 15,000), indicating the bed aggraded in that area. Thalweg slopes did not vary much between 2016 and 2021 when examined at a reach scale. At smaller scales, slope changes were apparent due to local thalweg change, but we did not observe a pattern of steepening or flattening on the J2 Return Channel during this period. The gradual shift from shallow slopes in the J2 Return Channel (0.00075 to 0.00095 ft/ft) to steeper slopes downstream of the North Channel confluence to the KCD (0.00106 to 0.00111 ft/ft) appears to be stable or changing too gradually to observe over this timescale (Figure 3.6).

Figure 3.7 provides annual thalweg profiles for the J2 Return Channel smoothed using 1,005 ft centered running average elevations to highlight annual profile changes. Thalweg elevations in the sediment augmentation area generally increased during the augmentation experiment as sediment from floodplain terraces was mechanically spread across the active channel. Downstream near Station 70,000, the highest magnitude of incision occurred between 2018 and 2019, with more stability from 2019 through 2021. We explore this segment in greater detail in Section 3.8.
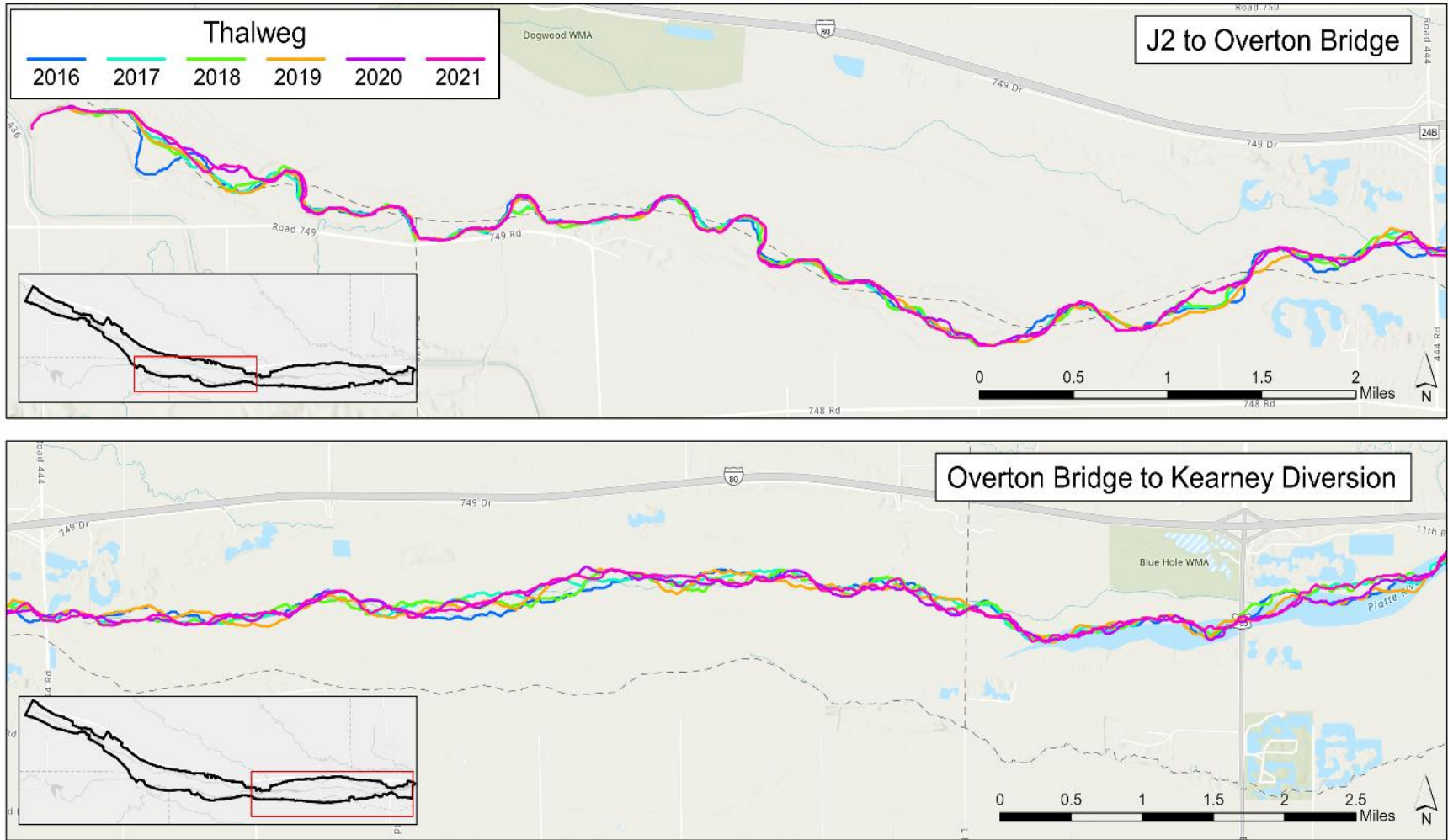
**Figure 3.5.** Annual thalweg alignments (2016–2021) derived from flow accumulation rasters. In the top panel, the transition from wandering to braided planform is present midway through the J2 Return Channel.
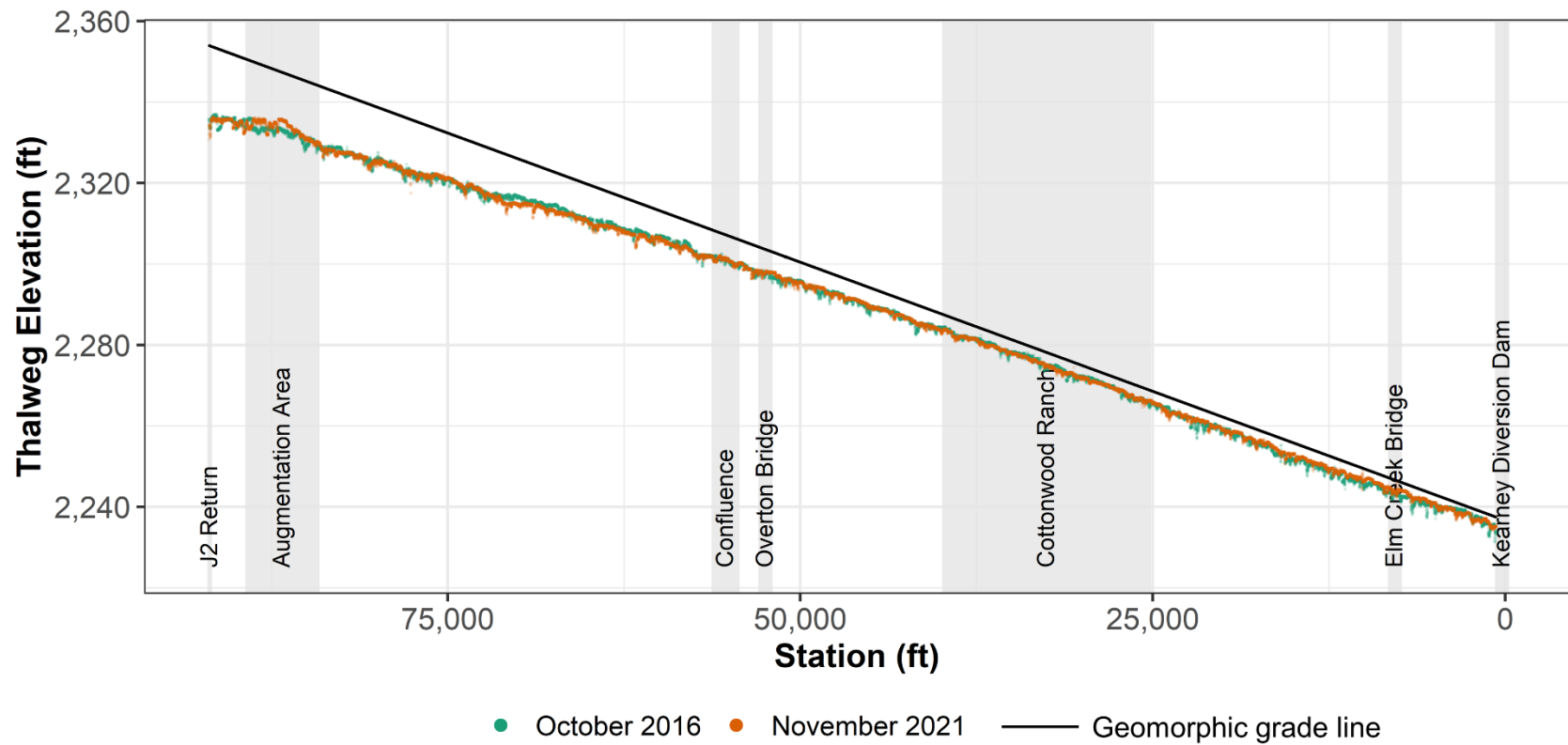
**Figure 3.6.** Longitudinal profile of thalweg elevation in 2016 (green) and 2021 (orange). The Geomorphic Grade Line (GGL) is shown in black as a reference for the magnitude of channel incision.
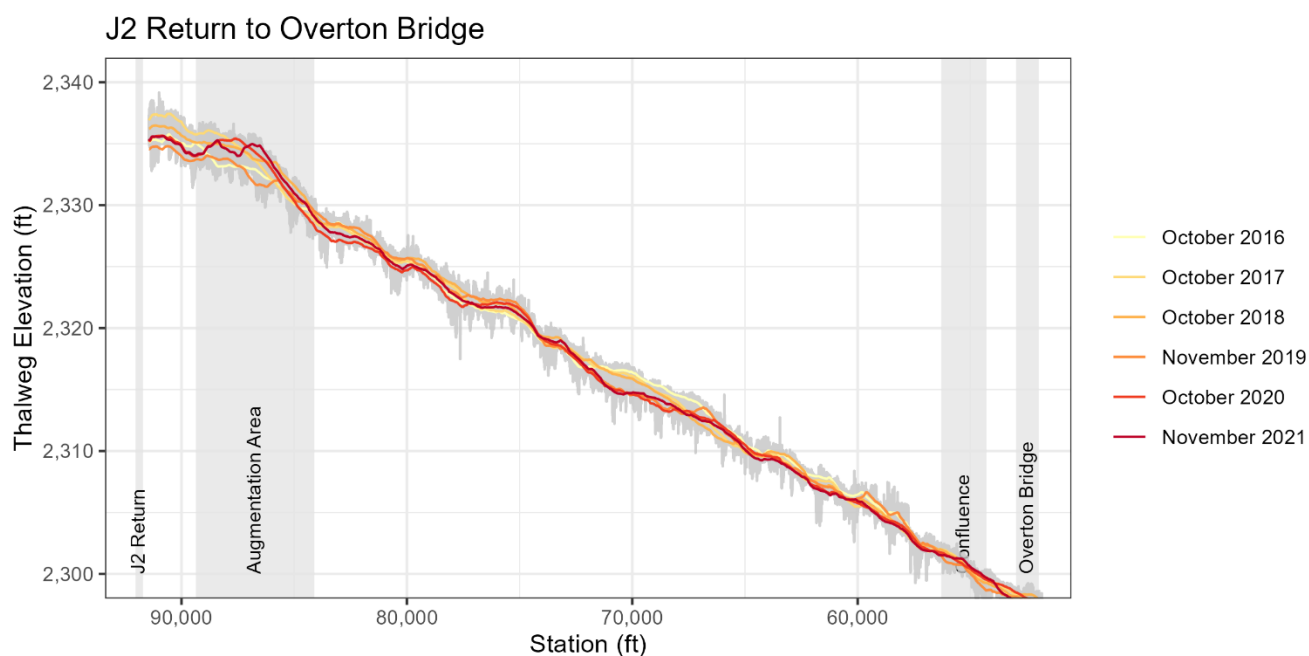
**Figure 3.7.** 2016–2021 annual moving average (1,005 ft) longitudinal profiles between J2 Return and Overton Bridge. Grey area behind profiles indicates the range of values for 2016–2021. Progressive thalweg aggradation is apparent in the sediment augmentation area and progressive degradation is apparent downstream in the vicinity of Station 70,000.

Segments of mean change derived from the changepoint analysis for the entire augmentation period (2016–2021) are presented in Figure 3.8 and mean change values are provided in Table 3.1. After five years of augmentation, mean change in thalweg elevation in the first 2.3 miles downstream of the augmentation area ranged from -0.3 to +0.4 ft. This is followed by an approximately one-mile reach with the most prominent incisional trend in the study area. The incisional reach extends from roughly Station 72,000 downstream to Station 66,000 with mean thalweg incision of -1.3 ft. The thalweg also incised in the reach immediately downstream with mean thalweg elevation loss of -0.64 ft. Continuing downstream, the channel transitioned to slight aggradation (+0.2 ft) near the J2 Return Channel confluence with the North Channel. Near Cottonwood Ranch, mean change shifted to slight thalweg incision (-0.2 ft). Downstream of Cottonwood Ranch, thalweg elevation increased by an average of 0.5 ft.
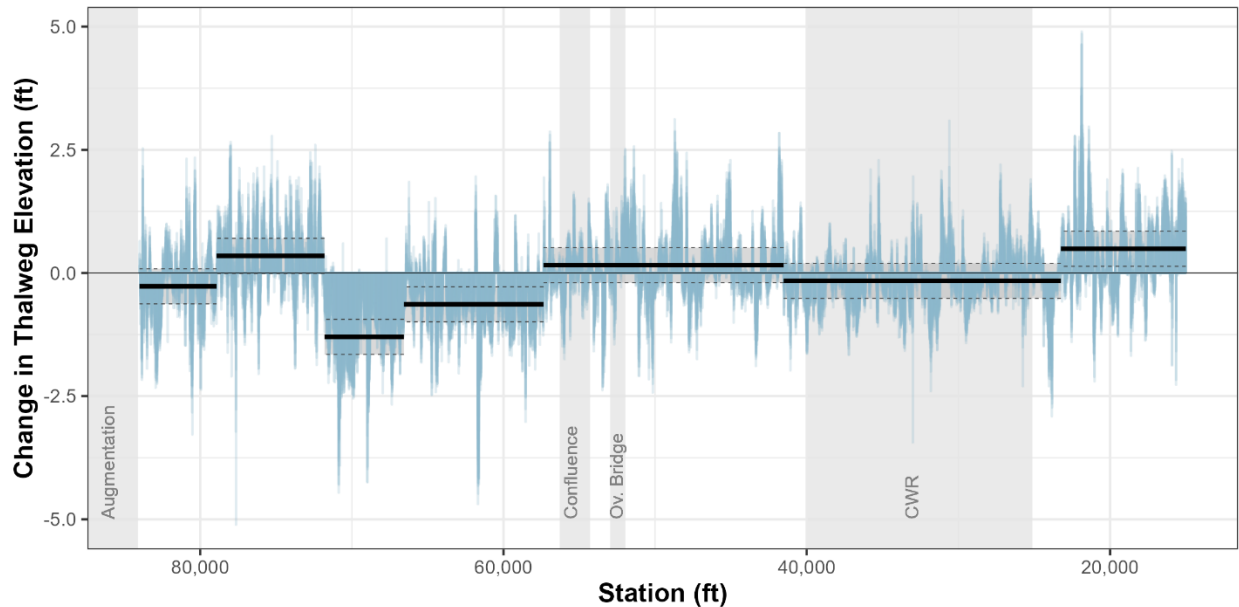
83

**Figure 3.8** 2016–2021 thalweg changepoint analysis results. Differences in thalweg elevations shown in blue. Mean segment change values shown in black. Negative numbers indicate thalweg incision and positive indicate thalweg aggradation. Shaded areas with bounding dotted lines represent the propagated error from LiDAR collection for 2016 and 2021 (0.356 ft).

**Table 3.1.** 2016–2021 thalweg changepoint analysis results.

| Station Range | Segment Length (mi) | Thalweg Elevation Change (ft) | | |
|---|---|---|---|---|
| | | **Mean** | **Minimum** | **Maximum** |
| 84,000–78,915 | 1.0 | -0.3 | -2.3 | 4.9 |
| 78,915–71,805 | 1.3 | 0.4 | -3.4 | 3.1 |
| 71,805–66,570 | 1.0 | -1.3 | -2.4 | 3.1 |
| 66,570–57,360 | 1.7 | -0.6 | -4.7 | 2.0 |
| 57,360–41,520 | 3.0 | 0.2 | -4.5 | 0.7 |
| 41,520–23,240 | 3.5 | -0.2 | -5.1 | 2.8 |
| 23,240–15,000 | 1.6 | 0.5 | -3.3 | 2.5 |

Changepoint analyses were also utilized to detect segments of mean change for each set of consecutive years during the augmentation experiment to evaluate inter-annual variability (Figure 3.9). In the J2 Return Channel, the segment around Station 70,000 shows persistent loss from 2016 to 2019, with the most loss occurring in 2019. The thalweg was stable in that area in 2020 and aggraded slightly in 2021. Downstream of the Overton Bridge, the annual changepoints indicate relative thalweg stability. Table 3.2 shows annual mean thalweg changes summarized by their location either upstream or downstream of Overton Bridge. See Section D.2 for further discussion on flow data.
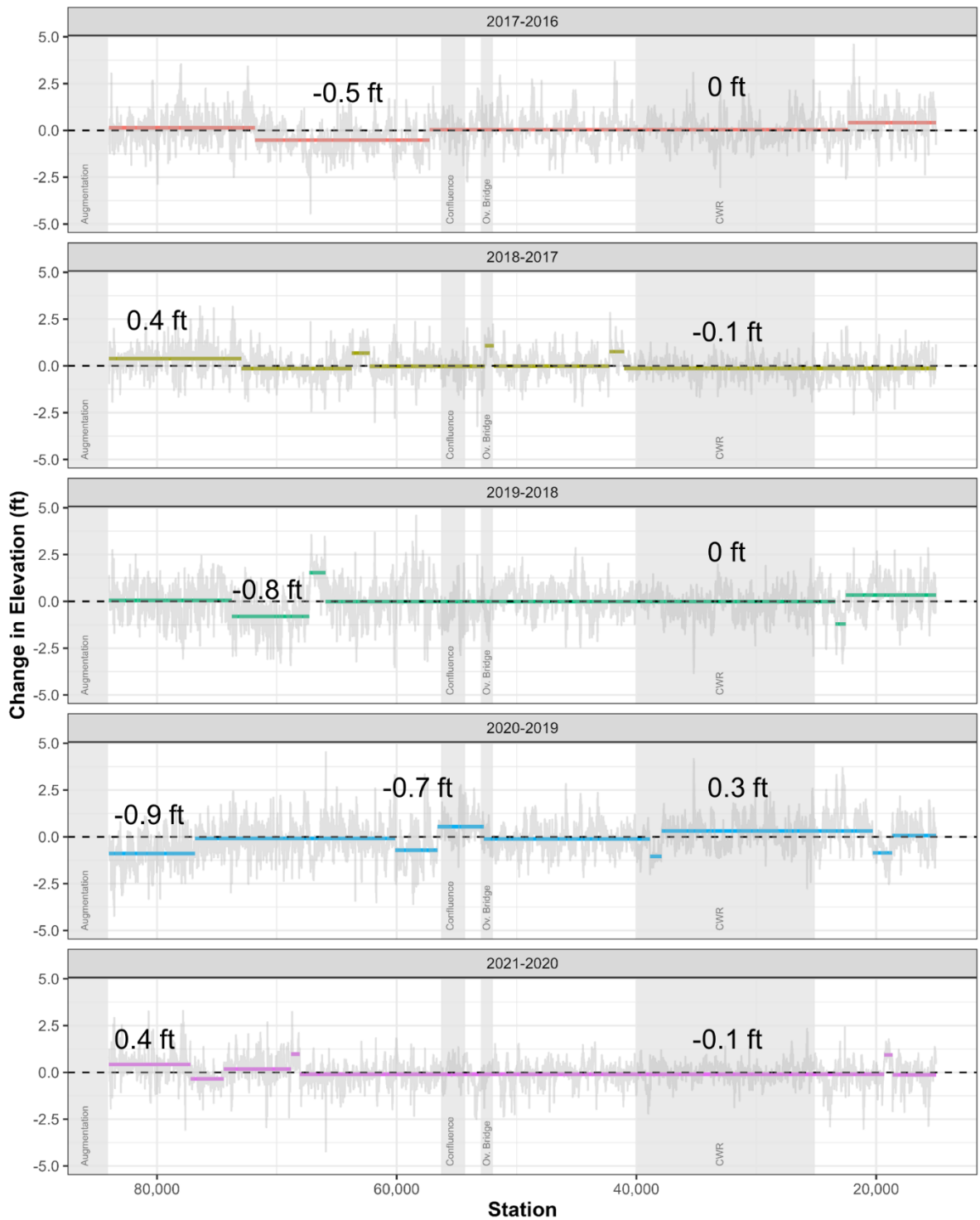
**Figure 3.9.** Annual changepoint analysis results of change in thalweg elevation between years. Colored lines show mean change values of changepoint segments. Light grey lines show at-a-station thalweg elevation difference.

**Table 3.2.** Average thalweg changes upstream and downstream of Overton Bridge with mean flow for comparison.

| Year | Mean Thalweg Change (ft) | | Mean Discharge at Overton Bridge (cfs) | Mean J2 Return Flow (cfs) |
|---|---|---|---|---|
| | J2 Return Channel | Downstream of Overton | | |
| 2016–2017 | -0.17 | 0.11 | 1,780 | 1,099 |
| 2017–2018 | 0.13 | -0.05 | 1,289 | 807 |
| 2018–2019 | -0.10 | 0.04 | 2,082 | 1,155 |
| 2019–2020 | -0.26 | 0.05 | 2,127 | 1,225 |
| 2020–2021 | 0.04 | -0.06 | 1,008 | 589 |

### 3.5    Longitudinal profile of mean channel elevation 2016–2021

Longitudinal profiles of thalweg elevations are useful in evaluating incision and slope change during the sediment augmentation experiment. However, they only describe changes to the deepest part of the channel. We also examined longitudinal profiles of average cross-sectional elevation to quantify dispersed channel change beyond the thalweg.

### 3.5.1   Methods

To calculate average cross-sectional elevation, we first clipped stationed channel transects to confine them to the active channel, defined as the portion of the channel wetted at a discharge of 2,500 cfs in the J2 Return Channel and 2,500 cfs in the North Channel. This results in a total flow of 5,000 cfs downstream of the J2 Return and North Channel Confluence. These flows represent the approximate bankfull (50% probability) flow for the reach. Wetted area was modeled for each year with SRH-2D  (Lai, 2008), using 2016–2021 LiDAR (PRRIP 2022b). Flow area polygons for each year were merged into a single polygon capturing the entire wetted area during the management experiment. After transects were clipped to the limits of the active channel, we sampled LiDAR DEM elevations at 3 ft intervals along each clipped transect and calculated the average elevation. Mean elevations were plotted by station for each year. At-a-station differences were calculated for each pair of consecutive years from 2016 through 2021, and for the difference between 2021 and 2016. Increases in mean channel elevation indicate aggradation due to depositing material. Material sources in this case include sediment augmentation, lateral erosion, and upstream transport. The merged polygon used to clip our transects includes inactive floodplain elevations that may have been incorporated into the active floodplain via lateral erosion over the course of the study period. As a result, reductions in mean channel elevation through time can be the result of either lateral erosion or bed erosion.

### 3.5.2   Results

The longitudinal profiles of average cross-sectional elevation for 2016 and 2021 are plotted in Figure 3.10 along with the GGL. Like the channel thalweg, the longitudinal profile of average cross-sectional elevation diverges from the GGL due to incision downstream of J2 Return. Maximum divergence from the GGL occurs near the J2 Return. The profile gradually converges with the GGL in a downstream direction. Through the Cottonwood Ranch Reach, the average

cross-sectional elevation is nearly parallel with the GGL and close to the predicted GGL elevation. Downstream of Station 12,000 (near Elm Creek Bridge) the profile of mean elevation converges with GGL due to the backwater effect and consequent upstream aggradational influence of the KCD. The average elevation in the sediment augmentation area (above Station 84,000) decreased between 2016 and 2021 as a result of augmentation (Figure 3.10). Station 71,250 also experienced a decrease in mean elevation. Overall, elevation change from 2016 to 2021 was more evident in the J2 Return Channel than downstream of Overton Bridge.
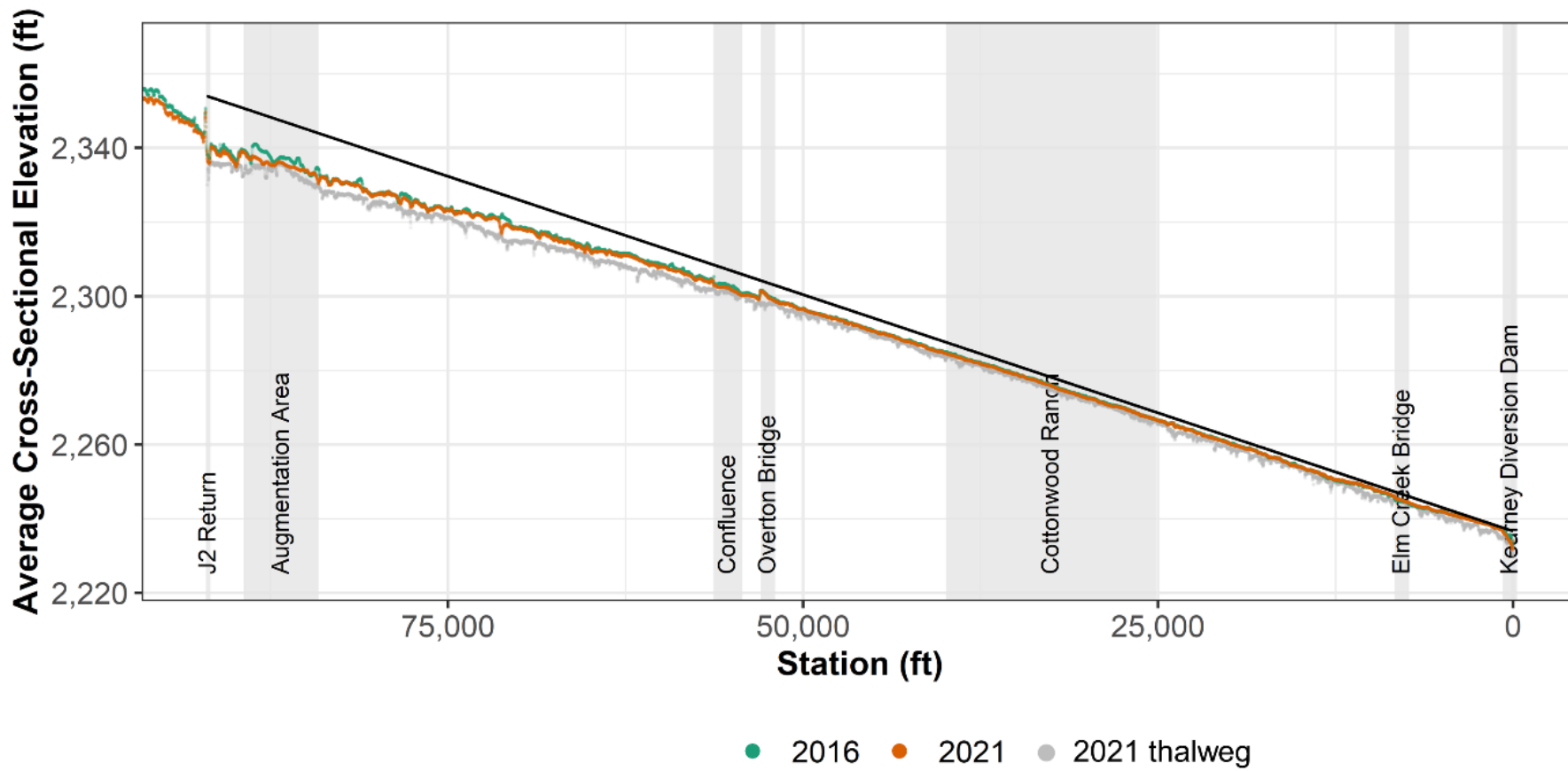
**Figure 3.10.** Average cross-sectional elevation longitudinal profile. The geomorphic grade line and 2021 thalweg are shown for reference.

Figure 3.11 provides annual mean channel elevation profiles for the J2 Return Channel smoothed using 1,005 ft centered running average elevations to highlight annual profile changes. Mean channel elevation decreased in the sediment augmentation area through the augmentation experiment due to mechanical removal of sediment from floodplain terraces and placement into the active channel. Downstream of the augmentation area, areas of large progressive decline in mean channel elevation are apparent near Stations 82,000, 78,000 and 72,000. These are areas with meanders that are actively migrating via lateral erosion of cutbanks and deposition on point bars. Progressive decline is also a pattern downstream of 72,000 to Overton Bridge between 2016 and 2021.
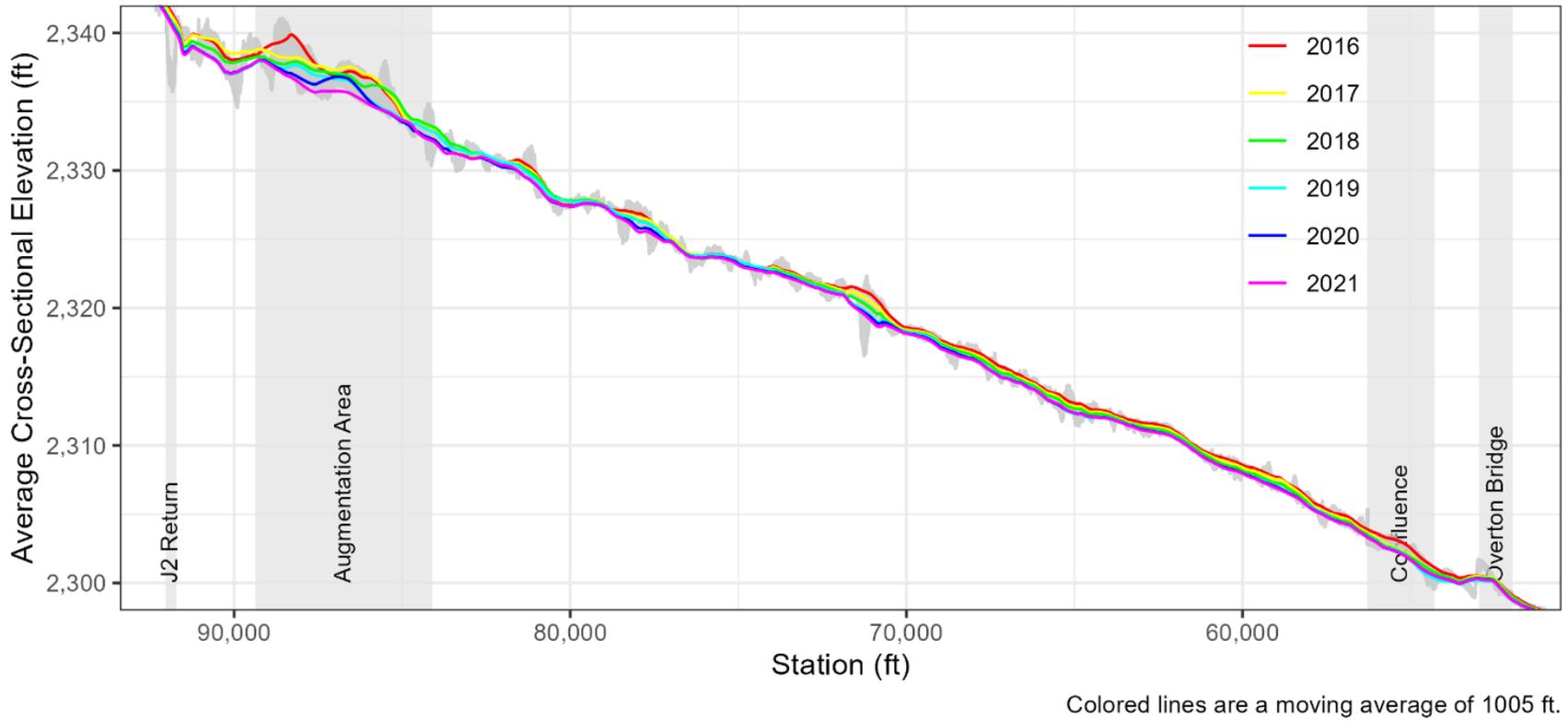
## J2 Return to Overton Bridge



**Figure 3.11.** Average cross-sectional elevation longitudinal profile in the J2 Return channel. Colored lines are a moving average of 1005 ft and grey lines show the range of values for 2016–2021.

Combining thalweg and mean channel elevation changes into one figure (3.12) provides a comprehensive view of in-channel changes during the augmentation experiment. General degradation can be detected when both thalweg and average elevations decrease (see Station 72,000 to Overton Bridge), while lateral erosion or channel widening can be detected by a decrease in average elevations accompanied by increase in thalweg elevations (see the augmentation area). Downstream of Overton Bridge, changes in average and thalweg elevations are not strongly positive or negative until station 25,000 where aggradation is indicated.  These patterns of erosion and deposition can be more directly assessed through a three-dimensional analysis of volume change that discriminates between lateral and bed erosion. That analysis is presented in Chapter 4.
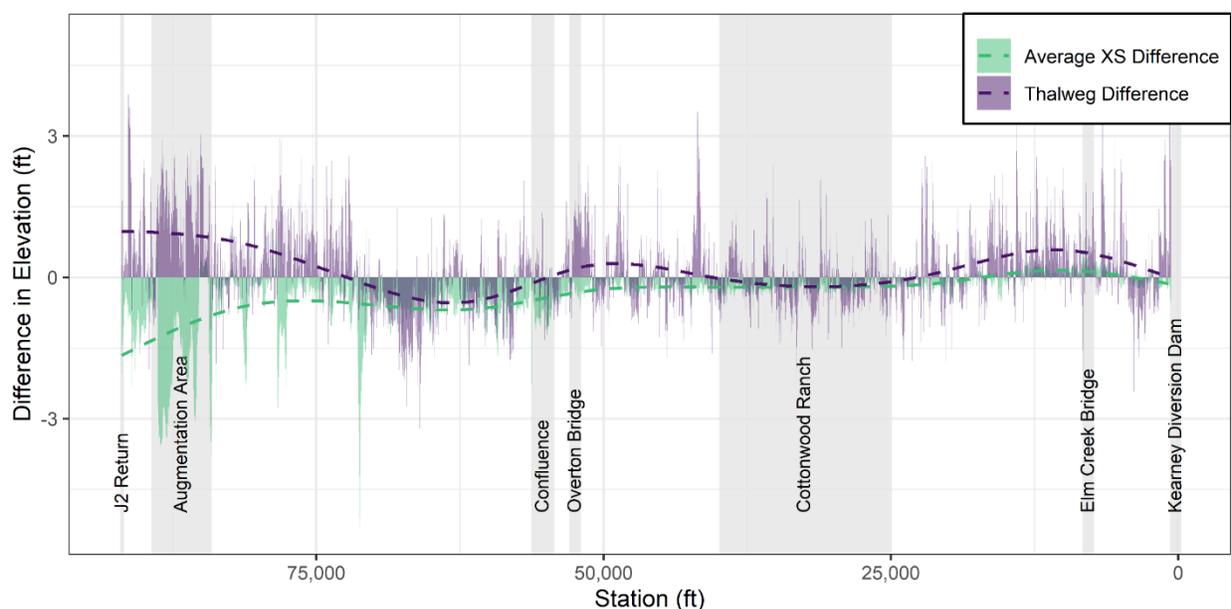


**Figure 3.12.** Differences in thalweg and average cross-sectional elevation from 2016 to 2021. A line depicting general trends was estimated with a generalized additive model.

### *3.6    Wetted Width*

As discussed previously, a portion of the J2 Return Channel transitioned from a historically wide braided planform to a narrow wandering planform over several decades after the J2 Return began operations in the 1940s. Evaluating spatial and temporal trends in wetted width, or the width of channel inundated by water during a reference flow, provides clues about the progression of incision and narrowing in the J2 Return Channel as well as potential effects of sediment augmentation.

### 3.6.1    Methods

Analyses of wetted widths are necessarily tied to one or more reference flows. For this analysis, we used a flow of 2,000 cfs to remain consistent with ongoing system-scale monitoring efforts (PRRIP EDO, 2022a). In general, 2,000 cfs is the approximate flow in the J2 Return Channel when

the return is operating at full capacity.[13] Downstream of Overton, a flow of 2,000 cfs was chosen for system-scale analyses of wetted width as it is sufficient to inundate bedforms and fill the entire channel without overtopping banks.

Wetted widths prior to and during the augmentation experiment were modeled using a combination of one-dimensional (1D) and two-dimensional (2D) hydraulic models of the study area. Wetted widths in 2009 and 2012 were modeled in 1D HEC-RAS at 78 cross-sections (PRRIP 2022a, HEC-RAS 2008) spaced an average of 1,165 ft apart through the study area. These models pre-dated topo-bathymetric LiDAR and relied on a combination of terrestrial LiDAR and supplemental field surveys. Once topo-bathymetric LiDAR were available in 2016, the Program shifted to annual two-dimensional hydraulic modeling using the Bureau of Reclamation SRH-2D modeling platform (Lai 2008) See Section D.3 for further discussion of hydraulic models, calibration, and validation. To provide for a direct comparison of HEC-RAS and SRH-2D wetted widths, we clipped HEC-RAS cross station lines to SRH-2D water surface polygons (2016, 2017, 2021) which allowed us to report 2D wetted widths at 1D cross section locations. Statistical tests of differences between mean width in three reaches (augmentation area, J2 Return Channel, and downstream of Overton) were completed with the emmeans package in R version 4.2.2 (Lenth 2023).

### 3.6.2   Results

The results of the wetted width analysis can be viewed as a continuum from upstream to downstream (Figure 3.13) or broken into three reaches and averaged (Table 3.3). The first reach is from the J2 Return to the downstream boundary of the augmentation area. This is the reach in which the channel was mechanically widened by bulldozing terraces and spreading the terrace sediment over the channel bed. Because of augmentation activities, widths in this reach increased dramatically in 2017, the first year of sediment augmentation. The second reach extends from the downstream boundary of the augmentation area to the Overton Bridge. This reach shows year-to-year width variations, but on average no progressive widening or narrowing (Table 3.3). In this reach, Tukey-adjusted pairwise comparisons of mean width between years do not reveal significant change in sequential years but do detect a significant difference between 2009 and 2016 wetted widths, with 2009 having higher width on average in the J2 Return Channel between stations 84,000 and 55,000 (mean difference 120 ft, $p < 0.025$ at the 95% confidence level). Pre-2016 widths are derived from a 1D model while post-2016 widths are derived from a 2D model. While this inconsistency should not obfuscate large changes, it precludes fine-scale analysis of year-to-year variation. Downstream of the Overton Bridge, the channel receives water inputs from both the J2 Return Channel and the North Channel, making it subject to natural high flow events in a way that the J2 Return Channel is not.  A high flow event in 2015 had a large morphological impact on the reach downstream of Overton including substantial bank erosion (Figure 3.14). The result of this event can be seen in the 50% increase in width from 2012 to 2016 below the confluence. This increase in width was maintained with additional slight increases during the sediment augmentation experiment. These width increases had a positive impact on Whooping Crane habitat.

---

[13] J2 Return flow of approximately 1,800 cfs and an additional 200 cfs of groundwater return flows.
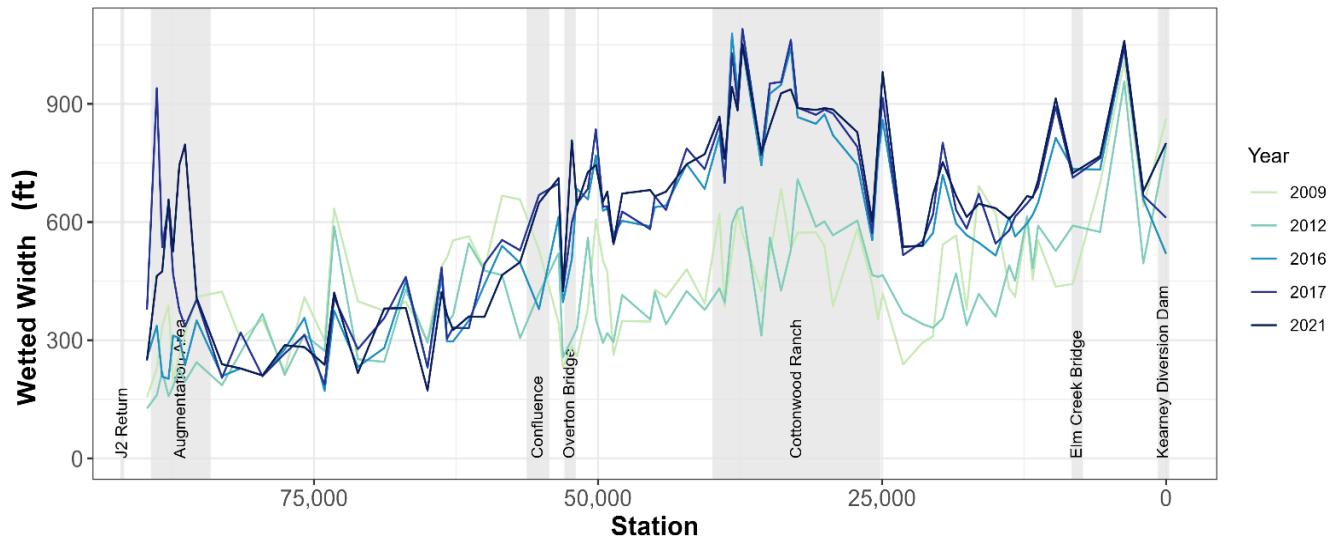
**Figure 3.13** Wetted width at HEC-RAS cross-sections in 2009–2021 at a flow of 2,000 cfs. Widening due to augmentation (2017, 2021) is visible upstream of the Augmentation Boundary and widening due to the 2015 flood visible downstream of Overton Bridge.



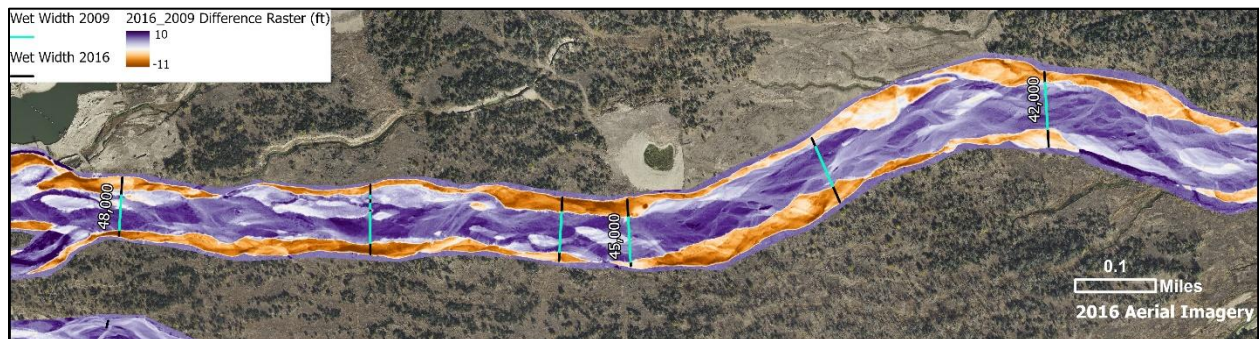**Figure 3.14** Significant channel widening is evidenced in the 2016 to 2009 difference raster by the regular pattern of erosion (orange) along channel banks between stations 48,000 and 42,000. This pattern begins at the confluence of the J2 Return and North Channels and continues to Elm Creek Bridge. Year by year comparison of LiDAR data indicates that the majority of the widening occurred in 2015.

**Table 3.3** Mean wetted width and standard deviation (SD) in three reaches, measured at 78 HEC-RAS cross-section locations. Augmentation beginning in 2017 increased width in Reach 1. Flooding in 2015 caused Reach 3 to widen between 2012 and 2016.

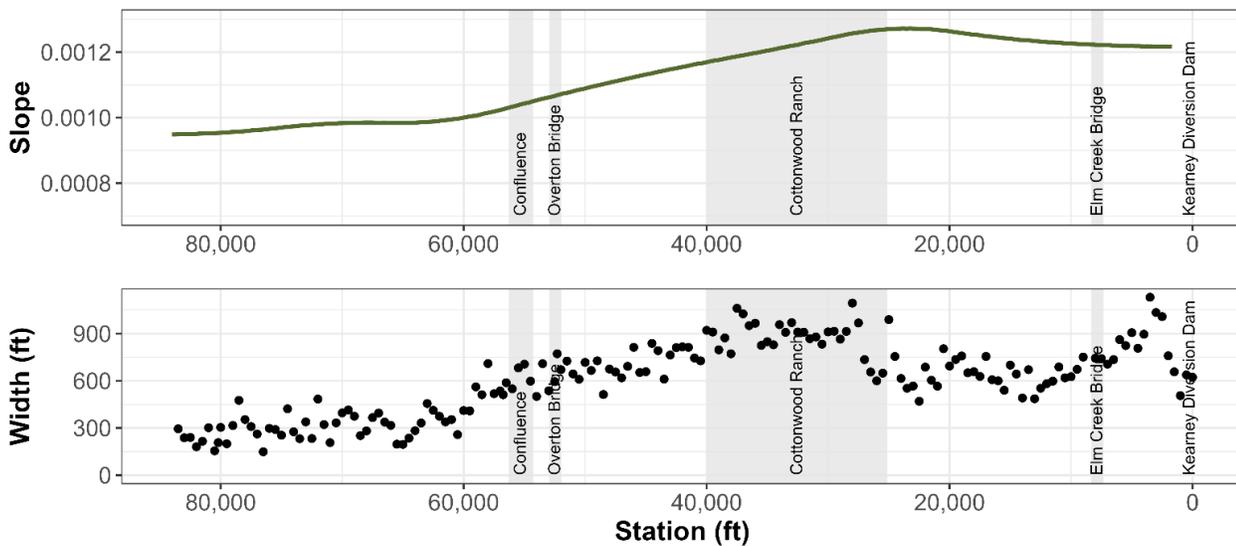| | Reach 1 J2 to Augmentation Boundary | | Reach 2 Augmentation Boundary to Overton | | Reach 3 Overton to KCD | |
|---|---|---|---|---|---|---|
| Year | Mean (ft) | SD (ft) | Mean (ft) | SD (ft) | Mean (ft) | SD (ft) |
| 2009 | 290 | 90 | 440 | 130 | 490 | 150 |
| 2012 | 190 | 40 | 360 | 120 | 480 | 140 |
| 2016 | 280 | 60 | 350 | 120 | 720 | 160 |
| 2017 | 510 | 200 | 380 | 150 | 740 | 150 |
| 2021 | 540 | 180 | 360 | 140 | 760 | 130 |



**Figure 3.15.** 2021 channel slope of the GAMM-modeled thalweg (top) and wetted width at 2,000 cfs (bottom). Width and slope increase together between Station 60,000 and 30,000.

We compared 2021 wetted width with channel slope to examine slope-width relationships in the study area (Figure 3.15). To reduce noise in our slope data, we used a Generalized Additive Mixed Model (GAMM) with a sampling distance of 100 ft to fit a line to the thalweg profile and calculated slope with a moving window. In 2021, there is an upward inflection in both slope and wetted width near Station 60,000. Between Station 60,000 and 30,000, both width and slope appear to increase together. Below Station 30,000, both width and slope decrease. However, width decreases more substantially than slope. This mirrored pattern suggests links between slope and width behavior; however, we acknowledge that many other variables such as flow and sediment supply are likely impacting these characteristics.

### 3.7   Sinuosity of the J2 Return Channel

Similar to wetted width, evaluating spatial and temporal trends in sinuosity provides clues about the progression of incision and narrowing in the J2 Return Channel as well as potential effects of sediment augmentation.

### 3.7.1   Methods

We analyzed pre-augmentation changes in channel sinuosity in the J2 Return Channel between 1969 and 2016 using hand-delineated channel thalwegs from aerial imagery (see Chapter 2). For the analysis of post-augmentation sinuosity, we used geoprocessing techniques described in Section 2.3.1 to delineate thalwegs from topo-bathymetric LiDAR. These lines were then smoothed in ArcGIS Pro version 3.0.3 using polynomial approximation with an exponential kernel smoothing algorithm and a tolerance of 300 ft. We compared the smoothed LiDAR-derived thalwegs to hand-delineations for overlapping years and found results to be similar, although hand-delineations yielded a higher average sinuosity by 0.01. Therefore, we plot and interpret sinuosity derived from both methods together.

### 3.7.2   Results

Sinuosity results are presented in Figure 3.16. Prior to initiation of sediment augmentation, sinuosity of the J2 Return Channel had increased steadily, though with low magnitude, since the early 2000s. Sinuosity declined in 2017 due to the construction of a meander cutoff immediately below the J2 Return (see Chapter 1). The cutoff rerouted the channel to avoid erosion of private property and straightened the alignment of the channel, decreasing length by about 1,300 ft. After 2017, sinuosity continued to increase throughout the duration of the augmentation management experiment. This is due to the continued development of meanders in the wandering segment of channel. The increase in sinuosity of the J2 Return Channel is not dramatic but the pattern shows a consistent increase in recent decades that is evidence for the onset and development of the observed changes in channel pattern. While sinuosity is not high enough to signify the existence of a clear and consistent transition to meandering, the trend in sinuosity increase supports visual analysis that this transition has begun and could continue.
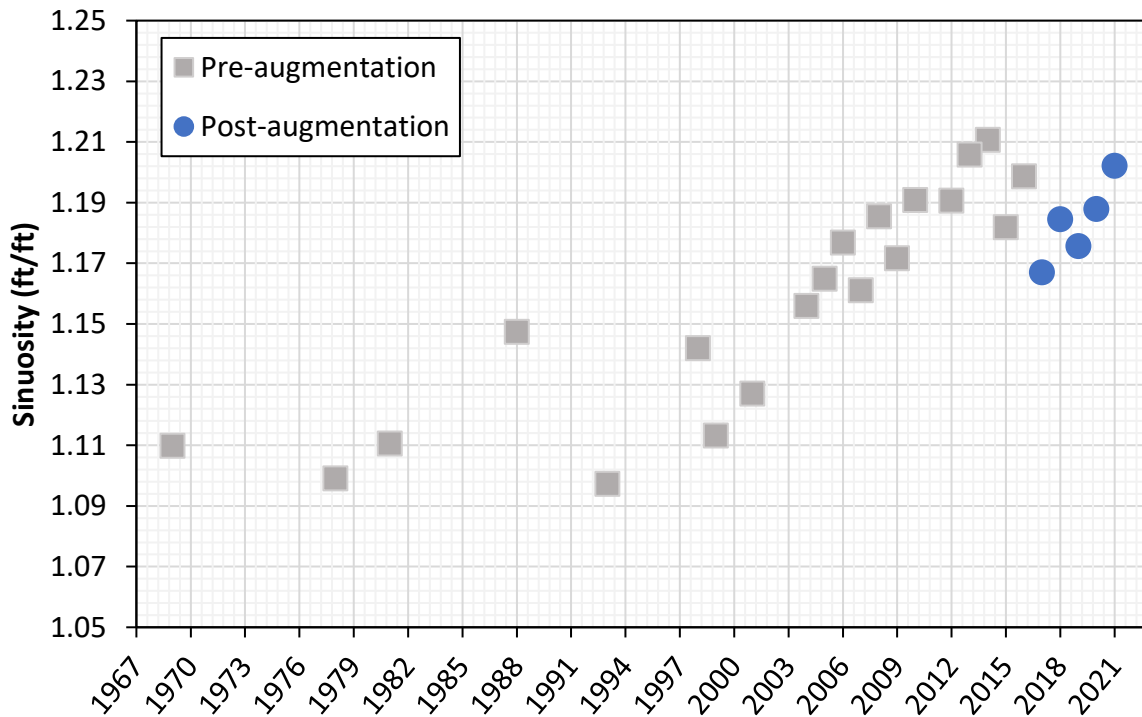
**Figure 3.16** Ratio of thalweg to straight-line length (sinuosity) in the J2 Return Channel between 1969 and 2021. Figure shows a trend in increasing sinuosity beginning in the early 2000s. Sinuosity declined in 2017 due to the construction of a meander cutoff as part of augmentation operations. Despite the cutoff, the trend of increasing sinuosity continued during the augmentation experiment.


### 3.8    Focused analysis of incision in the vicinity of Station 70,000

We identified a reach of river extending from Station 72,000 to 65,000 that required deeper investigation due to higher magnitude of change relative to other river segments. The reach is referred to as Reach 70,000 due to its proximity to River Station 70,000. In addition to a more detailed evaluation of prior analyses, we measured six channel cross sections from LiDAR data in this reach to provide a cross-sectional view of channel change during the augmentation experiment.

A detailed plot of 2016 and 2021 longitudinal profiles of the thalweg, 1,005 ft centered moving average thalweg elevations, and GAMM-predicted thalweg elevations (see section 3.6.2) is presented in Figure 3.17 with planview alignments presented as a reference in Figure 3.18. Comparison of the profiles indicates at-a-station change was highly variable with the highest magnitude of incision near Station 71,000 at the apex of a meander. Overall, the modeled thalweg profiles indicate significant incision of the thalweg beginning at Station 73,000 and ending at approximately Station 57,000. Within this reach the maximum magnitude of modeled thalweg incision (> 2 ft) occurred in the vicinity of Station 70,000.
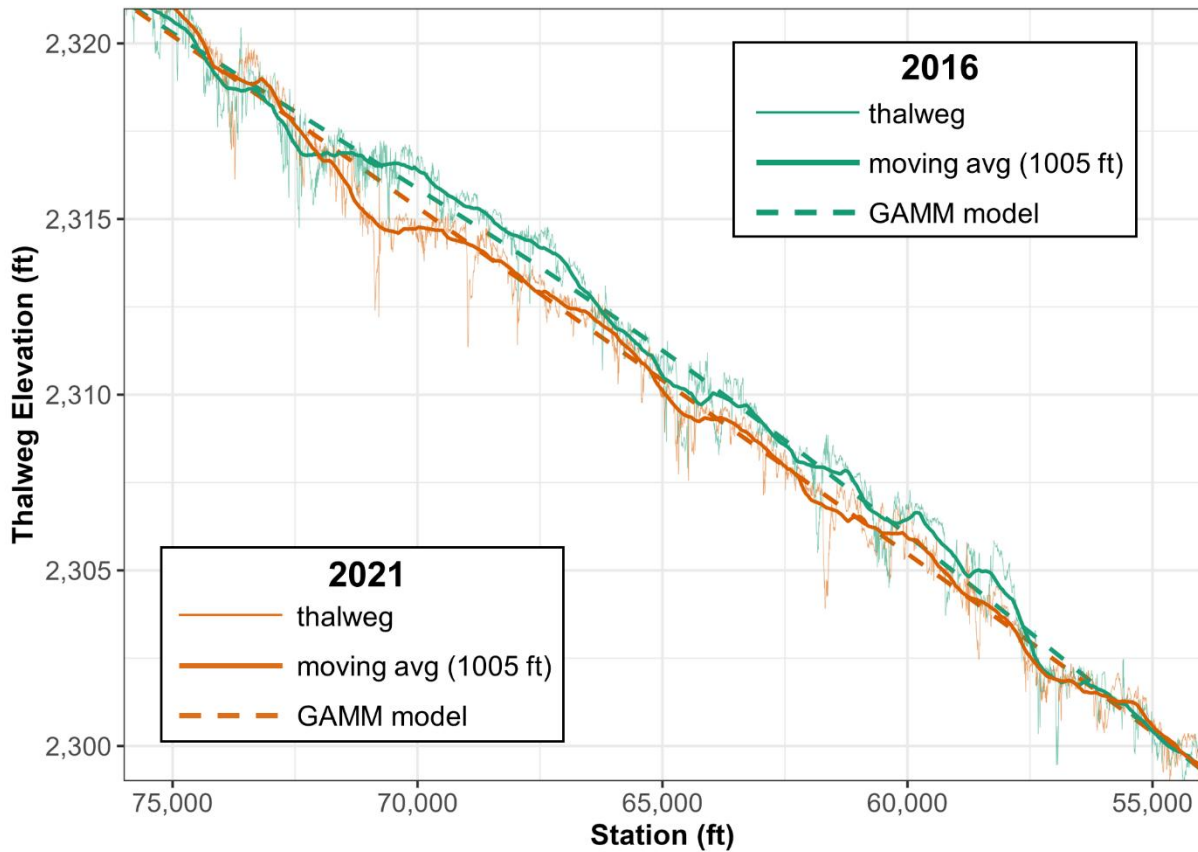
**Figure 3.17.** Longitudinal thalweg profiles and thalweg models (GAMMs) for 2016 and 2021 between Station 75,000 and 55,000.
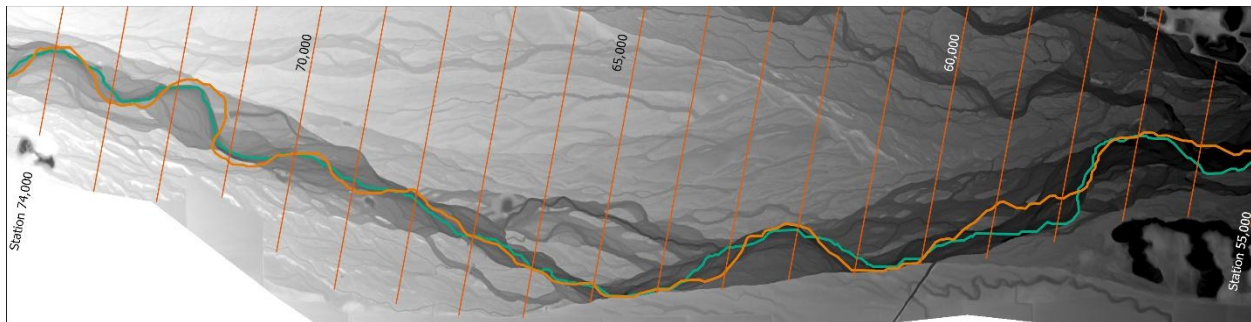


**Figure 3.18**. Planview of thalweg alignments in 2016 (green) and 2021 (orange) between station 74,000 and 55,000.

Annotated Reach 70,000 REMs for 2016 and 2021 are presented in Figure 3.19. The REMs indicate intensification of the existing meander and formation of a new meander just downstream of Station 70,000. Incision is apparent in the downstream extension of the eight ft and ten ft REM classes between 2016 and 2021. Figure 3.20 provides the location of cross sections between Station 71,580 and 68,940 within 2016 and 2021 aerial imagery.
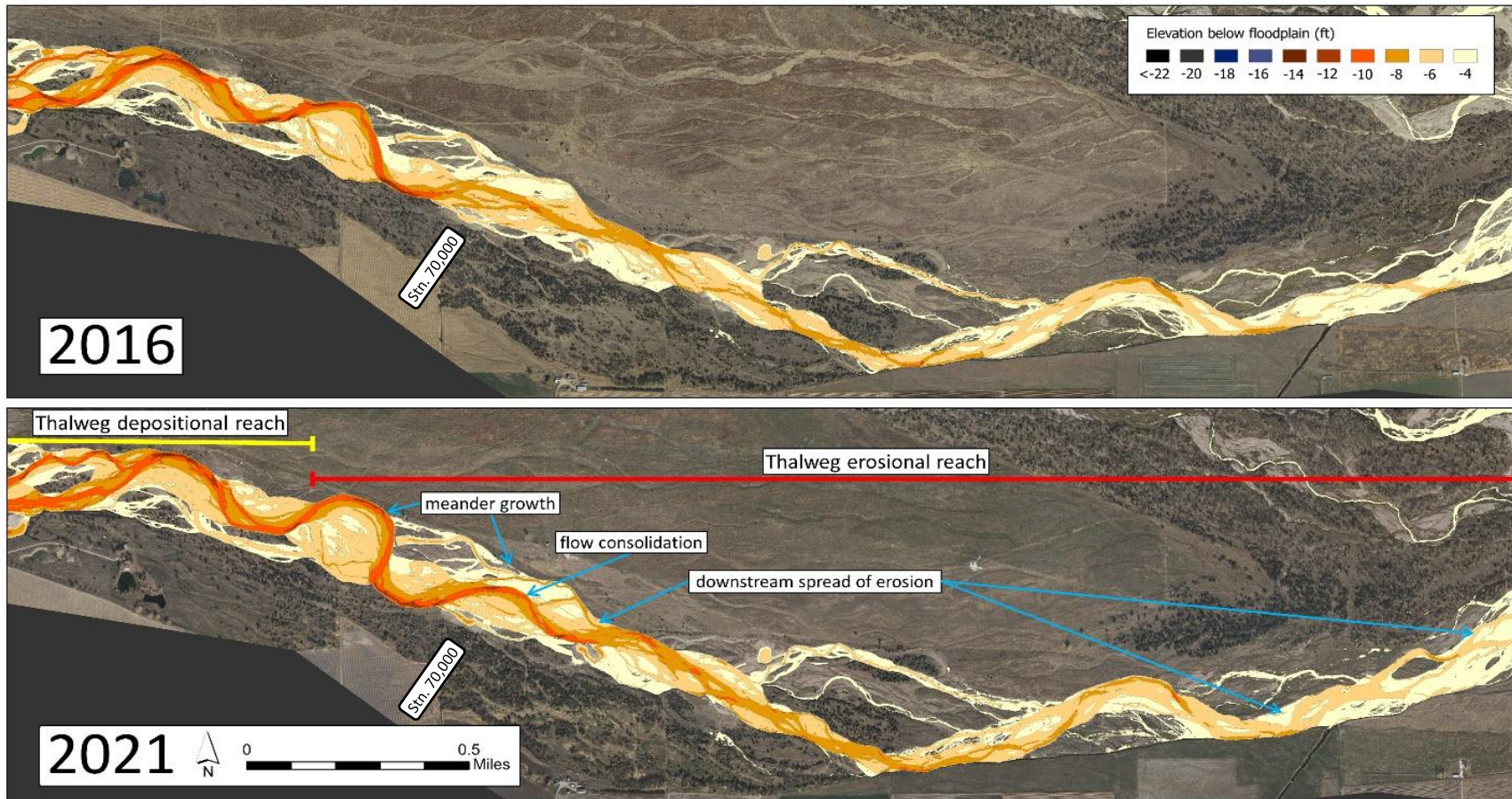
**Figure 3.19.** Annotated relative elevation models (REMs) of the downstream section of J2 Return Channel ending at Station 58,000. The relative elevation model is contoured into 2 ft intervals below -4 ft relative to the floodplain. Blue arrows in the bottom panel highlight changes since sediment augmentation. Yellow and red lines indicate regions of erosion and deposition detected by changepoint analysis.

**Figure 3.20.** Aerial imagery of Reach 70,000 in 2016 (top) and 2021 (bottom). A black rectangle extends from Station 71,835 to Station 66,435 and delineates the reach with the most change. Cross section locations are noted in red.

LiDAR-derived transect plots for the six cross sections between Station 71,580 and 68,940 are provided in Figure 3.21. All cross sections show some degree of lateral erosion between 2016 and 2021. This is most apparent at Station 71,580, 71,070, 68,940 and 68,050 transects which are all located at or near the apices of developing meanders. In terms of thalweg incision, the three 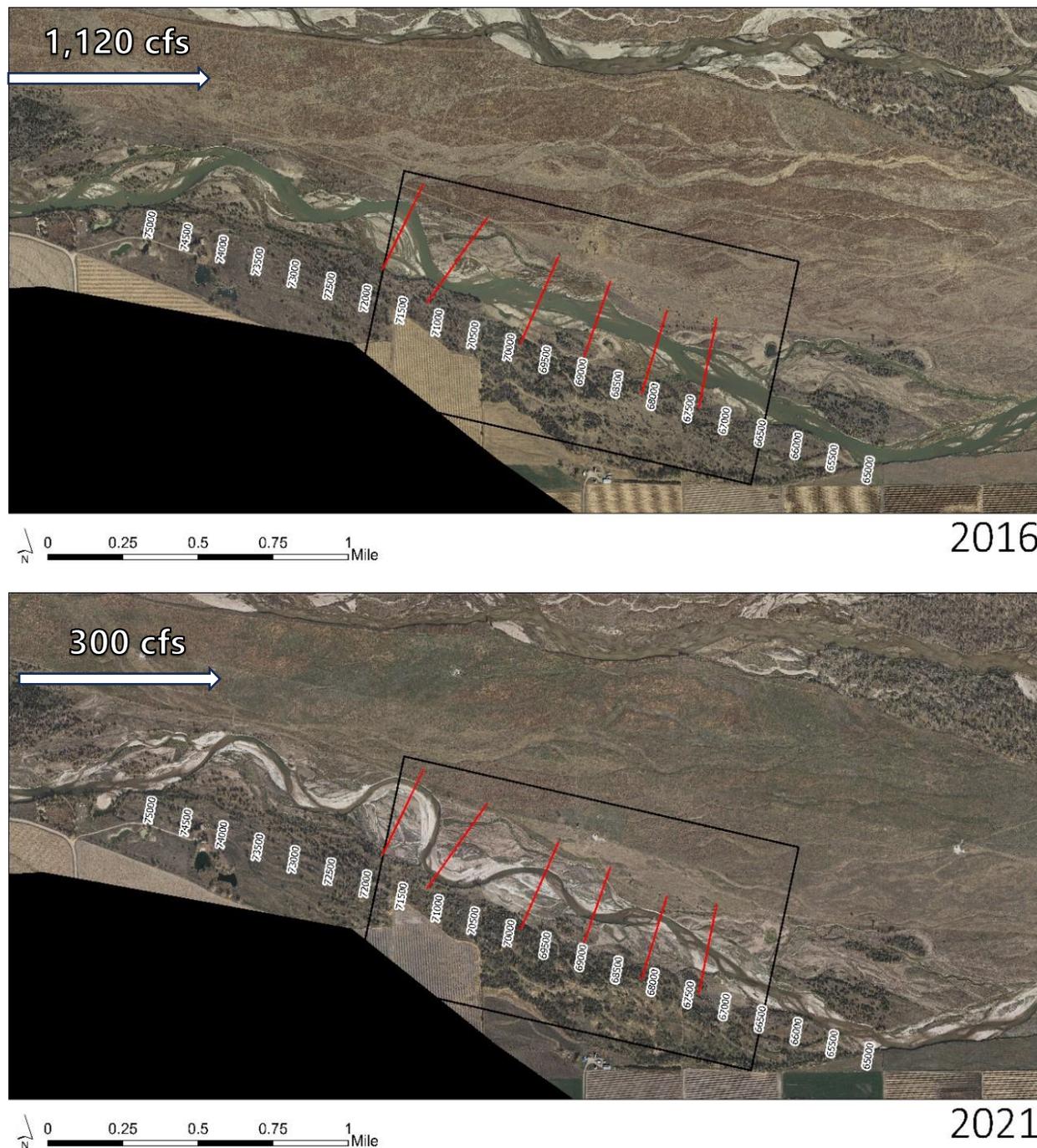most upstream cross sections experienced the highest magnitudes of incision in 2019 with some thalweg infilling in subsequent years. The three downstream cross sections did not experience thalweg infilling after 2019. Change in channel geometry at the furthest downstream cross section (67,355) indicates a planform shift at that location in 2019 with the development of an incised low flow channel near the midpoint of the cross section that persisted through 2021.
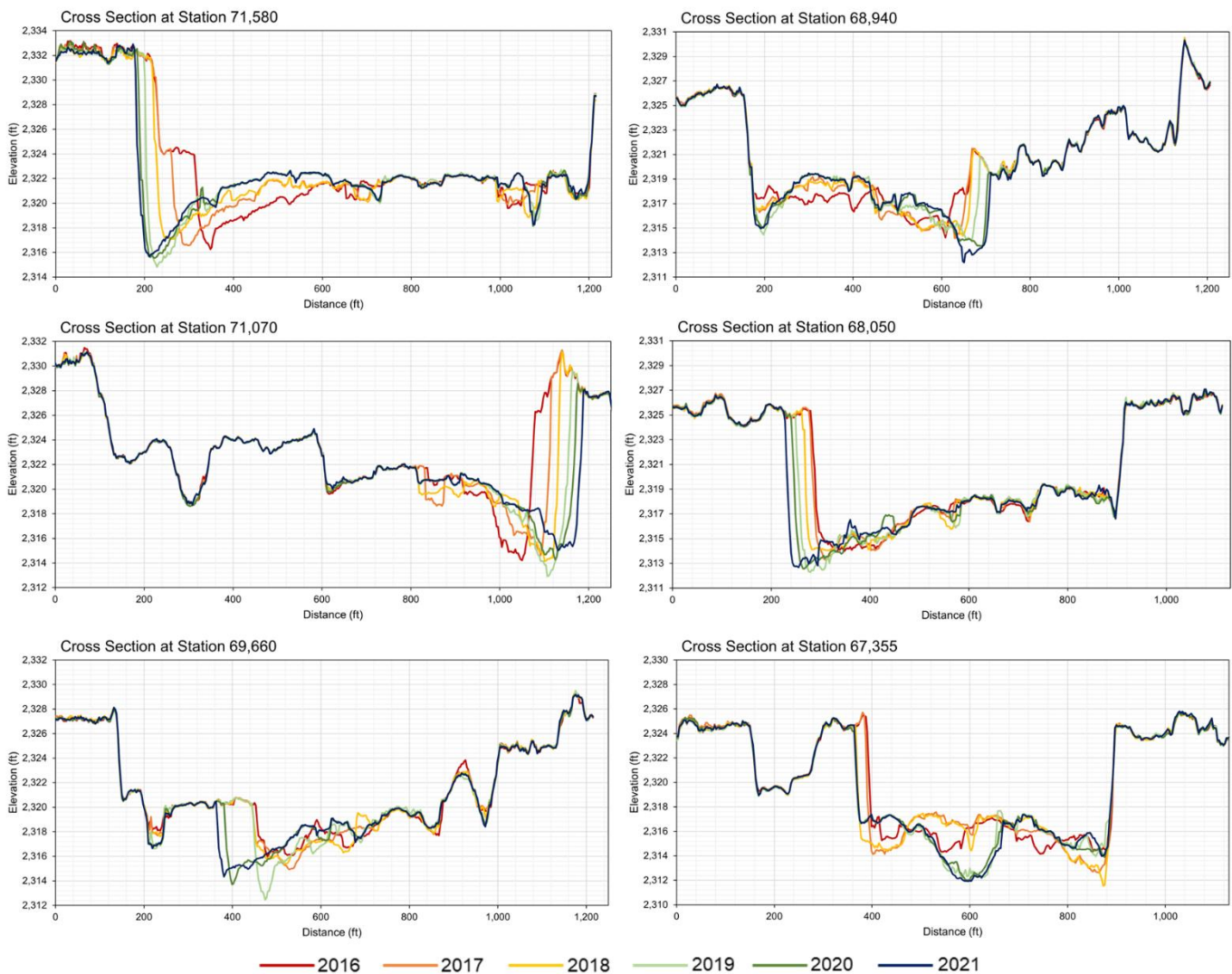


**Figure 3.21.** Cross sections viewed from river left to right, looking in the downstream direction at 6 locations in Reach 70,000 of the J2 Return Channel.

Sinuosity in Reach 70,000, calculated as thalweg length within the black rectangle in Figure 3.19, increased from 2016 to 2021 (Figure 3.22a). This is evident in REMs and aerial imagery as
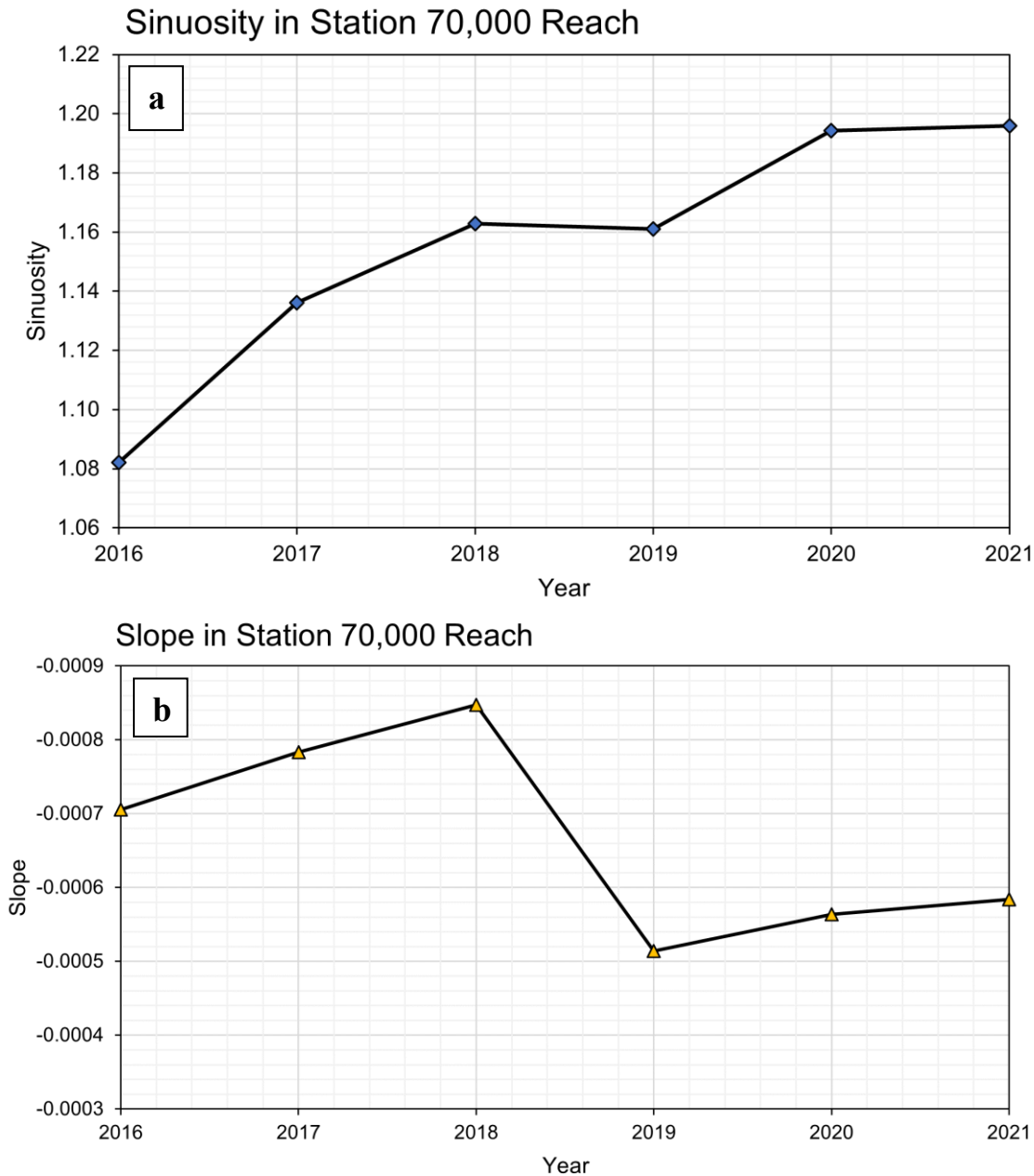


**Figure 3.22.** (a) Sinuosity of Reach 70,000, measured in the area delineated by the black rectangle in Figure 3.20. Sinuosity is the ratio of along-channel distance to straight line distance. (b) Slope of reach 70,000, measured as the slope of a linear regression between elevation and along-thalweg distance within the black rectangle in Figure 3.20.

meanders expanded during this period (Figures 3.19–3.20). Over the same period, channel slope decreased in this area due to events in 2019, although slight increases occurred before and after 2019 (Figure 3.22b).

This area is evolving and appears to have been the focal point of incision and planform change in the J2 Return Channel during the sediment augmentation experiment. The pace of this migration should be monitored, especially in absence of sediment augmentation, to evaluate how the channel continues to evolve.

## 3.9    Discussion

To evaluate sediment augmentation effectiveness since sediment augmentation began below the J2 Return, we examined longitudinal change starting in 2016, the year immediately prior to sediment augmentation. Analyses extended through 2021 to incorporate the first five years of the sediment augmentation management experiment. Using results from relative elevation to the floodplain, thalweg elevation, average cross-sectional elevation, and channel geometry, we found evidence of an aggradational augmentation response in the upper portion of the J2 Return Channel. The lower portion of the J2 Return Channel degraded during augmentation, especially as a result of high flows in 2019. Downstream of Overton Bridge, minor aggradation and degradation was observed at much smaller magnitudes than in the J2 Return Channel.

Upstream of Station 70,000 (the first 2.3 miles below sediment augmentation), the channel elevation increased. Sediment inputs during this time formed bars, decreased pool depths, and generally aggraded the channel. Though low magnitude when averaged through the reach, this gain in elevation could be partially attributed to sediment augmentation efforts, with some additional sediment inputs from the breakthrough channel prior to 2019. The breakthrough channel is described in D.2 and discussed further in Chapter 4.

Moving downstream of the aggradational reach within the J2 Return Channel, the remaining length of the reach upstream of the North Channel confluence continued to degrade during the first few years of the sediment augmentation experiment. Thalweg and average cross-sectional elevation decreased, and the reach surrounding Station 70,000 experienced the most negative change. Within this reach, meanders grew and migrated downstream. Although already incising, the reach experienced a large magnitude incisional event in 2019. Since 2019, when high flows occurred and the breakthrough channel berm was repaired (Section D.2), bed elevations in this reach have been stable though sinuosity has continued to increase.

Annual changes to thalweg planform patterns depict many areas along the J2 Return Channel where meanders are actively evolving as concentrated flows cut into unconsolidated banks (Figure 3.5). This lateral migration recruits additional sediment to the channel and is therefore not considered a negative outcome, but increased lateral migration can result in lowered channel slope, which in turn may affect planform. In the remaining braided section of the J2 Return Channel, both width and slope increase steadily in the downstream direction but have not changed much in the past five years. As meanders continue to expand and add channel length in this vicinity, slope is expected to decrease and planform transition will continue shifting further downstream. It is possible that upstream portions of the J2 Return Channel have adjusted to a relatively constant slope that yields a consistent wandering planform and may not evolve further under the current discharge and sediment regime. However, without sediment augmentation or

regular contributions from the breakthrough channel, the previously adjusted channel length is subject to additional change.

Changes downstream of Overton Bridge were generally subtle and lower magnitude than changes within the J2 Return Channel. Some bars dissipated during the study period. This change could be attributed to low magnitude degradation and management actions (e.g. vegetation disking in 2018) between 2016 and 2021. Generally, the reach downstream of Overton retained high wetted widths since 2015 with little to no detectable change in channel elevations and geometry. The channel is aggrading upstream of Elm Creek Bridge. This aggradation is potentially associated with the buildup of sediment upstream of the constriction at Elm Creek Bridge and behind KCD.

The J2 Return Channel, especially Reach 70,000, is sensitive to high flows and experienced overall average loss in elevation during the three highest flow years within the study period (2016–2017, 2018–2019, and 2019–2020; Table 3.2; Section D.2). During the two drier years (2017–2018 and 2020–2021), elevation gained on average in the J2 Return Channel. During all years measured, reach-averaged losses and gains have opposite signs in the J2 Return Channel versus downstream of Overton Bridge, i.e., when the J2 Return Channel experiences elevation loss, the channel downstream of Overton experiences elevation gain. Losses versus gains relative to flow magnitudes are reversed within the reach downstream of Overton Bridge. During lower flow years, the channel degraded downstream of Overton, and during high flow years the channel aggraded (Table 3.2). This behavior may assist future assessment of the general fate of augmented sediment. We hypothesize that during dry years, more augmented sediment remains within the J2 Return Channel, and during wet years more sediment (both augmented and stored) is transported downstream of Overton. Because the system upstream of Overton Bridge continues to receive insufficient sediment supply for sediment balance, high sediment transport years lead to channel degradation and threat of planform migration downstream within the J2 Return Channel. Though incision may be present in the J2 Return Channel during years with high flow, high transport years also yield important sediment inputs to downstream habitat. We will continue to evaluate this hypothesis as we collect more years of data on the system

A primary goal of sediment augmentation is to halt downstream progression of incision and narrowing. The transition from wandering to braided planform is roughly 3 miles upstream of Overton Bridge (see E.2 for our definition of these planform types). Here, our evaluation of channel planform and cross-sections indicated that the downstream end of the wandering planform reach migrated roughly 2,000 ft downstream during the augmentation experiment. This length estimate of channel planform migration over 5 years, and the approximate distance of 3 miles downstream to Overton Bridge, indicate that a wandering planform could migrate to the Overton Bridge on the order of 40 years. Though this estimate is general, it implies that the timescale for complete planform transition of the J2 Return Channel is decadal. Incision and planform change are measurable threats to habitat downstream of the Overton Bridge, but the confluence with the North Channel provides significant sediment inputs which are not quantified in this study. Analogous to sediment inputs from tributary confluences (Benda et al., 2004), water and sediment inputs from the North Channel offset some of the risk associated with incision caused by the J2 Return. Thus, related channel changes downstream of the confluence are likely to occur at a slower pace than within the J2 Return Channel.

Future analyses to advance our understanding of channel behavior downstream of the J2 Return include more detailed analysis of changes in channel width and slope, quantification of lateral migration of the channel thalweg, and statistical or morphodynamic models to relate channel response to sediment supply and flow. There are limitations to examining change with one metric at a time longitudinally. For example, confining analysis of change within the channel thalweg leads to continued uncertainty regarding the active channel and floodplain outside of the deepest portion of the channel and omits information about overbank deposition and secondary flow paths. Thus, we extend our analyses in the following chapter with examination of volume change to quantify sediment erosion and deposition within the study reach.

## *3.10  References*

Benda, L.E.E., Poff, N.L., Miller, D., Dunne, T., Reeves, G., Pess, G. and Pollock, M., (2004). The network dynamics hypothesis: how channel networks structure riverine habitats. BioScience, 54(5), pp.413-427.

Haynes, K., Eckley, I.A. and Fearnhead, P. (2017). Computationally efficient changepoint detection for a range of penalties. Journal of Computational and Graphical Statistics 26(1):134-143.

HEC-RAS. (2008). Hydraulic Reference Manual. U.S. Army Corps of Engineers, Hydrologic Engineering Center.

Killick, R., Eckley, I.A. (2014). changepoint: An R Package for Changepoint Analysis. Journal of Statistical Software 58(3): 1-19. https://www.jstatsoft.org/article/view/v058i03.

Killick, R., Fearnhead, P. and Eckley, I.A. (2012). Optimal detection of changepoints with a linear computational cost. Journal of the American Statistical Association 107(500):1590-1598.

Killick, R., Haynes, K., Eckley, I.A. (2022). changepoint: An R package for changepoint analysis. R package version 2.2.4. https://CRAN.R-project.org/package=changepoint.

Lai, Y. (2008). SRH-2D Version 2: Theory and User's Manual. Bureau of Reclamation Technical Service Center Sedimentation and River Hydraulics Group.

Lenth R (2023). emmeans: Estimated Marginal Means, aka Least-Squares Means. R package version 1.8.5. https://CRAN.R-project.org/package=emmeans.

Platte River Recovery Implementation Program (PRRIP). (2022a). System-scale geomorphology and vegetation monitoring report. Prepared for PRRIP Governance Committee, June 2022.

Platte River Recovery Implementation Program (PRRIP) Executive Director's Office (EDO). (2022b). First Increment Extension Science Plan.

Powers, P.D., Helstab, M. and Niezgoda, S.L. (2019). A process-based approach to restoring depositional river valleys to Stage 0, an anastomosing channel network. River Research and Applications 35(1): 3-13.

R Core Team (2022). R: A language and environment for statistical computing. R Foundation for Statistical Computing, Vienna, Austria. https://www.R-project.org/.

# CHAPTER 4   Volume change analysis

## *4.1   Abstract*

We used topo-bathymetric elevation data to calculate volumes of sediment that deposited or eroded between the Johnson No. 2 Hydropower Return (J2 Return) and the Kearney Canal Diversion (KCD). Using hydraulic modeling results, we separated lateral erosion from bed aggradation and degradation. We found that the study reach became less degradational in years since sediment augmentation began. Bed erosion has decreased 45% to 60% upstream of Overton Bridge. Our data indicate that a combination of hydrology, natural sediment sources, and augmented sediment have played a role in this reduction.

## *4.2   Introduction*

As discussed in Chapter 1, the Platte River Recovery Implementation Program (PRRIP or Program) attempted to estimate the sediment deficit in the Program's Associated Habitat Reach (AHR) created by the J2 Return structure using various measured and theoretical sediment transport functions that tie transport to flow. The estimated deficit ranged from 50,000 tons per year (35,000 yd$^3$/yr) between Overton Bridge and Kearney (Tetra Tech, 2017), to a 109,000 tons per year  (73,000 yd$^3$/yr) deficit between Overton and Elm Creek (The Flatwater Group, Inc, 2010). The 2017 estimate is less than half that of the 2010 estimate, despite covering a longer stretch of river with no major sediment sources. This disparity underlines the uncertainty and difficulty in comparing theoretical and field sediment data.

The Program began a full-scale sediment augmentation management experiment in 2017 with the purpose of offsetting the deficit and assessing effectiveness of augmentation in stabilizing the J2 Return Channel. Specifically, the Program began to augment 60,000–80,000 tons (40,000 – 60,000 yd$^3$) of sediment immediately downstream of the J2 Return each year. Effectiveness is assessed using Light Detection and Ranging (LiDAR) topographic data and hydraulic modeling data to measure actual volumetric change in our study area. This application of the morphological method (Ashmore and Church, 1998; Anderson, 2019; Vericat, et al., 2017), makes the most of our high-resolution LiDAR data to calculate change under known (or mostly known) circumstances.

Chapter 3 focuses on evaluation of longitudinal change in channel morphology during full-scale augmentation operations. Two of the primary limitations of that effort were 1) inability to quantify sediment flux through the study area and 2) lack of differentiation between lateral and bed erosion. Lateral erosion is sediment removal from banks and islands due to horizontal stress, while bed erosion is sediment removal from the riverbed due to vertical stress. Lateral erosion is a natural result of channel migration or width adjustment due to increased flow. With lateral erosion, sediment that was previously stored in the bank is added to the system. This sediment is incorporated into downstream bars and may reduce downstream deficits. In this way, lateral erosion is fundamentally different from bed erosion which signals channel deepening and further disconnection from the floodplain.

In this chapter, we expand LiDAR-derived longitudinal analysis into three-dimensional estimates of annual volume change during the sediment augmentation experiment that differentiate between bed and lateral erosion. To increase the utility of our findings, we also expanded the

analysis to include the years of 2009–2016 prior to augmentation activities. During that period, the Program collected topographic bare earth LiDAR. From 2016 to present, bathymetric LiDAR has been collected. Topo-bathymetric LiDAR penetrates the water surface and returns highly accurate estimations of the river bottom. Lack of bathymetry prior to 2016 adds uncertainty to volume change estimates, which is described in more detail below. Throughout this chapter, volume change estimates for 2009–2016 are referred to as Pre-Augmentation. Annual estimates during the augmentation experiment are referred to as Post-Augmentation.

Table 4.1 shows the amount of sediment that was made available for transport via augmentation in each year. The volume for 2017 is lower than other years because some excavated sediment was used to restore eroded cropland and construct a berm to arrest lateral erosion that was threatening a home along the south bank. Volumes were calculated using LiDAR differencing methods described in the following section of this chapter.

In years when the breakthrough channel was active, large amounts of sediment were also eroded and transported into J2 Return Channel in approximately the same location as the mechanical augmentation. The volume of sediment contributed via the breakthrough channel was calculated using the same method of analyzing difference rasters that was used across the entire study reach (see Section 4.3.2). Prior to annual topo-bathymetric data collection beginning in 2016, volume change below water surface is calculated as a range of values (Section 4.3.2). Prior to augmentation, the only known source of sediment to the J2 Return Channel was the breakthrough channel which contributed an annual average of 32,800–33,500 yd$^3$ between 2009 and 2016 (Table 4.1, Figure 4.1). Years in which augmentation and breakthrough channel activation both occurred had the highest sediment inputs, with a maximum of 104,000 yd$^3$ in the 2017–2018 year.

**Table 4.1** Sediment added to the J2 Return Channel.

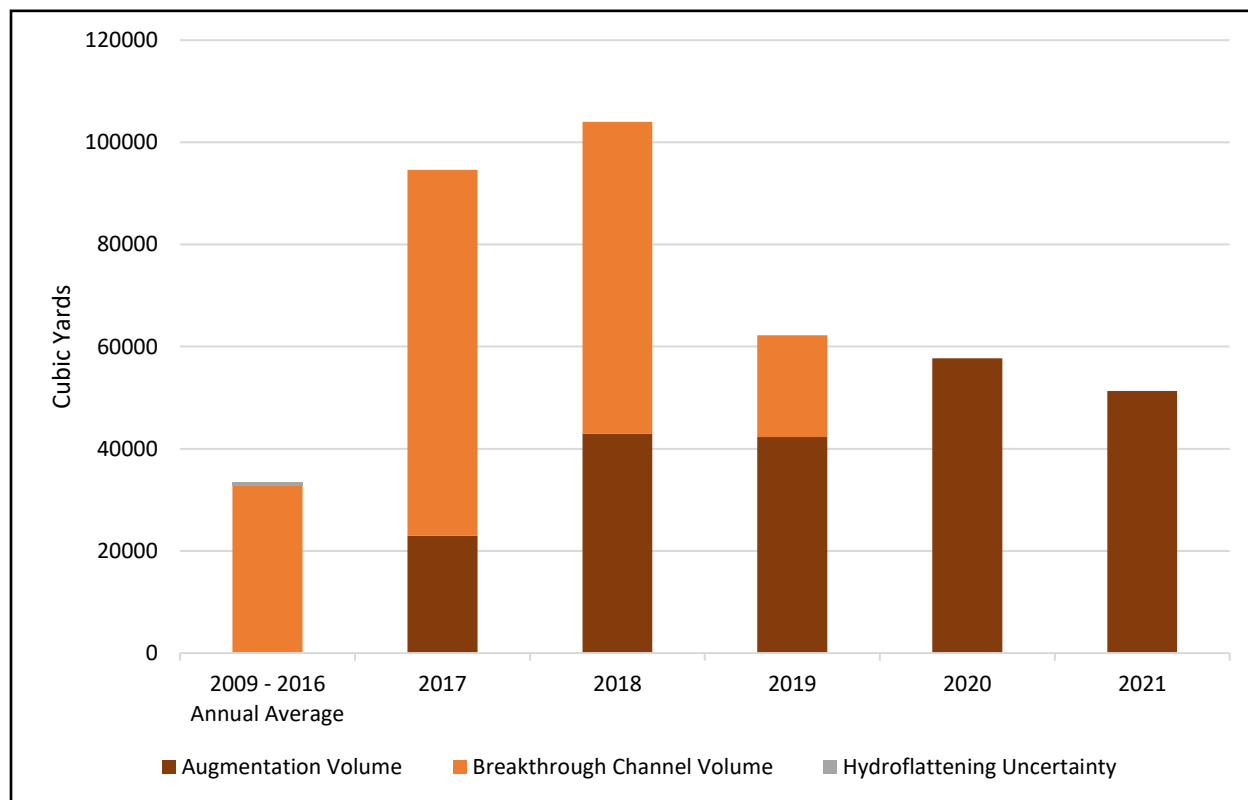|               | Breakthrough Channel Volume (yd$^3$) | Augmented Volume (yd$^3$) | Total (yd$^3$)    |
|---------------|--------------------------------------|---------------------------|-------------------|
| 2009 – 2016   | 262,000–268,300                      | 0                         | 262,000–268,300   |
| 2016 – 2017   | 71,600                               | 23,000                    | 94,600            |
| 2017 – 2018   | 61,100                               | 42,900                    | 104,000           |
| 2018 – 2019   | 19,900                               | 42,300                    | 62,200            |
| 2019 – 2020   | 0                                    | 57,700                    | 57,700            |
| 2020 – 2021   | 0                                    | 51,300                    | 51,300            |

**Figure 4.1** Sediment added to the J2 Return Channel downstream of the return through erosion in the breakthrough channel (orange) and sediment augmentation (brown).

## *4.3    Methods*

### 4.3.1    Volume change (LiDAR raster differencing)

Annual volume change estimates were developed via LiDAR raster differencing. We created annual difference elevation rasters by subtracting the earlier year from the more recent year.  We then clipped the difference rasters to the active channel (Figure 4.2; Appendix A) to remove dry floodplain areas that were not altered by flow. Removing these areas improved our accuracy because we found non-random error in LiDAR data for many floodplain areas due to year-to-year changes in vegetation. The active channel clip area was based on the hydraulic modeling results (see Section D.3) that identified the active flow conveyance area. These areas were then manually widened in places to include areas of bank failure that were not wet. The hydraulic model results represented an approximate bankfull discharge of 2,500 cfs in the J2 Return Channel and 2,500 cfs in the North Channel, resulting in 5,000 cfs in the reach downstream of the confluence. The active channel changes every year, so delineations are unique for each analysis year.

To convert 1D model results to 2D water extent polygons for pre-augmentation years 2009 and 2012, we exported water surface elevation (WSE) data to ArcGIS using HEC-GeoRAS (HEC-RAS, 2008) and created a digital triangulated irregular network (TIN) of the water surface. We then subtracted LiDAR data from the TIN of the modeled WSE, producing a raster of positive

depth values where the ground was below the water surface. We then manually removed puddles, abandoned channels, and other low-lying areas that were not hydraulically connected to the river. The full set of differenced rasters and their clipped area extents can be seen in Appendix A.
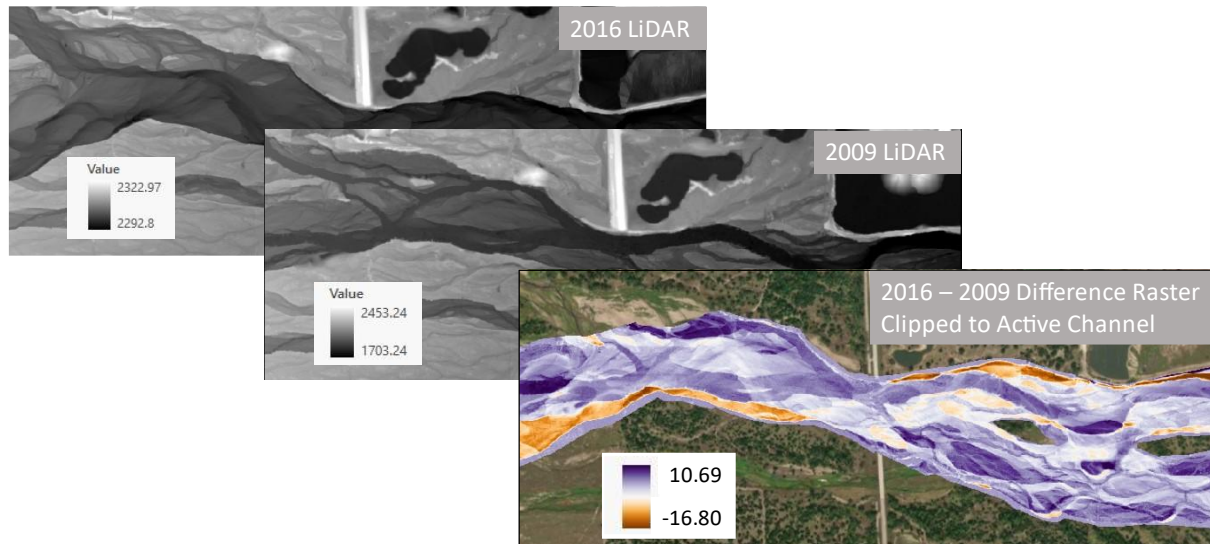


**Figure 4.2**. Example of raster differencing and clipping to the active channel at the Overton Bridge. 2009 elevations were subtracted from the 2016 elevations, resulting in a raster ranging from 10.69 ft of aggradation (purple) to 16.80 ft of erosion (orange).

In 2009, LiDAR rasters were hydroflattened within the wetted areas so change is presented as a range of possible values based on potential erosion and aggradation below the 2009 water surface. The hydroflattened areas often experienced aggradation as the channel migrated during the intervening years. In the 2016–2009 difference raster, this resulted in a net positive change above the 2009 hydroflattened elevation, meaning that the channel below the 2009 water surface filled in completely with sediment in many places. Based on the 2009 hydraulic model, the average depth of flow on the date of LiDAR collection was one ft. Multiplying this by the hydroflattened area gives a total underwater volume of 156,000 yd$^3$ in the J2 Return Channel reach. We used this estimate to represent maximum potential aggradation not accounted for during raster subtraction due to missing bathymetry data in the 2009 LiDAR.

We defined lateral erosion as areas that experienced bank erosion or failure due to hydraulic activity. Following this erosion, previously dry areas become accessible to flow. To identify these "newly wet" areas and thus areas of lateral erosion, we converted HEC-RAS and SRH-2D modeled water extents into 3x3 ft WSE raster grids (Figure 4.3A). We then intersected the rasters (2,500 cfs in the J2 Return Channel and 5,000 cfs below the North Channel confluence) and identified cells where water was newly present to create a mask of lateral erosion for each difference raster (Figure 4.3B).
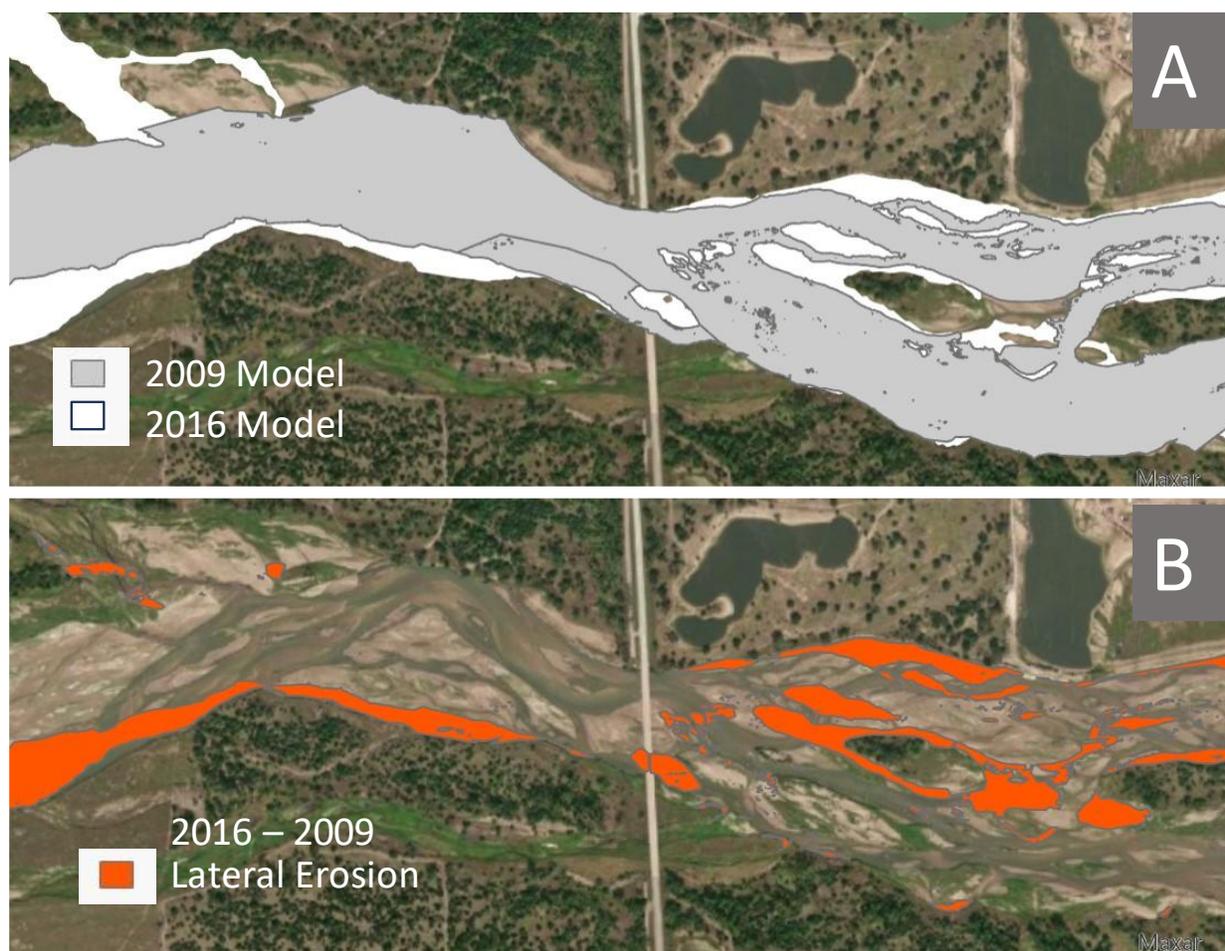
**Figure 4.3.** Lateral erosion was delineated by differencing hydraulic model results (A) and isolating newly wet areas (B).

Based on results of the System Scale Monitoring Report (PRRIP EDO, 2022b), the average wetted width of the J2 Return Channel is 450 feet. We chose to quantify sediment volume flux from year to year at a resolution of approximately two channel widths (900 feet) along the study reach. To accomplish this, we generated 900-foot-wide rectangles along the channel centerline that encompassed the entire channel. Using these rectangles as regions and values from the difference rasters clipped to the active main channel, we then summarized the data in each region using the ArcGIS Pro Zonal Statistics as Table tool (Figure 4.4). The sum of raster values in each region was multiplied by the area of the difference raster cell (9 ft$^2$) to compute the change in volume for that region. This sum includes all volume change including lateral erosion. We then used the same process to calculate volume change under the lateral erosion masks. Bed erosion was quantified by subtracting the lateral erosion quantity from the total volume difference for each region.
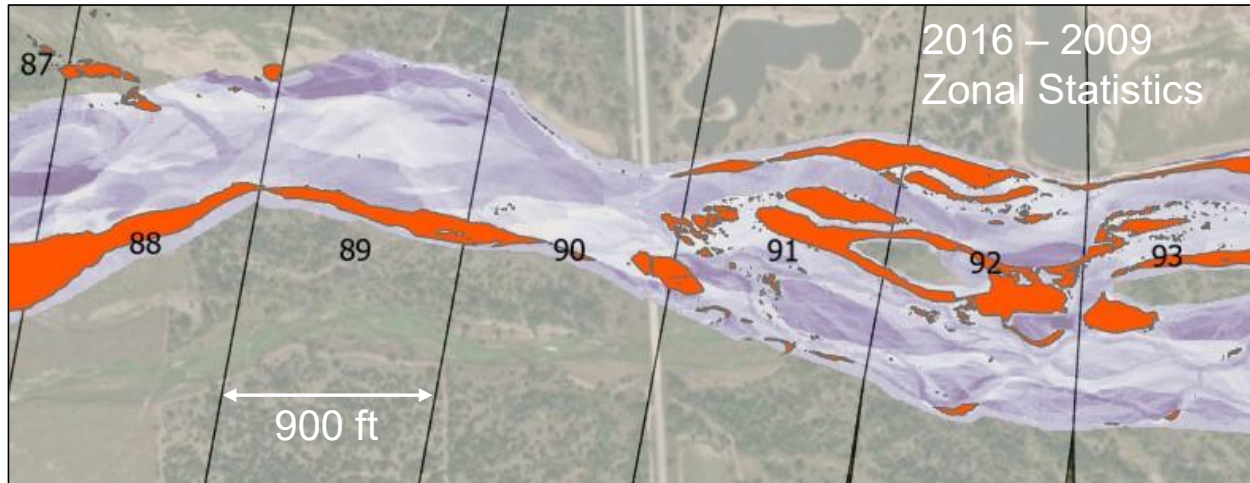
**Figure 4.4.** Using the zonal statistics tool, elevation differences in each 900-ft wide zone were summed. Zones are bounded in black and numbered 87-93 in this figure. The sums were then converted from ft to ft$^3$ by multiplying the elevation difference by the raster cell area (9 ft$^2$). The process was repeated to look only within the lateral erosion mask, shown in orange, to obtain the volume of lateral erosion in each zone.

### 4.3.2   Flow normalization of volume change

In most instances, volume change is divided by the number of years over which the change occurred. Another method to examine the volume change is to normalize the results by flow rather than year. This type of normalization allows us to control for the exponential relationship between flow and sediment transport, meaning that we can observe results without needing to account separately for wet and dry years. This procedure can only be used for normalization of volume change downstream of Overton Bridge because we do not have a complete set of flow data for the upstream reach due to ungaged flow from the breakthrough channel.

Normalization by flow was calculated by dividing volume change by the q dividend (Equation 4.1). The q dividend is the square of the flow volume that passed through the channel during the time that the volume change occurred. It is calculated by converting the daily mean flow rate to units of cubic yards per day, then squaring this value. Finally, the squared values are summed, and the resulting quantity is in units of 1/yd$^3$. Sediment transport capacity is often related to a power function of flow, with common exponents ranging from 1.4 to 2.4 (Julien & Simons, 1985). For the purposes of this analysis, we chose an exponent of 2.0 as recommended by our Independent Science Advisory Committee (ISAC, 2023).

*Equation 4.1* $$q\ dividend = \sum Q^2$$

## *4.4   Results*

### 4.4.1   Pre- and post-augmentation volume change results

To understand the relative influence of sediment augmentation on volume change and sediment flux within the study area, it is helpful to compare data grouped into pre- and post-augmentation time periods. The earliest Program LiDAR data was collected in 2009 and the first augmentation project occurred in the fall of 2017, prior to LiDAR collection. Therefore, our pre-augmentation

period spans 2009–2016 and post-augmentation spans 2016–2021. Given the different lengths of these timespans, results have been annualized or normalized by flow for easier comparison.

The net volume change at each station is shown in Figure 4.5, while Figure 4.6 shows the cumulative, or running sum, of volume change beginning at the downstream end of the sediment augmentation area. Figure 4.5A shows that total volume change was primarily negative (degradational) over the full reach for both time periods. Much of this negative change can be attributed to lateral erosion (Figure 4.5B). Sediment augmentation and lateral erosion both produced concentrated signatures in the J2 Return Channel due to mechanical widening and evolving meanders. When lateral erosion is subtracted from total change, the remaining volume can be attributed to changes that occurred in the channel bed (Figure 4.5C). Bed changes were a mix of positive (aggradational) and negative (degradational) across the reach.

In the post-augmentation period, areas of aggradation included the upstream end of the reach to Station 70,000 and downstream near the Elm Creek Bridge. In the pre-augmentation period, the reach upstream of the Overton Bridge was primarily negative, but the uncertainty due to the absence of 2009 bathymetry prevents a clear conclusion on the downstream reach. Viewing net change in relation to channel station is helpful for observing variability and identifying specific areas of interest, however, summing change over a longer reach can give more concise conclusions. Table 4.2 gives the sum of volume changes upstream and downstream of Overton Bridge. Sums in the upstream reach do not include change in the augmentation project area, instead focusing on non-mechanical change downstream of the projects. Figure 4.6 shows the running sum of change over the full area of interest.
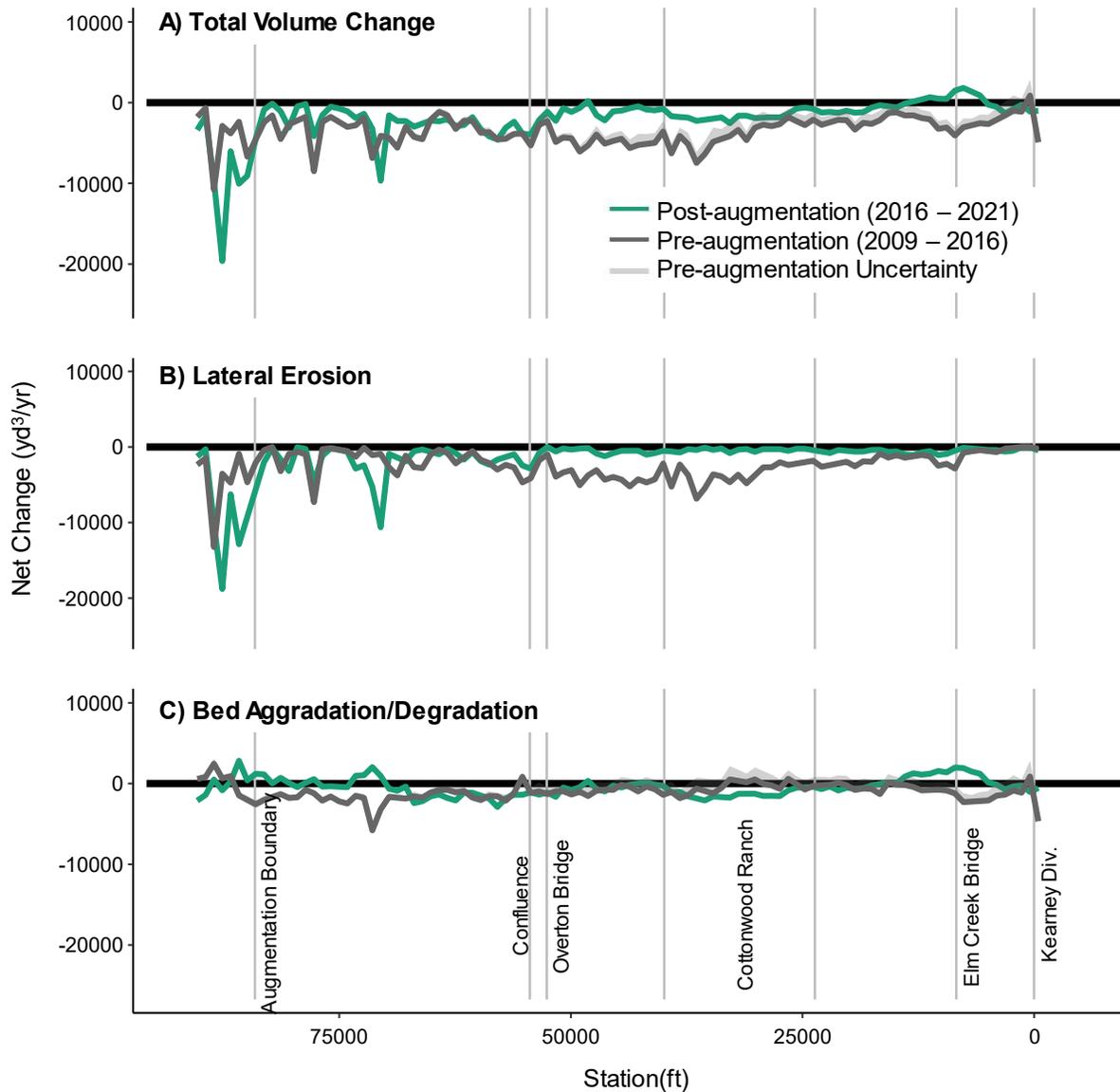
**Figure 4.5**. Net volume change per year by station. The figure shows the total volume change (A), which is the sum of the lateral erosion (B) and the bed aggradation/degradation (C). Upstream of Overton Bridge lateral erosion was high both pre- and post-augmentation while bed degradation reduced. Downstream of Overton Bridge much less lateral erosion occurred post-augmentation while bed volume change fluctuated around zero during both periods.

**Table 4.2.** Pre- and post-augmentation volume change broken into two reaches. Negative values indicate net degradation for the reach. Orange cells indicate an increase in degradation from pre- to post-augmentation, while green cells indicate a decrease in degradation.

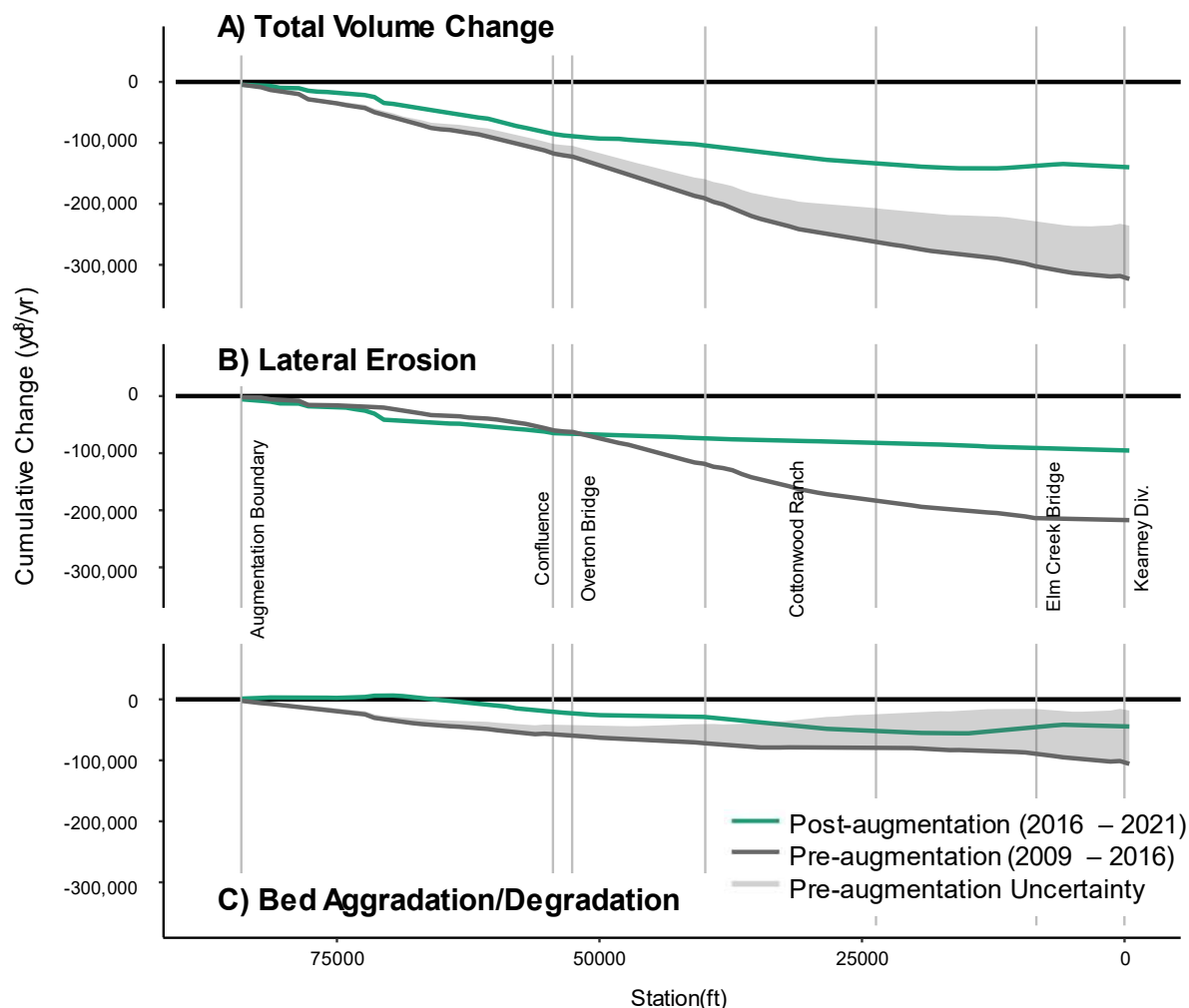| | Augmentation Boundary to Overton Bridge (yd$^3$/yr) | | Overton Bridge to KCD (yd$^3$/yr) | |
|---|---|---|---|---|
| | Pre-Augmentation | Post-Augmentation | Pre-Augmentation | Post-Augmentation |
| Lateral | -63,000 | -65,800 | -154,400 | -29,600 |
| Bed | -59,700 to -42,000 | -23,000 | -46,100 to 23,700 | -21,500 |
| Total | -122,700 to -105,000 | -88,800 | -200,400 to -130,700 | -51,100 |

**Figure 4.6**. Cumulative volume change in the pre- and post-augmentation time periods. Lines represent the running sum of all change starting at the downstream end of augmentation projects. Gray shaded area represents the uncertainty in the pre-augmentation period due to lacking bathymetry data.

While volume change remained negative in the post-augmentation period, Table 4.2 and Figures 4.5 and 4.6 show that this change became less negative compared to pre-augmentation. Upstream of the Overton Bridge, the channel bed was degrading at a rate of 0.8 to 1.1 in/yr, averaged over the total area. After augmentation, this rate decreased to 0.4 in/yr, a decrease of 45% to 60% while lateral erosion had a slight increase of 4%. Downstream of the bridge a large reduction in lateral (80%) and total degradation (61%–75%) was observed. At KCD, total volume change and lateral erosion were lower during the post-augmentation period, while the difference in bed degradation is within the uncertainty for the pre-augmentation period.

### 4.4.2   Flow-normalized volume change results

Given sediment transport increases nonlinearly with flow, it can be helpful to remove flow variability from the analysis to compare volume change under approximately equal flow conditions. For example, given equal flow, we would expect an unstable reach to change more than a stable one. As will be further discussed in Section 4.4.3, the pre-augmentation period experienced greater flow than the post-augmentation period, and Figure 4.7A shows that the pre-augmentation period also experienced greater total volume change. Figure 4.7B shows that when these results are normalized by flow, the difference between pre- and post-augmentation values shrinks to be within the uncertainty bounds over most of the reach[14]. The contrast between change normalized by flow (Figure 4.7B) and change not normalized by flow (Figure 4.7A) This indicates that flow is a primary factor in the reduction in downstream volume change in the post-augmentation period. This further suggests that the reach has not become more or less prone to erosion with time. It continues to be degradational on average, with the magnitude of degradation varying with flow.

---

[14] Note that flow normalized data is only available downstream of Overton Bridge due to incomplete flow data upstream of the bridge.
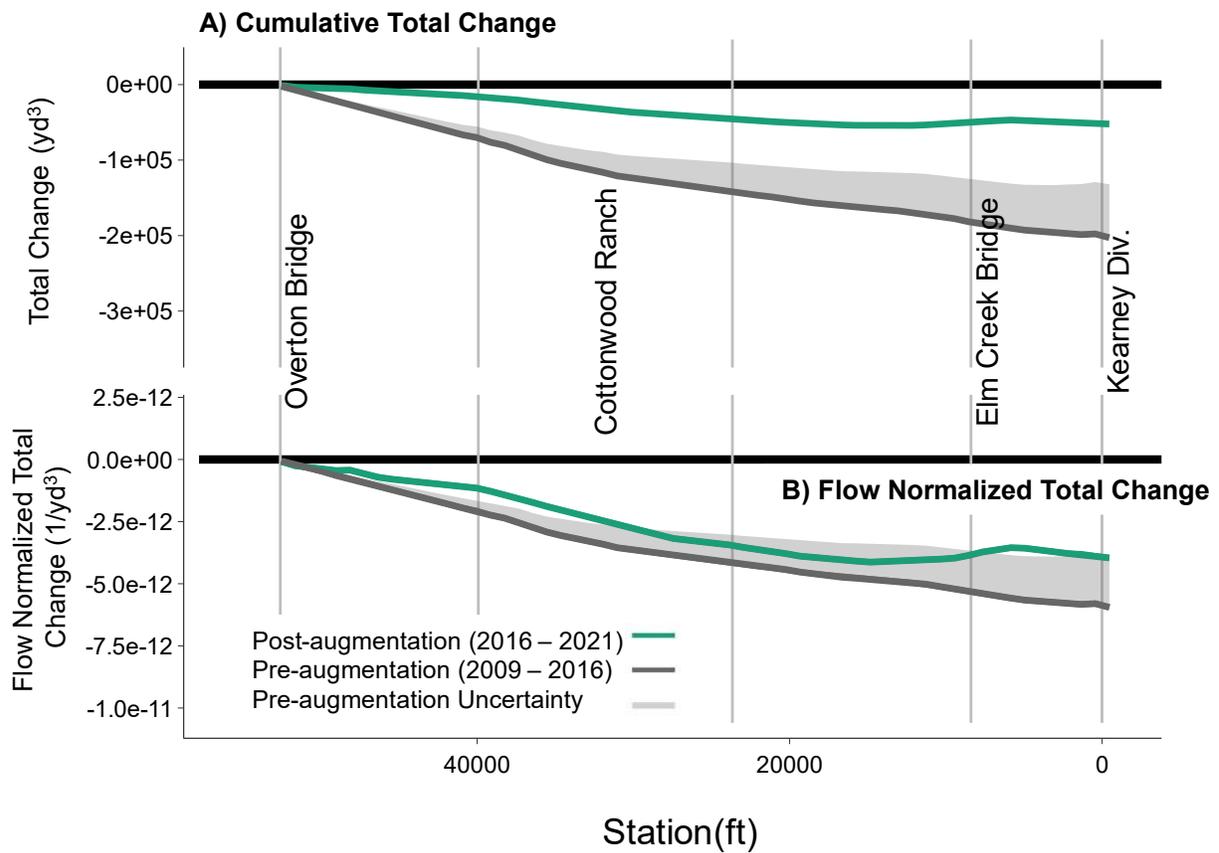
**Figure 4.7**. Cumulative total volume change downstream of the Overton Bridge. Values in panel B are normalized by flow at the Overton USGS gage, while values in A are not. Normalizing by flow reduces the difference between pre- and post-augmentation volume change.

### 4.4.3    Effectiveness of sediment augmentation

Our analysis indicates that conditions became less degradational in our study area since the implementation of sediment augmentation. To isolate the part that sediment augmentation played in this improvement, we must consider the other main variable in our system, flow. Downstream from the confluence of the J2 Return Channel and the North Channel, the Overton Bridge USGS gage shows that the pre- and post-augmentation periods were distinct. Figure D.4 shows that monthly average flow exceeded 6,000 cfs five times in the pre-augmentation period and not once in the post-augmentation period. In addition, the high flow event in June of 2015 brought a maximum daily flow of 15,300cfs, much higher than the maximum daily flow of 9,750cfs during the drier post-augmentation period (Table 4.3).

**Table 4.3** Summary of flow during the pre and post-augmentation periods.

|  | Pre-augmentation | | Post-Augmentation | |
|---|---|---|---|---|
|  | J2 Return | Overton Bridge | J2 Return | Overton Bridge |
| Average Daily Flow (cfs) | 960 | 2,150 | 970 | 1,650 |
| Maximum Daily Flow (cfs) | 2,030 | 15,300 | 1,780 | 9,750 |

These differences in flow make it difficult to isolate the effect of sediment augmentation. Fortunately, our full flow record at the Overton gage allows us to approximate volumetric change on the downstream reach independent of flow (Figure 4.7B). Doing so indicates that degradation potential was similar on this reach pre- and post-augmentation. While the post-augmentation change is slightly less degradational in a few locations, the differences are small enough to be within the uncertainty bounds over most of the reach. The high lateral erosion (Table 4.2) and large increases to wetted width (see Chapter 3) in the pre-augmentation period also point towards high flow events being the main driver of change rather than augmentation project sediment. Channel-forming events such as the flood in 2015 caused high lateral erosion, which in turn introduced new sediment to the riverbed. Without high flow events, the post-augmentation period saw only 20% of the pre-augmentation annual lateral erosion downstream of the Overton Bridge.

Upstream of Overton Bridge, flow entering the J2 Return Channel is typically regulated and ranges from 0 to 2,000 cfs. The average release from the Supply Canal was very similar in the pre- and post-augmentation periods (Table 4.3). This indicates that the additional sediment introduced to the system via sediment augmentation projects is likely a key factor in the reduction in bed degradation and total degradation observed in the J2 Return Channel. Figure 4.8 shows the relative volumes of sediment that eroded from the most upstream part of the J2 Return Channel where augmentation projects have occurred (orange). In the post augmentation period, the amount of sediment that eroded, including what was augmented, from the upstream reach increased by 35,500–38,300 yd$^3$/yr. Given that flow was similar in the post-augmentation period, this increase in erosion can be attributed to an increased availability of sediment (23,000 to 57,700 yd$^3$/yr) from sediment augmentation and the breakthrough channel, see Figure 4.1). Relative to this, we see a decrease in bed erosion from downstream of the augmentation area to the Overton Bridge of 16,200 to 33,900 yd$^3$ per year. The similarity between the values of the upstream increase and downstream decrease in erosion indicates that sediment is leaving the augmentation area and reducing bed degradation downstream.
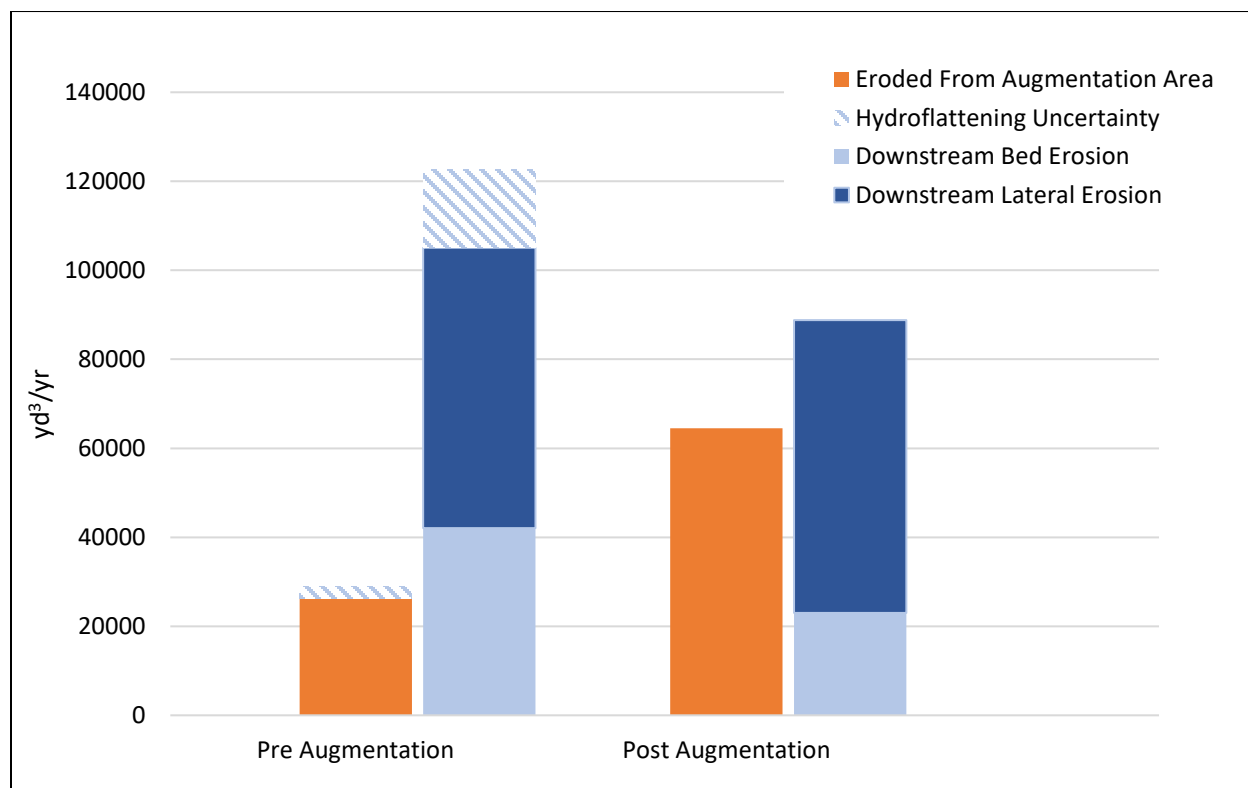
**Figure 4.8** Volumes eroded from the J2 Return Channel upstream and within the augmentation project area (orange), and downstream of augmentation projects to the Overton Bridge (blue) in pre- and post-augmentation periods. In the post augmentation period, upstream sediment supply increased and downstream bed erosion decreased. The similarity between the values of increase and decrease indicate that sediment is leaving the augmentation area and reducing bed erosion downstream.

### 4.4.4   Year-by-Year Volume Change During Augmentation

In the post-augmentation period, annual topo-bathymetric LiDAR data enables a year-by-year examination of volume change. Table 4.4 shows there is high variation, but generally less degradation was observed in the most recent two years when the breakthrough channel has been closed. Examining the year-by-year post-augmentation data spatially (Figures 4.9 and 4.10), it is possible to see an expanding zone of positive change just downstream of the augmentation boundary from 2016–2019 (4.11a). This signal is not evident in 2019–2021, perhaps becoming more dispersed as total degradation is reduced in those years.

**Table 4.4** Post-augmentation year-by-year volume change divided into two reaches at Overton Bridge. Negative values are in parentheses and indicate net degradation or erosion.

| | Downstream augmentation boundary to Overton Bridge | | | Overton Bridge to KCD | | |
|---|---|---|---|---|---|---|
| | Total Volume Change (yd$^3$) | Lateral Erosion (yd$^3$) | Bed Agg/Deg (yd$^3$) | Total Volume Change (yd$^3$) | Lateral Erosion (yd$^3$) | Bed Agg/Deg (yd$^3$) |
| 2017-2016 | (117,200) | (76,800) | (40,300) | 18,500 | (23,300) | 41,800 |
| 2018-2017 | (91,100) | (39,300) | (51,800) | (170,300) | (18,300) | (152,000) |
| 2019-2018 | (123,800) | (73,900) | (49,900) | (116,300) | (50,300) | (66,000) |
| 2020-2019 | (77,500) | (40,200) | (37,400) | 12,100 | (26,600) | 38,700 |
| 2021-2020 | (38,900) | (41,600) | 2,700 | (2,100) | (300) | (1,900) |
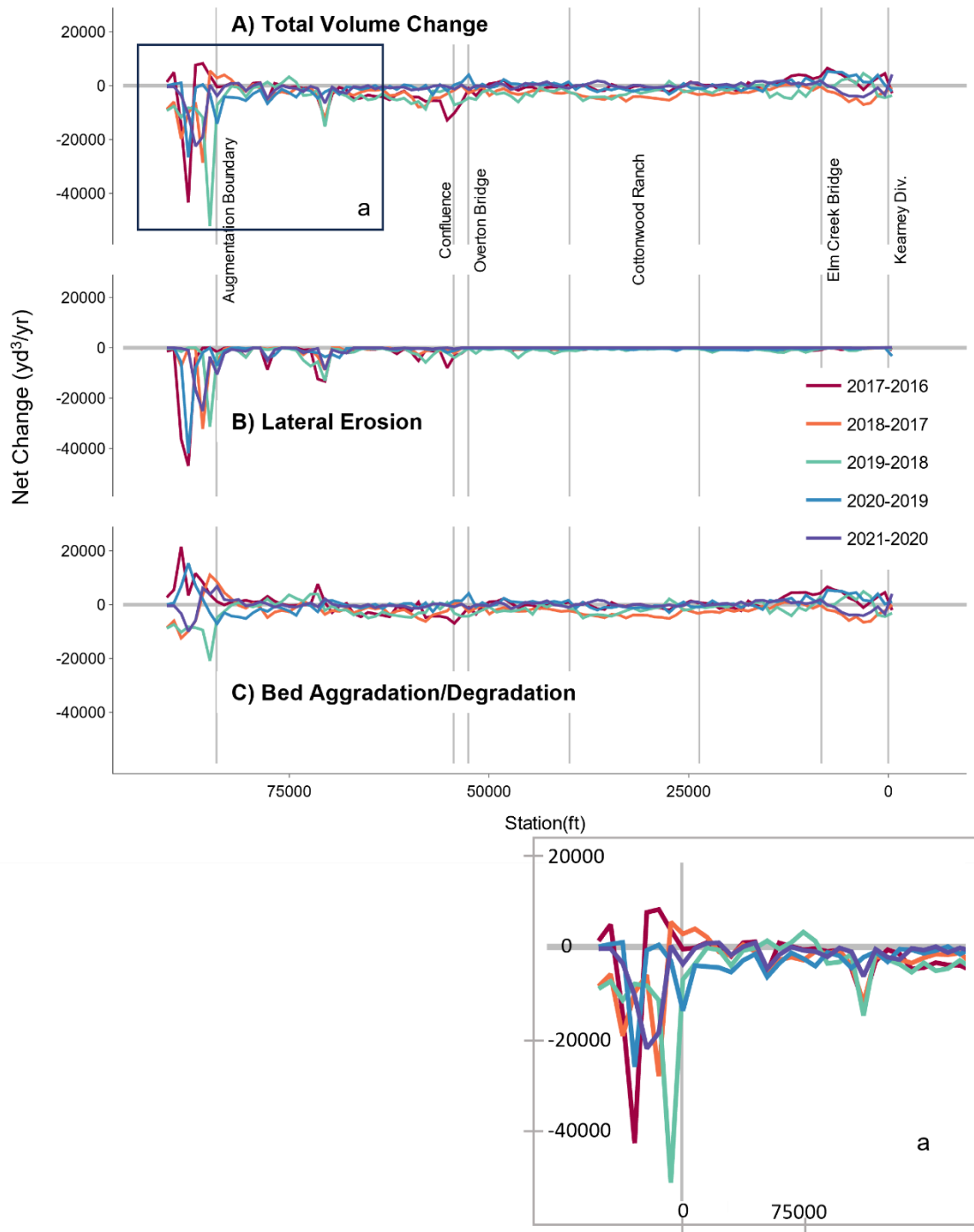
**Figure 4.9** Post-augmentation year-by-year net volume change. Inset 'a' depicts positive volume change that moves downstream from the augmentation zone in 2016 to 2019. This pattern is disrupted in 2019-2021, perhaps becoming more dispersed as total degradation is reduced in those years.
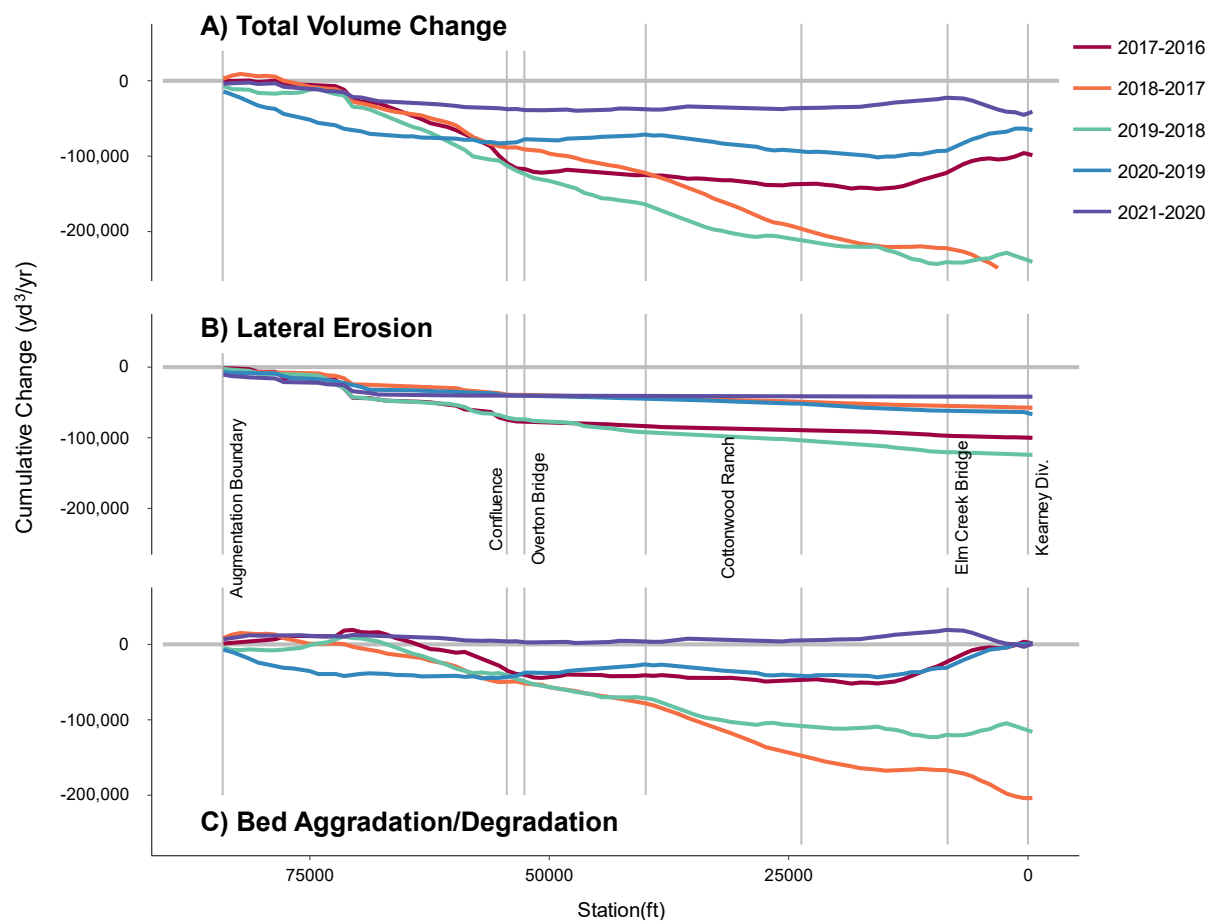
**Figure 4.10** Cumulative year-by-year volume change in the post-augmentation period. (A) Lines represent the running sum of all change starting at the downstream end of augmentation projects. The nearly flat lines downstream of Overton Bridge indicate very little lateral erosion occurred (B). Steep slopes indicate high local change, such as the high bed degradation at Cottonwood Ranch from 2017–2019 (C).

Noise due to varying flow and sediment inputs makes the year-by-year data difficult to interpret. General trends seem to be decreasing degradation in the reach upstream of Overton Bridge, though higher flows in 2019 seem to have caused more bed degradation in the 2020–2019 year. Some years (2016 - 2018) have a distinct hump that is likely the signature of augmentation and breakthrough sediment moving downstream (Figure 4.9 inset 'a'), but in other years no distinct signature is visible and a more dispersed reduction in erosion can be seen. While the reach downstream of Overton Bridge is largely stable, there is year-by-year variation here as well. The steep negative slope in the Cottonwood Ranch area (Figure 4.10) in 2017–2019 shows that this area was degradational during that time, likely due to disking activities in 2018 and higher flow in 2019 (Figure D.4). After the large-scale lateral erosion that occurred in the flood of 2015, very

little additional lateral erosion occurred in the downstream reach during the drier post-augmentation period. This can be observed from the nearly flat slope of lines in Figure 4.10B.

## 4.5    Discussion

In our full-scale augmentation experiment we evaluated whether 60,000–80,000 tons (40,000–60,000 yd$^3$) of sediment placed immediately downstream of the J2 Return each year could offset the sediment deficit sufficiently to stabilize the J2 Return Channel and prevent incision from progressing downstream. In this chapter we evaluated the effectiveness of augmentation via the morphological approach, using LiDAR data (constrained by hydraulic modeling) to measure actual volumetric change during the experiment. Our findings indicate that the J2 Return Channel remained degradational during the experiment, but bed erosion was reduced, and some areas of aggradation were observed in the first three miles downstream of augmentation. We also found that a large portion of sediment supply in the J2 Return Channel came from lateral erosion of channel banks. Finally, we found that the net volume change downstream of the J2 Return Channel between Overton Bridge and the KCD is dynamic but stable, with no observable signal from augmentation.

In terms of quantitative change, bed degradation in the J2 Return Channel decreased by 45%–60% during the augmentation experiment. We attribute this reduction to augmentation activities because the decrease in erosion (approx. 20,000 to 40,000 yd$^3$/yr) was roughly equal to the augmented material leaving the sediment augmentation project area. The movement of augmented material downstream away from the augmentation area is visible in Fig. 4.11. Given full-scale sediment augmentation arrested approximately half of bed degradation in the J2 Return Channel, the volume, location of augmentation, grain-size distribution, or other design factors may need to be adjusted to address the continued incision in the lower half of the channel. Doubling the annual augmentation volume could hypothetically offset remaining bed degradation, but mechanically augmenting 80,000–120,000 yd$^3$/yr may incur challenges in terms of cost, physical supply, and ability to mobilize the sediment. The Program's current United States Corps of Engineers (USACE) Section 404 permit identifies seven sites from which sediment can be sourced with varying degrees of difficulty. At the current rate of augmentation, these sites have enough sediment for a total of 21 more augmentation projects. Without alteration to the existing permit, doubling the volume of augmented sediment would reduce the number of potential projects by half, with four years of source material from Jeffrey Island and six years of source material from more challenging sites along Plum Creek.

Downstream of Overton Bridge, volume change analysis indicates a dynamic channel with a high degree of spatial and temporal variability during the augmentation period. Spatially, the reach from the Overton Bridge to CWR was stable to slightly aggradational, the CWR reach was slightly degradational, and the reach from CWR to the KCD structure was aggradational during augmentation years. Temporally, the channel bed (excluding lateral erosion) between Overton and KCD was net aggradational or relatively stable in three out of five years, but degradational from 2017–2019. When compared to the pre-augmentation period and normalized for discharge, we observed no major difference in bed erosion during the pre- and post-augmentation periods downstream of Overton Bridge.

The one difference we did observe was substantial lateral erosion that occurred because of the prolonged peak flow event in 2015 which increased mean channel width by more than 200 ft. Channel widths have remained stable since 2015, despite much lower flows in recent years (Chapter 3).

Overall, sediment augmentation reduced bed degradation in the J2 Return Channel, but there was no pre- and post-augmentation difference in sediment balance downstream of Overton within the limits of our uncertainty from hydroflattened DEMs. Much of the sediment supply in the J2 Return Channel originates from lateral erosion, which recruits stored sediment from the banks. Theoretically, degradation will continue to slowly progress downstream toward the Overton Bridge and will negatively impact habitat at an unknown point in the future. As such, some form of permanent ongoing augmentation in J2 Return Channel is necessary to reduce future risk to downstream habitat, but near- and long-term benefits are difficult to quantify and weigh against the annual cost of augmenting sediment. Accordingly, it may be necessary to evaluate alternatives that allow for some degree of long-term sediment replenishment into the J2 Return Channel without the cost and supply limitations of ongoing mechanical augmentation. This includes alternatives like retrofitting of the Jeffrey Island Sand Dam to pass sediment into the J2 Return Channel in a controlled manner. Investigations into passive sediment replenishment and augmentation alternatives will likely begin in late 2023.

## 4.6   References

Anderson, S. (2019). Uncertainty in quantitative analyses of topographic change: error propagation and the role of thresholding. *Earth Surface Processes and Landforms, 44*, 1015-1033.

Ashmore, P., & Church, M. (1998). Sediment transport and river morphology; a paradigm for study. In *Gravel Bed Rivers in the Environment* (pp. 115-148). Highlands Ranch, CO: Water Resources Publications LLC.

Bangen, S., Hensleigh, J., McHugh, P., & Wheaton, J. (2016). . Error modeling of DEMS from topographic surveys of rivers using fuzzy inference systems. *Water Resources Research, 52*, 1176– 1193.

Brierley, G., & Fryirs, K. (2005). *Geomorphology and River Management: Applications of the River Styles Framework.* Malden, MA: Blackwell Publishing.

Dewberry. (2010). *LiDAR Quality Assurance (QA) Final Report Sub-Project 1: Platte River Corridor Nebraska/Kansas LiDAR.*

Federal Geographic Data Committee (FGDC). (1998). *National Standard for Spatial Data Accuracy.*

HEC-RAS. (2008). *Hydraulic Reference Manual.* U.S. Army Corps of Engineers, Hydrologic Engineering Center.

Hensleight, J. (2013). *Geomorphic Change Detection Using Multi-beam SONAR.* Master's Thesis, Utah State University, Logan, UT.

Independent Scientific Advisory Committee (ISAC). (2023). *ISAC Report on February 2023 PRRIP Science Plan Reporting Session (SPRS).* Platte River Recovery Implementation Program (PRRIP).

Julien, P., & Simons, D. (1985). Sediment Transport Capacity of Overland Flow. *Transactions of the ASAE, 28*(3), 755-762.

Lai, Y. (2008). *SRH-2D Version 2: Theory and User's Manual.* Bureau of Reclamation Technical Service Center Sedimentation and River Hydraulics Group.

Lane, S., Westaway, R., & Hicks, M. (2003). Estimation of erosion and deposition volumes in a large, gravel-bed, braided river using synoptic remote sensing. *Earth Surface Processes and Landforms, 28*, 249-271.

Leopold, L., & Wolman, M. (1957). *River Channel Pattern: Braided, Meandering and Straight.* Washington DC: U.S. Geological Survey Professional Papers.

Platte River Recovery Implementation Program (PRRIP) Executive Director's Office (EDO). (2022). *First Increment Extension Science Plan.*

Platte River Recovery Implementation Program (PRRIP) Executive Director's Office (EDO). (2022). *System-Scale Geomorphology and Vegetation Monitoring Report 2017-2020.*

Quantum Spatial Inc. (QSI). (2016). *Platte River, Nebraska – Fall 2016: Topobathymetric LiDAR Technical Data Report.*

Quantum Spatial Inc. (QSI). (2017). *Platte River, Nebraska – Fall 2017: Topobathymetric LiDAR Technical Data Report.*

Quantum Spatial Inc. (QSI). (2018). *Platte River, Nebraska – Fall 2018, Nebraska: Topobathymetric LiDAR Technical Data Report.*

Quantum Spatial Inc. (QSI). (2019). *Platte River Fall 2019, Nebraska: Topobathymetric LiDAR Technical Data Report.*

Quantum Spatial Inc. (QSI). (2020). *Platte River Fall 2020, Nebraska: Topobathymetric LiDAR Technical Data Report.*

Quantum Spatial Inc. (QSI). (2020). *RE: Platte River Recovery Implementation Program, Update of baseline data for 2018 and 2017.*

Quantum Spatial Inc. (QSI). (2021). *Platte River Fall 2021, Nebraska: Topobathymetric LiDAR Technical Data Report.*

Rosgen, D. (1994). A Classification of Natural Rivers. *Catena, 22*, 169-199.

Tetra Tech. (2017). *Final 2016 Platte River Final Data Analysis Report.*

The Flatwater Group, Inc. (2010). *Platte River from the Lexington to Odessa Bridges Sediment Augmentation Experiment Alternatives Screening Study Summary Report.*

Vericat, D., Wheaton, J., & Brasington, J. (2017). Revisiting the Morphological Approach: Opportunities and Challenges with Repeat High-Resolution Topography. In D. Tsutsumi, & J. Laronne, *Gravel-Bed Rivers* (pp. 121-158). Chichester, UK: John Wiley & Sons, Ltd.

Wheaton, J., Brasington, J., Darby, S., & Sear, D. (2010). Accounting for uncertainty in DEMs from repeat topographic surveys: improved sediment budgets. *Earth Surface Processes and Landforms, 35*, 136-156.